Analysis of metabolic alterations in carbon utilization pathways during virus infection

Krystal Ann Fontaine

A dissertation

submitted in partial fulfillment of the

requirements for the degree of

Doctor of Philosophy

University of Washington

2014

Reading Committee:

Michael Lagunoff, Chair

Adam P. Geballe

Jason G. Smith

Program Authorized to Offer Degree:

Microbiology

University of Washington

Abstract

Analysis of metabolic alterations in carbon utilization pathways
during virus infection

Krystal Ann Fontaine

Chair of the Supervisory Committee:
Professor Michael Lagunoff
Department of Microbiology

Viruses are dependent on the metabolic machinery of the host cell to supply the energy and molecular building blocks needed for their replication. Substantial research has focused on understanding how viruses alter host cellular metabolism in the hopes of identifying metabolic pathways that are critical for successful infection. In this thesis, we explore how two viruses important for biodefense, vaccinia virus (VACV) and dengue virus (DENV), manipulate the global cellular metabolome during infection. In Chapter III, we examine the impact VACV has on the host metabolic network and discover that VACV implements a strikingly unique carbon utilization program during infection. Specifically, we define an important role for glutamine during VACV infection and show that glucose is dispensable for replication. We show that the glutaminolytic pathway of glutamine metabolism is markedly altered in VACV-infected cells and is necessary to replenish the TCA cycle during infection. We further demonstrate that glutaminolysis is required for optimal VACV replication by facilitating the robust viral protein synthesis needed for infectious virion production. In Chapter IV, we find that DENV

significantly alters glucose metabolism during infection. In particular, we show that DENV infection activates glycolysis via the upregulation of multiple glycolytic mediators. Moreover, we demonstrate that the glycolytic pathway is essential for efficient DENV replication. Therefore, this body of work reveals how viruses dramatically reprogram central carbon metabolism and offers further evidence that metabolic inhibitors may provide promise in the treatment of virus infections in the future.

TABLE OF CONTENTS

Page

List of Figures iii

List of Tables iv

Chapter I: Introduction 1
- Viruses and host cellular metabolism 1
- Viral-induced changes in central carbon metabolism 6
- Objectives of this thesis 8
- Vaccinia virus 9
- Dengue virus 12
- Hypotheses 14

Chapter II: Materials and Methods 17
- Cells 17
- Inhibitors 17
- Antibodies 18
- Viruses and determination of DENV infection rates 18
- Virus infections for metabolic analysis 19
- Cell viability assays 20
- Nutrient starvation and metabolic inhibitor treatment studies 20
- DENV focus-forming unit reduction assays 22
- Glucose uptake assays 22
- Quantitative real-time RT-PCR 23
- Western blot analysis 24
- Transmission electron microscopy 25
- Statistical analysis 26

Chapter III: Vaccinia virus requires glutamine but not glucose for efficient replication 27
- Summary 27
- Introduction 28
- Results 30
- Discussion 36

Chapter IV: Dengue virus requires the induction of glycolysis for productive infection 52
- Summary 52
- Introduction 53
- Results 55

Discussion 60

Chapter V: Conclusions and Future Directions 74
Summary 74
Conclusions 75
VACV 75
DENV 76
Future Directions 77
VACV 77
DENV 79

References 86

LIST OF FIGURES

Figure Number		Page
1-1	Viruses alter carbon metabolism in mammalian cells	16
3-1	Glutamine metabolism is altered during VACV infection	47
3-2	Glutamine is necessary for optimal infectious VACV production	48
3-3	Glutamine is an essential anaplerotic substrate for the TCA cycle during VACV infection	49
3-4	Glutamine is required to maintain the TCA cycle for VACV protein synthesis	50
3-5	Glutamine deprivation results in reduced virion formation in VACV-infected cells	51
4-1	The glycolytic pathway of glucose metabolism is altered during DENV infection	69
4-2	Glutamine metabolism is perturbed in DENV-infected cells	70
4-3	Exogenous glucose is necessary for optimal infectious DENV production	71
4-4	Glycolysis is induced during DENV infection	72
4-5	Glycolysis is required for maximal DENV replication	73
5-1	Glutaminolytic enzyme levels are not elevated during VACV infection	84
5-2	HIF-1α mRNA levels are increased during DENV infection	85

LIST OF TABLES

Table Number Page

3-1 VACV infection alters global host cellular metabolism 40

4-1 DENV infection alters global host cellular metabolism 64

ACKNOWLEDGEMENTS

There are many people I would like to thank for supporting me during my graduate career. First and foremost, I thank my mentor Michael Lagunoff for his committed guidance in helping me to become an independent scientist. He provided me with clear direction, yet also allowed me the freedom to pursue scientific endeavors that I was excited to explore. I would also like to thank my previous mentors, Sharon Isern and Scott Michael, for the inspiring introduction to research and for the continuous encouragement they have given me over the years. I would simply not be where I am today if it were not for these three individuals. I am also indebted to my committee members (Jason Smith, Adam Geballe, Keith Jerome, and Elaine Raines) for years of advice and insight. Thank you to all the members of the Lagunoff lab, past and present, for helping to make my graduate experience such a memorable one. Specifically, I am beyond thankful for Erica Sanchez and the expansive role she has played in my life. To Roman Camarda, I will continue to try to find the words to convey just how truly grateful I am that you joined the lab. I would also like to express my gratitude to my dear friends, including my fellow classmates, for sharing the path with me on such a monumental journey. Lastly, I am forever grateful for my family and their ferocious love and endless support. To Daddy, Momma, Gramma, and Pop Pop, in particular: thank you, thank you, thank you, thank you.

DEDICATION

I dedicate this dissertation to my Daddy and Momma, the two greatest parents a girl could have hoped for. How lucky I have been and continue to be to have you always by my side.

To you both, I love you with all of my heart.

CHAPTER I

Introduction

Viruses and host cellular metabolism

Cellular metabolism is a complex and tightly controlled network of pathways that provide the energy and molecular building blocks necessary to maintain the life of the cell. Similarly, viruses are also dependent on the generation of ATP and macromolecular precursors for critical processes, including genome replication, viral protein synthesis, membrane production, and virion assembly. In recent years, significant focus has been placed on understanding how viruses manipulate host cellular metabolism to support viral replication. Such studies have the power to identify metabolic pathways that are required for successful virus infection and could potentially lead to the discovery of future therapeutic avenues based on metabolic inhibitors.

Many laboratories have utilized a global approach to investigate virus-induced alterations in host cellular metabolism. Nuclear magnetic resonance (NMR) spectroscopy, gas chromatography-mass spectrometry (GC-MS), and liquid chromatography-tandem mass spectrometry (LC-MS/MS) have been used to quantify the intracellular and extracellular levels of numerous metabolites following virus infection. Occasionally, platforms combining multiple analytical techniques have been applied to obtain greater metabolome coverage. These methods have given rise to the systems-level measurement of metabolites, called metabolomics, and metabolic fluxes, known as fluxomics (1-3).

Much of our knowledge on the global metabolic consequences of virus infection stems from several studies focused on members of the *Herpesviridae* family. Viral metabolomic analysis was first conducted to examine metabolic alterations caused by human cytomegalovirus (HCMV) lytic infection (4). HCMV is a large, enveloped, double-stranded DNA virus that

latently infects a significant portion of the human population and can cause serious disease in immunologically naïve or immunocompromised individuals. LC-MS/MS was utilized to measure the levels of 63 different intracellular metabolites at multiple time points following HCMV infection of primary human foreskin fibroblasts. This analysis showed that levels of metabolites involved in glycolysis, the citric acid (TCA) cycle, and nucleotide biosynthesis increase with the progression of HCMV infection. Furthermore, several glycolytic and TCA cycle enzymes are transcriptionally upregulated in HCMV-infected cells. Together, these data suggest that flux through these metabolic pathways is increased during HCMV infection. Systems-level metabolic flux profiling confirmed that flux through glycolysis, the TCA cycle, and nucleotide biosynthesis is indeed upregulated in HCMV-infected fibroblasts (5). HCMV infection also increases flux through the lipid biosynthetic pathway, and pharmacologically inhibiting fatty acid synthesis or very long chain fatty acid generation significantly impairs replication (5, 6), potentially by affecting virion envelope formation. A follow-up study comparing the changes in global metabolic flux between HCMV and a related herpesvirus, herpes simplex virus-1 (HSV-1), reported that these two viruses execute largely divergent metabolic programs within the host cell (7). While HCMV increases glycolytic flux and the movement of glucose carbon to the TCA cycle to support fatty acid biosynthesis, HSV-1 redirects central carbon metabolism toward pyrimidine nucleotide production. Moreover, inhibiting the flux of glucose carbon toward pyrimidine nucleotide synthesis blocks replication of HSV-1, but not HCMV (7). These studies reveal that although herpesviruses share similar requirements for their life cycles, such as the synthesis of nucleic acids and envelopes, distinct virus-specific metabolic programs are implemented during infection to promote successful replication.

Global metabolic profiling has also been performed on Kaposi's sarcoma-associated herpesvirus (KSHV)-infected cells. This was the first metabolomic study to examine changes in host cellular metabolism induced during latent herpesvirus infection (8). KSHV is the etiologic agent of Kaposi's sarcoma (KS), an endothelial cell-based tumor that is the most common malignancy in AIDS patients worldwide (9). GC-MS and LC-MS/MS were used in combination to measure intracellular metabolite levels following latent KSHV infection of endothelial cells. Data from this metabolomic screen suggest that several metabolic pathways are altered following KSHV infection, including glycolysis, the pentose phosphate pathway, and the fatty acid synthesis pathway. Furthermore, lipid biosynthesis is required for the survival of latently KSHV-infected endothelial cells, as pharmacological inhibition of this pathway results in the apoptotic death of infected cells (8). Together, these studies identify the fatty acid synthesis pathway as a potential target to develop novel antiviral therapies to treat both latent and lytic herpesvirus infections.

Much focus has also been placed on investigating the global impact members of the *Flaviviridae* family have on host cellular metabolism. The proteome and lipidome of human hepatoma cells were analyzed during a time course of acute hepatitis C virus (HCV) infection (10). Proteomic analysis of HCV-infected Huh-7.5 cells suggested early perturbations in glycolysis, the TCA cycle, and the pentose phosphate pathway following infection (10). Numerous reports have since shown that glycolysis is activated by HCV and have provided mechanistic insight into its regulation during infection (11-13). Data from both the lipidomic (10) and global metabolomic (14) profiling of HCV-infected Huh-7.5 cells identified alterations in the levels of select lipid species, although the perturbations described in each study were different. As lipid droplets and the endoplasmic reticulum (ER)-derived "membranous web"

facilitate HCV genome replication and virion assembly (reviewed in references (15, 16)), significant focus has been directed toward elucidating the complex role lipid metabolism plays in the HCV life cycle.

The requirement of membrane formation and lipid metabolism is also intensely investigated for dengue virus (DENV) infection, as electron tomography has demonstrated that replication occurs on double-membrane vesicles that neighbor the ER (17). Furthermore, a key enzyme involved in fatty acid biosynthesis, fatty acid synthase (FASN), relocalizes to sites of DENV replication, and pharmacologically inhibiting this metabolic pathway abrogates DENV infection in Huh-7.5 cells (18). DENV also replicates within the *Aedes* mosquito vector, and DENV-infected mosquito cells exhibit virus-induced membrane structures similar to those observed in human cells (19, 20). Lipidomic analysis of the C6/36 *Aedes* mosquito cell line revealed that DENV dramatically perturbs the lipid profile of infected cells, particularly affecting levels of lipids that influence membrane structure and those that function as potent signaling molecules (21). A parallel lipidomic analysis of DENV-infected human cells has yet to be performed. However, NMR spectroscopy and LC-MS were used to examine extracellular changes in metabolite levels of DENV-infected EA.hy926 cells, a human endothelial hybrid cell line. This metabolomic screen confirmed that DENV infection alters fatty acid metabolism and also identified changes in levels of amino acids, TCA cycle intermediates, and tryptophan catabolism products in medium from cultured DENV-infected endothelial cells (22). As this analysis only investigated metabolites that are taken up or secreted into the extracellular milieu, a more comprehensive examination of the metabolome during DENV infection of human cells would be informative. However, the studies conducted thus far identify fatty acid synthesis as a promising pathway to target to inhibit flavivirus infection.

Lastly, the global metabolic impact has been examined for other viruses, including members of the *Retroviridae* and *Orthomyxoviridae* families. LC-MS/MS technology was applied to monitor the metabolic alterations associated with human immunodeficiency virus type 1 (HIV-1) infection of CD4+ T cells and macrophages (23). This metabolomic analysis revealed that HIV-1 implements a distinct metabolic program depending on the host cell it infects. Although certain HIV-induced alterations in host metabolism are conserved between the two cell types, such as changes in the pentose phosphate pathway and the TCA cycle, other metabolic pathway perturbations are target cell type specific. For example, increased glucose uptake and elevated levels of glycolytic intermediates were observed in CD4+ T cells infected with HIV-1, whereas HIV-infected macrophages exhibit decreased glucose uptake and a reduction in glycolytic metabolite levels. Conversely, significant differences in the intracellular pools of nucleoside triphosphates (NTPs) were only observed in macrophages infected with HIV-1 (23). Together, these results identify specific HIV-induced metabolic alterations that may be critical for the short-lived infection of CD4+ T cells and the survival of persistently infected macrophages. Likewise, LC-MS/MS was used to measure changes in intracellular metabolite concentrations during influenza A (IAV) infection of human fibroblasts (HFs). Surprisingly, IAV infection induces only modest changes in the cellular metabolome compared to the extensive metabolic reprogramming exhibited by HCMV and HSV-1 infection of HFs (24). This observation was confirmed in IAV-infected MDCKs, a canine kidney epithelial cell line. However, a striking perturbation in glycolysis was noted during IAV infection of MDCK cells. Elevated concentrations of glycolytic intermediates corresponded with both increased glucose uptake and lactate production in IAV-infected cells, thus indicating that IAV infection of MDCKs induces the upregulation of glycolysis (25). Ultimately, these studies highlight the

ability viruses have to implement distinct metabolic programs during infection, and demonstrate how these programs can vary depending on the host cell type the virus infects.

In summary, the research conducted thus far on viral-induced alterations in global host cellular metabolism reveal several unanticipated findings. First, closely related viruses that share similar life cycles can execute markedly disparate metabolic programs to promote successful replication, as was observed with the *Herpesviridae* family members HCMV and HSV-1. Second, highly divergent viruses can require the same metabolic perturbation(s) during infection, with the necessity for increased fatty acid synthesis being a primary example. However, the role these metabolic alterations play in viral replication may differ between viruses. Lastly, viruses can implement remarkably unique cell type specific metabolic programs during infection, reflecting a striking ability for viruses to adapt to a particular host cellular environment. Though we have learned a great deal about virus-host metabolic interactions in recent years, further work is necessary to provide a more complete understanding of how and why viruses alter host cellular metabolism.

Viral-induced changes in central carbon metabolism

All viruses examined to date have been shown to dramatically perturb the host cell metabolome, particularly pathways involved in central carbon utilization (4, 5, 7, 8, 10, 14, 22-25) (Figure 1-1). Glucose and glutamine represent the main carbon sources utilized by mammalian cells to support energy homeostasis and biosynthesis. In general, glucose is considered the primary contributor of cellular ATP production through its oxidation via glycolysis and the TCA cycle. Normal cells, as well as cancer cells, use the glycolytic pathway to convert glucose to pyruvate. Typically, pyruvate then enters the TCA cycle, where its

catabolism to CO_2 ultimately promotes mitochondrial oxidative phosphorylation. However, in most cancer cells, glucose carbon is directed away from the TCA cycle to produce lactate or to be used biosynthetically. The latter occurs when some of the pyruvate produced from glucose proceeds through the TCA cycle to generate citrate. From here, citrate can be shuttled out of the mitochondrion into the cytoplasm where it is converted into acetyl CoA (ACoA) and oxaloacetic acid (OAA). Cytoplasmic ACoA can then be used as a biosynthetic precursor, primarily for fatty acid synthesis (reviewed in references (26-29)) (Figure 1-1). Otto Warburg first described the unusual manner in which tumor cells metabolize glucose in 1924. He found that cancer cells convert glucose into lactate, even in normoxic conditions where sufficient oxygen is present to support oxidative phosphorylation (30). Known as the Warburg effect, this form of glucose utilization results in the generation of only 2 ATP molecules per molecule of glucose metabolized, whereas the complete oxidation of a glucose molecule by cellular respiration yields a theoretical maximum of 36-38 ATP molecules. Although this appears to be an inefficient means of utilizing glucose, we now know that cancer cells can use exogenous glutamine to support the carbon requirement for the TCA cycle (31-33), a phenomenon termed anaplerosis. Glutamine is converted to the TCA cycle intermediate α-ketoglutarate via glutaminolysis, a metabolic pathway consisting of two deamination steps. Glutamine is first deaminated to glutamate, which is subsequently deaminated to α-ketoglutarate (Figure 1-1). Thus, the anaplerotic usage of glutamine maintains the generation of TCA cycle intermediates and NADH, the latter of which is required for oxidative phosphorylation and ATP production (31, 32).

Numerous viruses induce alterations in host cellular central carbon metabolism that are commonly observed in cancer cells. A prime example is the induction of the Warburg effect by several human viruses, including KSHV, HCMV, and HCV (5, 7, 10, 11, 34), suggesting a

critical role for aerobic glycolysis during virus infection. Accordingly, suppressing glycolysis via pharmacological inhibition or glucose deprivation blocks HCMV and HCV replication (35, 36), and results in the apoptotic death of cells latently infected with KSHV (34). In addition, HCMV infection activates glutaminolysis to replenish the TCA cycle so that glucose carbon can accommodate the fatty acid biosynthetic needs of viral replication. HCMV increases exogenous glutamine uptake and upregulates the two enzymes of the glutaminolytic pathway, glutaminase and glutamate dehydrogenase (37). Because glucose carbon is shuttled out of the mitochondrion to be used biosynthetically during infection (7), HCMV-infected cells become dependent upon glutamine for ATP generation and virus production (37). Although much is known as to how HCMV alters central carbon metabolism, determining if other viruses utilize glucose and glutamine in similar manners for successful replication will be an important area of interest for future investigation.

Objectives of this thesis

The impact of virus infection on the host cell metabolome includes perturbations in nucleotide synthesis, amino acid metabolism, lipid biosynthesis, glycolysis, the TCA cycle, and the pentose phosphate pathway. These metabolic changes coincide with the specific phases of the virus life cycle and the energy input necessary for efficient virion production. However, these studies also bring to light the gaps in our understanding of how different viruses reprogram cellular metabolism to support replication. Importantly, the global metabolic consequence of vaccinia virus (VACV) infection was not known, as metabolomic analyses had not yet been performed on members of the *Poxviridae* family. Additionally, the impact of dengue virus (DENV) infection on the intracellular metabolome had not been thoroughly investigated. This

thesis work provided a parallel analysis of the metabolic alterations associated with VACV and DENV following infection of the same human cell type and revealed strikingly distinct perturbations in central carbon metabolism. As both of these viruses are important to study for biodefense, this work provides metabolic targets for the development of novel antiviral therapies to inhibit potential agents of biological terrorism.

Vaccinia virus

VACV is the most extensively studied member of the *Orthopoxvirus* genus of the *Poxviridae* family. Poxviruses are large, enveloped, double-stranded DNA viruses with genomes that range from 145 to 290 kilobases in size and encode approximately 200 genes. Unlike other DNA viruses that must access the nucleus for replication, the entire poxvirus life cycle occurs exclusively in the cytoplasm of infected cells (38). Poxvirus replication is an intricate cascade of cytoplasmic events that ultimately results in the production of two morphologically distinct forms of infectious virus: the intracellular mature virus (IMV) and the extracellular enveloped virus (EEV). These virion types differ in both membrane number and surface glycoprotein expression and play specific roles in the poxvirus life cycle. IMV represents the majority of infectious progeny produced during poxvirus replication and is released upon lysis of the infected cell (reviewed in references (39, 40)). EEV is required for efficient cell-to-cell spread both *in vitro* and *in vivo* (41, 42) and is thus responsible for long-range virus dissemination (39).

The VACV morphogenetic pathway is complex and begins with the formation of crescent-shaped membranes within virus factories, which are cytoplasmic regions of the cell largely devoid of organelles (43). These crescents will develop into spherical immature virus (IV), and subsequently into dense, brick-shaped, infectious IMV (reviewed in references (39,

40)). Although the majority of infectious virions produced during VACV replication are IMV (40), a portion of IMV will be transported away from sites of viral assembly to become enveloped in trans-Golgi or endosome-derived membrane cisternae (44-46). These virions are known as intracellular enveloped virus (IEV). Once transported to the cell surface by microtubules, IEV can become cell-associated enveloped virus (CEV) (42, 47), a morphogenetic intermediate that, along with EEV, is important for VACV dissemination (48). Actin tail formation beneath CEV (49) can propel virions toward neighboring cells, a process that is required for optimal cell-to-cell spread (50, 51). IEV that is not retained at the cell surface, but is instead directly released into the extracellular milieu is EEV (39, 40). Thus, each morphogenetic intermediate generated during the VACV life cycle serves a particular role in virus dissemination.

VACV is best known for its use as the live vaccine to eradicate smallpox, a devastating disease caused by variola virus, the most notorious member of the *Poxviridae* family. Smallpox is an acute, contagious disease with an estimated mortality rate that approached 50% or greater in naïve populations (52). Efforts to protect against smallpox occurred as early as the 10th century in China and India. The prophylactic intranasal or cutaneous inoculation of smallpox scab material, a procedure known as variolation, was used to prevent the development of serious smallpox disease. At the end of the 18th century, the English physician Edward Jenner described a safer alternative to variolation. Jenner found that the deliberate inoculation of infectious material from the related cowpox virus prevented the development of pustules following challenge by variolation (reviewed in reference (53)). In the 1960s, the World Health Organization (WHO) launched the Smallpox Eradication Programme, a systematic vaccination initiative that led to the global eradication of smallpox. As smallpox has killed more members of

the human population in recorded history than all other infectious diseases combined, its eradication represents one of the greatest triumphs in medicine (reviewed in references (53, 54)).

Although smallpox was declared eradicated in 1980, there remains considerable fear that variola virus could be used as a bioterrorism agent as two WHO-approved stocks of the virus are still in existence (reviewed in references (54, 55)). Furthermore, other poxviruses are able to exclusively or zoonotically infect humans to cause significant disease (56-58). The poxvirus molluscum contagiosum is an important human skin pathogen that can cause serious disfigurement and suffering in infected individuals, which are primarily children and young adults (reviewed in reference (59)). Zoonotic monkeypox virus (MPXV) infection of humans results in the development of a disease that is milder, but clinically similar to smallpox. MPXV is endemic to the tropical rain forest regions of Central and West Africa, and although the virus has been found in numerous African rodent species, the exact reservoir for MPXV remains unknown (60). Monkeypox was first discovered to cause human infection in 1970 in Central Africa. Several cases of human monkeypox outbreaks by different strains of MPXV have subsequently been reported (reviewed in reference (61)), including one variant found in the Democratic Republic of Congo that results in mortality rates of approximately 10-15% (62, 63). Since smallpox has been successfully eradicated, monkeypox is now considered the most severe orthopoxvirus infection in humans (reviewed in references (64-67)). The presence of such pathogenic poxviruses in the human population, as well as the possible re-emergence of variola virus due to deliberate bioterrorism, underscore the need to continue our research efforts in the poxvirus field in hopes of identifying novel approaches to inhibit poxvirus infections. Chapter III of this thesis investigates the potential metabolic requirements of poxvirus replication and defines a specific role for glutamine utilization during VACV infection.

Dengue Virus

DENV is a member of the *Flavivirus* genus of the *Flaviviridae* family, which contains several other medically important human pathogens, such as West Nile virus, Japanese encephalitis virus, and yellow fever virus. Flaviviruses are small, enveloped, positive-stranded RNA viruses with genomes approximately 11 kilobases in size that encode a single polyprotein. Post-translational cleavage of the polyprotein by both host and viral proteases results in the generation of three structural proteins and seven nonstructural proteins (reviewed in reference (68)). Similar to poxviruses, replication of flaviviruses also occurs in the cytoplasm of infected cells. Following translation and processing of the polyprotein, extensive remodeling of cytoplasmic membranes occurs to establish cytosolic sites of replication, known as replication complexes (reviewed in reference (69)). These structures may help to localize viral replication components and to sequester viral antigens from intracellular immune recognition. Budding of flaviviruses occurs on ER membranes and infectious virions are released into the extracellular milieu via the secretory pathway (17) (reviewed in references (69, 70)).

Like many flaviviruses, DENV is transmitted to the human host via an arthropod vector. In particular, the four serotypes of DENV (DENV-1, DENV-2, DENV-3, and DENV-4) are transmitted through the bite of the *Aedes aegypti* and *Aedes albopictus* mosquito (reviewed in references (71, 72)). Unlike other mosquito-transmitted viruses, DENV does not require an enzootic amplification host and is successfully maintained by a human-to-mosquito-to-human cycle of transmission (73). The *Aedes* mosquito inhabits tropical and subtropical areas of the world and its geographical range continues to expand due to several factors, including increased international travel, unrestrained urbanization, and inadequate water management (74). The four DENV serotypes are the most prevalent mosquito-borne viruses that impact human health

(reviewed in reference (75)), as it is currently estimated that nearly half of the global population in over 100 countries is at risk for contracting DENV (76-79).

All four serotypes of DENV are capable of causing the broad spectrum of clinical manifestations associated with infection, which range from an asymptomatic disease to the potentially fatal dengue hemorrhagic fever (DHF) and dengue shock syndrome (DSS). Typically, DENV infections are either asymptomatic or only moderately symptomatic (80, 81). The majority of symptomatic infections present as dengue fever, a self-limiting disease that involves the sudden onset of fever accompanied with other symptoms, such as retro-orbital headache, myalgia, abdominal pain, and nausea. The more life-threatening diseases DHF and DSS are characterized by fever, thrombocytopenia, severe bleeding, and plasma leakage, which can lead to hypotensive shock (reviewed in references (71, 82, 83)). Interestingly, DHF/DSS often occurs in patients following a secondary, heterotypic DENV infection or in primary DENV-infected infants with maternally transferred dengue immunity (84, 85). A phenomenon known as antibody-dependent enhancement (ADE) has been proposed as a potential pathogenic mechanism of DHF/DSS (reviewed in references (84, 86, 87)). Infection with DENV results in the production of broadly cross-reactive antibodies that are either non-neutralizing or weakly neutralizing (88, 89). Upon secondary infection with a different serotype of DENV, the presence of these sub-neutralizing antibodies enhances binding of DENV to Fcγ receptor-bearing host cells, leading to increased uptake and replication of the virus (85). Although ADE of DENV infection has been demonstrated both *in vitro* and *in vivo* (90-94), the details of how this phenomenon mediates disease severity remain largely unknown.

It has been recently estimated that a total of 390 million DENV infections occur annually worldwide (77). Furthermore, these infections result in approximately 500,000 hospitalizations

and 25,000 fatalities each year, with children carrying much of the disease burden (78). Currently, there are no commercially available vaccines or specific antiviral treatments to combat DENV, though much effort has been directed toward these areas of research. Studies such as the one described in this thesis work may reveal new therapeutic strategies to target DENV and other flavivirus infections. Chapter IV of this thesis explores the impact of DENV infection on the host cellular metabolome and identifies the activation of glycolysis as an essential metabolic alteration for DENV replication.

Hypotheses

All viruses hijack the host cellular metabolic machinery to supply the energy and biosynthetic precursors needed for their replication. Recently, several reports have described the extensive reprogramming of global cellular metabolism following virus infection (4, 5, 7, 8, 10, 14, 21-25, 34). These studies identified metabolic perturbations that appear to be broadly important for viral replication, such as altered glycolysis and fatty acid synthesis. Additionally, other metabolic pathways, such as pyrimidine nucleotide biosynthesis, may be essential for only certain virus life cycles (7, 24). Going into this work, I hypothesized that VACV and DENV infection of primary human foreskin fibroblasts (HFFs) would induce dramatic alterations in the host cellular metabolome. Furthermore, I hypothesized that although VACV and DENV may display common metabolic signatures, these two viruses would also exhibit unique metabolic requirements, reflecting their disparate life cycles. As reported below, I found that VACV and DENV implement distinct metabolic programs during infection with strikingly different alterations in carbon utilization pathways. Importantly, inhibition of these metabolic pathways significantly impairs virus production, revealing perturbations in cellular metabolism that are

critical for viral replication. Thus, investigating viral-induced changes in the host cell metabolome can lead to the potential use of metabolic inhibitors to treat future viral outbreaks.

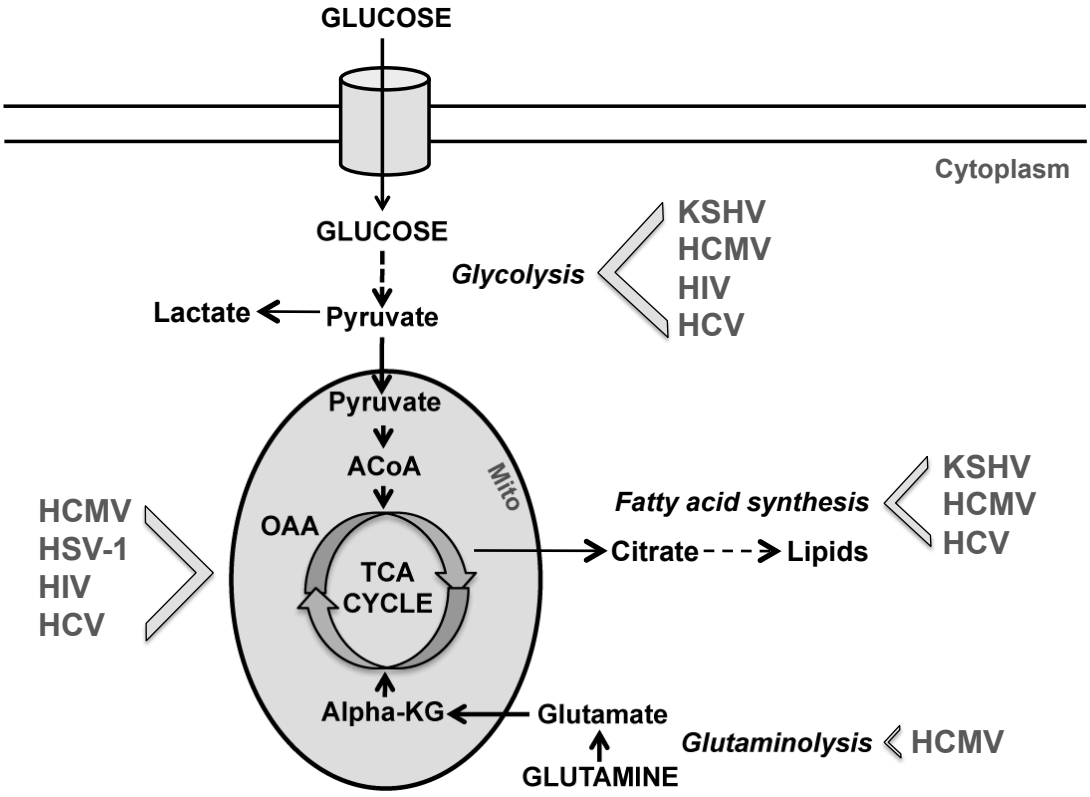

Figure 1-1. Viruses alter carbon metabolism in mammalian cells. Basic diagram of cytoplasmic and mitochondrial (Mito) carbon metabolism. Listed are some of the viruses that have been shown to perturb the pathways included in the schematic. A dashed arrow represents multiple enzymatic reactions within a given metabolic pathway. Abbreviations: alpha-KG, α-ketoglutarate; OAA, oxaloacetic acid; ACoA, acetyl coenzyme A.

CHAPTER II

Materials and Methods

Cells

Primary human foreskin fibroblasts (HFFs) (ATCC PCS-201-010) were propagated and maintained at 37°C in 5% CO_2 in Dulbecco's modified Eagle Medium (DMEM) supplemented with 10% fetal bovine serum, 2 mM L-glutamine, 100 U/ml penicillin, and 100 μg/ml streptomycin. BSC40 cells (ATCC CRL-2761), Vero cells, and Huh-7.5 cells (provided by Michael Gale, Jr., University of Washington) were cultured in a similar fashion. Tert-immortalized human microvascular endothelial cells were maintained in EGM-2 medium (Lonza). For the glucose and glutamine depletion studies, DMEM lacking D-glucose, L-glutamine, sodium pyruvate, and phenol red (catalog number A14430-01; Invitrogen) was used. This medium was supplemented with 2% dialyzed fetal bovine serum (catalog number SH30079.03; HyClone), and for replete medium, 1 g/liter D-glucose and 2 mM L-glutamine were added. Dialyzed serum was utilized in these studies, as it has been thoroughly depleted of small molecules, including glucose and glutamine. The glucose concentration reported for the lot of dialyzed HyClone serum used was <20 mg/dl; therefore, when used at 2%, there is less than <0.004 g/liter of glucose present in the medium.

Inhibitors

Bis-2-(5-phenylacetamido-1,3,4-thiadiazol-2-yl)ethyl sulfide (BPTES) (catalog number SML0601) was obtained from Sigma-Aldrich and solubilized in dimethyl sulfoxide (DMSO) to a stock concentration of 10 mM. Additional dilutions of BPTES were made in methanol and used at the indicated final concentrations. Sodium oxamate (O2751) and deferoxamine mesylate salt

(DFO) (D9533) were also obtained from Sigma-Aldrich. Both drugs were solubilized in deionized water and used at the indicated final concentrations.

Antibodies

Primary antibodies used in these studies include: anti-E3L (a gift from Stuart Isaacs, University of Pennsylvania), anti-P4a (kindly provided by Dennis Hruby, Oregon State University), anti-β-actin (catalog number A5441; Sigma-Aldrich), anti-1.6D (a generous gift from Sharon Isern and Scott Michael, Florida Gulf Coast University), anti-4G2 (also provided by Sharon Isern and Scott Michael, Florida Gulf Coast University), anti-DENV 3H5.1 (catalog number MAB8702; Millipore), anti-hexokinase 2 (HK2) (catalog number sc-6521; Santa Cruz Biotechnology), anti-glucose transporter 1 (GLUT1) (catalog number G3900-01J; US Biological), anti-glutaminase (GLS) (catalog number ab60709; Abcam), and anti-glutamate dehydrogenase (GDH) (catalog number ab89967; Abcam). Secondary antibodies used in these studies include: horseradish peroxidase-conjugated goat anti-mouse (catalog number 115-036-062; Jackson ImmunoResearch), horseradish peroxidase-conjugated goat anti-rabbit (catalog number 111-036-045; Jackson ImmunoResearch), horseradish peroxidase-conjugated goat anti-mouse (catalog number 31410; Pierce), anti-human Alexa Fluor® 488 (catalog number A11013; Invitrogen), and anti-mouse/rabbit/goat IRDye® secondary antibodies (LI-COR).

Viruses and determination of DENV infection rates

The VC-2 Copenhagen strain of vaccinia virus (obtained from Adam Geballe, Fred Hutchinson Cancer Research Center) was propagated in BSC40 cells, and titers were determined by plaque assays on HFFs. Stocks of dengue virus type 2/NG-C (a kind gift from Michael Gale,

Jr., University of Washington) were propagated in Vero cells and titers were determined by plaque assays on Vero cells. Experimental dengue virus (DENV) infection rates were determined by immunofluorescence. DENV-infected cells were fixed at 24 hours postinfection (hpi) with 10% (w/v) formalin, permeabilized with 70% (v/v) ethanol, and blocked with 3% bovine serum albumin (BSA) in Dulbecco's Phosphate-Buffered Saline (DPBS). Cells were then immunostained with 1 μg/ml of the DENV envelope glycoprotein-specific hMAb 1.6D and 2 μg/ml goat anti-human Alexa Fluor® 488, and counterstained with the mounting medium Vectashield® (Vector Laboratories).

Virus infections for metabolic analysis

For the VACV metabolomic analysis, HFFs were washed with DPBS and serum starved overnight in DMEM. Cells were then mock or VACV infected (multiplicity of infection [MOI] of 3) in serum-free DMEM for 1 h, after which the inoculum was replaced with fresh serum-free DMEM. For the DENV metabolomic analysis, HFFs were washed with DPBS and serum starved overnight in DMEM prior to infection. Cells were then mock or DENV infected (MOI of 9, determined as plaque-forming units (PFU)/Vero cell) in serum-free DMEM for 3 h, after which the inoculum was replaced with DMEM supplemented with 2% fetal bovine serum, 2 mM L-glutamine, 100 U/ml penicillin, and 100 μg/ml streptomycin. When infected at an MOI of 9, approximately 50% of HFFs expressed detectable DENV envelope (E) glycoprotein by 24 hpi, as measured by immunofluorescence. Cells were harvested at the indicated times with a cell scraper and washed once in cold DPBS, and pellets were snap-frozen in a dry ice-ethanol bath. Samples were stored at -80°C until shipment to Metabolon (Durham, NC).

A multitude of curation procedures were conducted by Metabolon to guarantee the quality of the data set presented. Metabolon data analysts used proprietary visualization and interpretation software to confirm peak identification consistency and to limit system artifacts, misassignments, and background noise among the various samples. Bradford assays were performed to normalize all samples by protein concentration, and each biochemical in the mock samples was rescaled to yield a median of 1. Following log transformation and imputation with minimum observed values for each compound, two-way analysis of variance (ANOVA) with contrasts tests was used to determine which metabolites were significantly altered by virus infection of HFFs at each time point across four biological replicates. Error bars on metabolite-level line plot graphs reflect standard errors of the means from the four separate infections.

Cell viability assays

HFFs or BSC40 cells were washed once with DPBS and fed replete medium, glutamine-free medium, or glucose-free medium. Attached cells were removed by trypsinization at 24 h posttreatment and collected, along with the culture medium and DPBS wash containing any detached cells. Cells were concentrated, mixed 1:1 with 0.4% trypan blue solution, and counted with a hemacytometer. Error bars reflect standard errors of the means from three separate experiments.

Nutrient starvation and metabolic inhibitor treatment studies

For the VACV study, HFFs or BSC40 cells were washed with DPBS and infected with VACV at an MOI of 5 for 1 h. Cells were washed once with DPBS and fed replete medium, glutamine-free medium, or glucose-free medium. For experiments where TCA cycle

intermediates were added to the medium, the final concentrations used were 7 mM dimethyl-α-ketoglutarate (catalog number 349631; Sigma-Aldrich), 4 mM oxaloacetic acid (catalog number 04126; Sigma-Aldrich), or 4 mM pyruvate (catalog number S8636; Sigma-Aldrich). For BPTES treatment experiments, VACV-infected cells were fed replete medium containing methanol (control), 10 μM BPTES, or 10 μM BPTES and 7 mM dimethyl-α-ketoglutarate. Infected cells were harvested at 24 hpi with a cell scraper, washed once in cold DPBS, and resuspended in 10 mM Tris-HCl (pH 9). Virus was released by subjecting the infected cells to three freeze-thaw cycles and sonication. Titers were determined by a plaque assay on BSC40 cells. Error bars reflect standard errors of the means from at least three separate experiments for the nutrient starvation and TCA intermediate rescue studies. Errors bars reflect standard errors of the means from two independent experiments for the BPTES treatment studies.

For the DENV study, HFFs were washed with DPBS and infected with DENV at an MOI of 3 in serum-free DMEM for 2 h. Cells were washed with DPBS and fed replete medium, glucose-free medium, or glutamine-free medium. For oxamate treatment experiments, DENV-infected HFFs were treated with 0 mM oxamate, 50 mM oxamate, or 100 mM oxamate. TIME cells were infected with DENV at an MOI of 1 for 2 h and treated with 0 mM oxamate or 100 mM oxamate. Supernatant was collected from infected cells 24 hpi, centrifuged to remove cellular debris, and titers were determined by focus-forming unit reduction assays on Vero cells. Error bars reflect standard errors of the means from three separate experiments for the glucose starvation and oxamate treatment studies with HFFs. Errors bars reflect standard errors of the means from two independent experiments for the oxamate treatment studies in TIME cells.

DENV focus-forming unit reduction assays

Monolayers of Vero cells in 6- or 12-well plates were infected with supernatants collected from DENV-infected cells. Supernatants were diluted in serum-free DMEM and allowed to infect the cells for 1 h, after which the monolayers were overlaid with plugs consisting of a 1:1 ratio of 1.8% Agar Noble (BD Biosciences) and 2X MEM (Lonza) supplemented with 20% FBS, 4 mM L-glutamine, 200 U/ml penicillin, and 200 μg/ml streptomycin. Four days postinfection, cells were fixed with 10% (w/v) formalin, permeabilized with 70% (v/v) ethanol, and subjected to immunostaining. Virus foci were detected using mouse anti-DENV mAbs 3H5.1 or 4G2, followed by horseradish-peroxidase conjugated goat anti-mouse immunoglobulin (Pierce) and developed using AEC chromagen substrate (Dako) or 3,3'-diaminobenzidine tetrahydrochloride (Sigma-Aldrich).

Glucose uptake assays

HFFs in 12-well plates were serum starved ~16 h prior to infection. Cells were then mock or DENV infected at an MOI of 9 in serum-free DMEM for 2 h, after which the inoculum was replaced with DMEM supplemented with 2% fetal bovine serum, 2 mM L-glutamine, 100 U/ml penicillin, and 100 μg/ml streptomycin. Complete medium was replaced 22 hpi with serum-free DMEM. At 24 hpi, cells were washed twice with DPBS (containing magnesium and calcium) and fed 0.5 μCi of deoxy-D-glucose, 2-[1,2-^{3}H(N)] (NET549A250UC; Perkin Elmer) in 500 μl of DPBS (containing magnesium and calcium) for 5 min at 37°C. Cells were then washed twice with ice-cold DPBS (without magnesium and calcium) and lysed in 300 μl 1% SDS for 20 min at room temperature. Next, 150 μl of lysate was added to 4 ml of Biofluor Plus (Perkin Elmer) and activity (disintegrations per minute) was measured by liquid scintillation counting. Cell-

associated radioactivity was normalized to protein concentration, which was determined using the BCA Protein Assay Reagent Kit (Pierce). Error bars reflect the standard errors of the means from three separate experiments.

Quantitative real-time RT-PCR

For the VACV study, total RNA isolation and quantitative real-time RT-PCR were performed as previously described (95), using 500 ng of total RNA from each sample for analysis. The primers used to examine VACV transcript levels were: E3L forward primer 5'-CGC AGA GAT TGT GTG TGA GG-3', E3L reverse primer 5'-AAC GGT GAC AGG GTT AGC AC-3'; F17R forward primer 5'-ATT CTC ATT TTG CAT CTG CTC-3', F17R reverse primer 5'-AGC TAC ATT ATC GCG ATT AGC-3'; hypoxanthine-guanine phosphoribosyltransferase (HPRT) forward primer 5'-GAA CGT CTT GCT CGA GAT GTG-3', and HPRT reverse primer 5'-CCA GCA GGT CAG CAA AGA ATT-3'. Relative abundances of E3L mRNA and F17R mRNA were normalized by the delta threshold cycle method to the abundance of HPRT mRNA, with VACV-infected cells fed replete medium being set to 1. Error bars reflect standard errors of the means from three separate experiments.

For the DENV study, total RNA was isolated from HFFs using the Nucleospin® RNA II kit (Macherey-Nagel). Two-step quantitative real-time reverse transcription-PCR (Bio-Rad) was used to measure transcript or DENV RNA levels. iScript™ Reverse Transcription Supermix for RT-qPCR (Bio-Rad) was used to synthesize one microgram of cDNA from one microgram of total RNA according to manufacturer's instructions. One hundred nanograms of cDNA were used in SsoAdvanced™ SYBR Green Supermix (Bio-Rad) according to manufacturer's protocols. The primers used for hexokinase 2 (HK2) (96), glyceraldehyde-3-phosphate

dehydrogenase (GAPDH) (97), DENV RNA (18), and HPRT (98) have been described previously. Relative abundances of HK2 mRNA or DENV RNA were normalized by the delta threshold cycle method to the abundance of GAPDH mRNA or HPRT mRNA, with mock-infected cells being set to 1 or DENV-infected cells fed replete medium being set to 100. Error bars reflect standard errors of the means from three separate experiments for the HK2 expression studies. Error bars reflect standard errors of the means from two independent experiments for the DENV RNA quantitation studies.

Western blot analysis

For the VACV study, mock- and VACV-infected cells were harvested by trypsinization and lysed in radioimmunoprecipitation assay (RIPA) buffer (50 mM Tris-HCl [pH 7.6], 150 mM NaCl, 1 mM EDTA, 1% NP-40, 0.5% deoxycholate, 0.1% sodium dodecyl sulfate) supplemented with protease and phosphatase inhibitors. Proteins were separated by SDS-PAGE (7.5% polyacrylamide gels) and transferred to Immobilon P polyvinylidene difluoride membranes (Millipore). Blots were incubated with the indicated primary antibody (dilutions of 1:4,000 for anti-E3L, 1:8,000 for anti-P4a, 1:1,000 for anti-GLS, 1:1,000 for anti-GDH, and 1:10,000-1:100,000 for anti-β-actin) and subsequently with horseradish peroxidase-conjugated secondary antibody (dilutions of 1:20,000 goat anti-rabbit and 1:10,000-1:30,000 goat anti-mouse). Immunoreactive proteins were visualized by chemiluminescence using Amersham ECL Plus Western blotting detection reagents (GE Healthcare Life Sciences). Differences in band intensity were quantified by densitometric methods using ImageJ (99).

For the DENV study, HFFs were mock or DENV infected at an MOI of 9 in serum-free DMEM for 2 h. Following infection, cells were treated with 0 μM DFO or 150 μM DFO and

harvested with a cell scraper at 24 hpi. Cytoplasmic and nuclear fractions were obtained using the NE-PER nuclear and cytoplasmic extraction kit (Thermo Scientific). Proteins were separated by SDS-PAGE and transferred to Immobilon FL polyvinylidene difluoride membranes (Millipore). Blots were incubated with the indicated primary antibody (dilutions: 1:1,000 for anti-GLUT1, 1:200 for anti-HK2, and 1:30,000 for anti-β-actin) and subsequently incubated with the appropriate IRDye® secondary antibody (LI-COR). Proteins were visualized and differences in band intensity were quantified using the Odyssey® CLx Infrared Imaging System (LI-COR).

Transmission electron microscopy

HFFs grown to ~80-90% confluence in 150-cm^2 cell culture flasks were infected with VACV at an MOI of 5 and fed replete medium, glutamine-free medium, or glutamine-free medium supplemented with 7 mM dimethyl-α-ketoglutarate. Infected cells were fixed at 24 hpi and processed for transmission electron microscopy (TEM). Briefly, VACV-infected cells were fixed with 2% paraformaldehyde and 2.5% glutaraldehyde in 0.2 M cacodylate buffer and were postfixed in 2% aqueous osmium tetroxide-0.2 M cacodylate buffer for 2 h at 4°C. After multiple washes, the samples were dehydrated in ethanol and embedded in Epon. Ultrathin sections were placed onto grids and stained with uranyl acetate and lead citrate. Samples were observed under a JEOL JEM-1400 transmission electron microscope (Fred Hutchinson Cancer Research Center electron microscopy facility) with a Gatan Ultrascan 1000XP camera and DigitalMicrograph software (Gatan, Pleasanton, CA).

Statistical Analysis

Standard errors of the means are shown, and statistical differences between groups were analyzed with Student's *t* test (two-tailed) or one-way ANOVA. A *P* value of ≤ 0.05 was considered significant and is indicated by an asterisk in the figures. A *P* value of ≤ 0.01 is indicated by a double asterisk, and a *P* value of <0.0001 is indicated by a triple asterisk in the figures.

CHAPTER III

Vaccinia Virus Requires Glutamine but not Glucose for Efficient Replication

Adapted from an article originally published in the Journal of Virology:

Fontaine Krystal A., Camarda R, Lagunoff M. 2014.
Vaccinia virus requires glutamine but not glucose for efficient replication.
J Virol 88:4366-4374.

SUMMARY

Viruses require host cell metabolism to provide the necessary energy and biosynthetic precursors for successful viral replication. Vaccinia virus (VACV) is a member of the *Poxviridae* family, and its use as a vaccine enabled the eradication of variola virus, the etiologic agent of smallpox. A global metabolic screen of VACV-infected primary human foreskin fibroblasts suggested glutamine metabolism is altered during infection. Glutamine and glucose represent the two main carbon sources for mammalian cells. Depriving VACV-infected cells of exogenous glutamine led to a substantial decrease in infectious virus production, whereas starving infected cells of exogenous glucose had no significant impact on replication. Viral yield in glutamine-deprived cells or in cells treated with an inhibitor of glutaminolysis, the pathway of glutamine catabolism, could be rescued by the addition of multiple tricarboxylic acid (TCA) cycle intermediates. Thus, VACV infection induces a metabolic alteration to fully rely on glutamine to anaplerotically maintain the TCA cycle. VACV protein synthesis, but not viral transcription, was decreased in glutamine-deprived cells, which corresponded with a dramatic reduction in all VACV morphogenetic intermediates. This study reveals the unique carbon utilization program implemented during poxvirus infection and provides a potential metabolic pathway to target viral replication.

INTRODUCTION

All viruses rely on host cellular metabolism for the energy and macromolecule synthesis required for their replication. Recently, significant focus has been placed on examining how virus infection alters the host cellular metabolic profile in the hopes of identifying metabolic pathways that are critical to virus life cycles. Viral metabolomic analyses were first conducted to determine changes in host cell metabolism caused by human cytomegalovirus (HCMV) lytic infection (4, 5). HCMV was shown to induce multiple metabolic alterations, including upregulation of the tricarboxylic acid (TCA) cycle, fatty acid synthesis, pyrimidine nucleotide biosynthesis, and glycolysis. The metabolic effects of virus infection on human cells have now been investigated for several other viruses, including Kaposi's sarcoma-associated herpesvirus (KSHV), herpes simplex virus-1 (HSV-1), hepatitis C virus (HCV), human immunodeficiency virus type 1 (HIV-1), and dengue virus (4, 7, 8, 10, 22, 23). These studies have identified numerous metabolic perturbations induced by virus infection. Importantly, one metabolic alteration that has been observed in most of these reports is the activation of glycolysis, suggesting a role for glucose as a critical carbon source during virus infection.

Glucose and glutamine are the primary sources of carbon for energy homeostasis and biosynthesis in mammalian cells. Normally, glucose is considered the main contributor of cellular ATP through its oxidation via glycolysis and the TCA cycle. However, in cells where glucose carbon is being directed away from the TCA cycle, such as in most cancer cells and HCMV-infected cells, glutamine carbon can be used to replenish the TCA cycle, a process termed anaplerosis (5, 7, 31-33, 37). Thus far, studies that have examined the impact of glucose and glutamine deprivation on virus production, including HCMV, HSV-1, and poliomyelitis

virus, have found that both carbon sources are required for optimal viral replication (37, 100, 101).

Global metabolic analyses have not previously been performed on members of the *Poxviridae* family. Poxviruses are large, double-stranded DNA viruses that, in contrast to other DNA viruses, replicate entirely in the cytoplasm of infected cells (38). Vaccinia virus (VACV) is the prototypical poxvirus and was used as the live vaccine against variola virus, the causative agent of smallpox. Although smallpox has been eradicated, other poxviruses are able to infect humans either exclusively or zoonotically to cause serious disease, including molluscum contagiosum virus and monkeypox virus (56-58). A highly pathogenic variant of monkeypox virus found in the Democratic Republic of Congo causes a smallpox-like disease and results in a mortality rate of approximately 10% (62, 63). Due to the potential use of variola virus as a bioterrorism agent, as well as the presence of other pathogenic poxviruses in the human population, furthering our understanding of poxvirus-host interactions remains an important challenge.

To identify perturbations in host cellular metabolic pathways during poxvirus infection, we performed a global metabolomic screen during a time course of VACV infection of primary human foreskin fibroblasts (HFFs). Of particular interest, data from this screen suggested that glutamine utilization is altered in VACV-infected cells compared to their mock–infected counterparts. Surprisingly, we found that exogenous glutamine is the critical carbon source for VACV replication and that glucose is dispensable for virus production. We also determined that glutamine, via its catabolism to α-ketoglutarate, is required to maintain the TCA cycle for VACV protein synthesis and that the loss of viral protein synthesis under glutamine-deprived

conditions results in reduced levels of all virion morphogenetic intermediates. Therefore, VACV infection induces a dependence on glutamine metabolism to support efficient viral replication.

RESULTS

VACV infection alters glutamine metabolism

To examine changes in host cell metabolism induced during VACV infection, we utilized a global intracellular metabolic profiling approach. Primary human foreskin fibroblasts (HFFs) were used for these experiments, as they are a commonly employed VACV-permissive primary cell type. Transformed cells are known to exhibit fundamentally altered metabolism; therefore, many transformed cell lines are often of limited value for examining viral-induced metabolic alterations (reviewed in references (32, 102, 103)). HFFs were serum starved for approximately 18 h prior to infection to synchronize the cells in the G_0/G_1 phase. Cells were then mock or VACV infected at an MOI of 3 and harvested at 4, 8, 12, and 24 hours postinfection (hpi) for metabolic analysis. Samples from four independent experiments were analyzed by using both gas chromatography mass spectrometry (GC-MS) and liquid chromatography-tandem mass spectrometry (LC-MS/MS). Our metabolomic screen identified numerous changes in host cellular metabolic pathways following VACV infection of HFFs (Table 3-1). Interestingly, we noted a striking perturbation in glutamine metabolism during the course of VACV infection. Glutamine is metabolized via glutaminolysis, a process consisting of two deamination steps. In the first step, glutamine is deaminated to glutamate. The second deamination reaction then converts glutamate to α-ketoglutarate, an intermediate that can enter the TCA cycle. Figure 3-1 shows that both glutamine and glutamate levels were elevated in VACV-infected cells at multiple time points postinfection. Glutamine levels were significantly elevated in VACV-

infected cells at both 4 and 8 hpi, whereas glutamate was found at increased levels in VACV-infected cells at all four time points examined. The metabolite α-ketoglutarate was not one of the 282 biochemicals detected in our samples. These data suggest that VACV infection alters glutamine utilization in HFFs.

Glutamine is required for maximal infectious VACV production

Because our metabolic screen identified an alteration in glutamine metabolism during VACV infection, we hypothesized that glutamine may be essential for viral replication. To test this, we investigated the impact both glutamine and glucose deprivation have on VACV production. HFFs were infected with VACV at an MOI of 5 and subsequently fed replete medium containing both glucose and glutamine or medium lacking either glucose or glutamine. At 24 hpi, cell-associated viral yields were determined by a plaque assay. As shown in Figure 3-2A, depriving VACV-infected cells of exogenous glutamine reduced the production of infectious virus by approximately 90%. Surprisingly, starving VACV-infected cells of glucose had no significant impact on viral replication. Importantly, in the time frame examined for infection, the small changes observed in the growth and viability of uninfected HFFs under conditions of glutamine or glucose deprivation were similar, indicating that the block in VACV production was not due to the effects of glutamine deprivation on cellular integrity (Figure 3-2B). While it was previously reported that HFFs lose viability when starved of glucose for 48 h (37), this was not the case following 24 h of glucose deprivation. These results reveal a dependence on glutamine, but not on glucose, during VACV infection.

In addition, we examined the impact of glutamine deprivation on VACV production in the permissive BSC40 cell line. As shown in Figure 3-2C, starving VACV-infected BSC40 cells

of exogenous glutamine resulted in an approximately 2-log reduction in viral yield. The observed block in VACV replication was not due to decreased cell viability under conditions of glutamine deprivation (Figure 3-2D). Titers could not be accurately measured for glucose-deprived infected BSC40 cells, as they are a transformed cell line and are highly sensitive to glucose starvation, exhibiting ~17% cell death following glucose starvation for 24 h (reviewed in references (32, 104, 105)). However, even with this significant impact on cellular integrity, it is interesting to note that viral yields obtained from glucose-starved infected BSC40 cells were still more than a log higher than those obtained from glutamine-starved infected BSC40 cells (data not shown). This set of experiments further implicates that glutamine is the critical carbon source for VACV replication and that the requirement for glutamine is not cell type specific.

Glutamine is an anaplerotic substrate for the TCA cycle during VACV infection

Many cancer cell types utilize exogenous glutamine, via its conversion to α-ketoglutarate, to fill the TCA cycle. This anaplerotic usage of glutamine allows the cell to use glucose-derived carbon for biosynthetic purposes instead of energy production (31-33) (Figure 3-3A). Similarly, it has been shown that HCMV-infected HFFs become dependent on glutamine to replenish the TCA cycle so that glucose carbon can be used primarily for fatty acid synthesis (26, 37). Our data indicate that glucose is not necessary for VACV replication, thus suggesting that a different carbon source is used to feed the TCA cycle during VACV infection. To determine if VACV-infected cells require glutamine to maintain the TCA cycle, we added a number of TCA cycle intermediates to the medium of glutamine-deprived infected cells. Following infection, HFFs were fed replete medium, glutamine-free medium, or glutamine-free medium supplemented with 7 mM dimethyl-α-ketoglutarate, 4 mM oxaloacetic acid, or 4 mM pyruvate. Cells were harvested

at 24 hpi, and viral yields were measured by a plaque assay. The addition of exogenous TCA cycle intermediates to glutamine-deprived infected cells significantly rescued VACV production (Figure 3-3B).

We also examined infectious virus production following pharmacological inhibition of glutaminolysis. VACV-infected cells were treated with bis-2-(5-phenylacetamido-1,3,4-thiadiazol-2-yl)ethyl sulfide (BPTES), a small molecule inhibitor of glutaminase, the enzyme that catalyzes the first step of glutaminolysis, the conversion of glutamine to glutamate. Figure 3-3C shows that blocking of glutaminolysis reduced viral yields to levels similar to those obtained from glutamine-deprived infected cells. Moreover, virus production in BPTES-treated cells was significantly recovered by α-ketoglutarate supplementation. Combined, these data indicate that exogenous glutamine, via its conversion to α-ketoglutarate, is required to replenish the TCA cycle in VACV-infected cells.

Glutamine is necessary to maintain the TCA cycle for viral protein synthesis

To identify at what stage in the VACV life cycle glutamine is required, we first examined viral mRNA synthesis by quantitative real-time RT-PCR. For this experiment, we measured transcript levels of the VACV early gene E3L, which encodes an antagonist of the innate immune response, and the VACV late gene F17R, which encodes a protein involved in mature virion assembly. HFFs were infected with VACV at an MOI of 5 and fed replete medium or glutamine-free medium. Total RNA was isolated from infected cells harvested at both 2 hpi and 8 hpi, and quantitative real-time RT-PCR was conducted by utilizing primers specific for E3L and F17R. Figure 3-4A shows that E3L and F17R mRNA synthesis was not inhibited at either

time point postinfection under glutamine-deprived conditions. These results indicate that exogenous glutamine is not required for VACV transcription.

We next examined early and late VACV protein expression via Western blot analysis. For this experiment, we measured the protein levels of the early gene E3L as well as the late gene P4a, which encodes the major VACV core protein precursor. Following infection, HFFs were fed replete medium, glutamine-free medium, or glutamine-free medium supplemented with either 7 mM dimethyl-α-ketoglutarate or 4 mM pyruvate, two TCA cycle intermediates that rescued infectious VACV production in glutamine-deprived cells (see Figure 3-3B). As shown in Figure 3-4B, early and late viral protein synthesis was blocked when VACV-infected cells were starved of exogenous glutamine. E3L and P4a protein levels were substantially recovered by the TCA cycle intermediate α-ketoglutarate or pyruvate in VACV-infected cells deprived of glutamine. In addition, VACV-infected cells treated with increasing concentrations of BPTES exhibited a dose-dependent decrease in P4a levels compared to those of vehicle-treated (control) cells. The impact of BPTES treatment on viral protein synthesis was examined as early as 6 hpi and showed similar results (Figure 3-4C). These data reveal that exogenous glutamine is necessary for VACV protein synthesis. Furthermore, these findings suggest that the need for glutamine extends beyond its role as an amino acid. When glutaminase is specifically inhibited, the utilization of glutamine as a TCA intermediate is prevented, but glutamine is still available to be used as an amino acid. Therefore, the requirement for glutamine during VACV infection is due largely to its use as an anaplerotic substrate to replenish the TCA cycle.

Levels of virion morphogenetic intermediates are reduced in glutamine-deprived infected cells

The above-described results show that glutamine is required at the stage of viral protein synthesis in the VACV life cycle. To determine if glutamine deprivation also affects VACV maturation, Western blot analysis was performed to measure P4a cleavage. P4a is a precursor polypeptide that is proteolytically cleaved to produce the major VACV core protein 4a and the protein p23 (106). The presence of these cleavage products serves as a marker for the conversion of immature virions (IVs) to mature virions (MVs). As shown in Figure 3-5A, although total protein levels were decreased in the absence of glutamine, the relative abundance of the cleavage product p23 was approximately equivalent to the relative abundance of the precursor P4a in glutamine-starved infected cells. These results suggest that glutamine deprivation does not inhibit VACV maturation.

To further investigate whether glutamine deprivation has an impact on VACV maturation, we next visualized virion morphogenesis by transmission electron microscopy (TEM). HFFs were infected with VACV at an MOI of 5 and fed replete medium, glutamine-free medium, or glutamine-free medium supplemented with 7 mM dimethyl-α-ketoglutarate. Cells were fixed at 24 hpi and prepared for examination by TEM. Figure 3-5B shows that no apparent block in VACV morphogenesis was observed in glutamine-deprived infected cells. All stages of virion morphogenesis were identified in VACV-infected cells under the three conditions, including crescents, IVs, and MVs. However, levels of these morphogenetic intermediates were strikingly reduced in VACV-infected cells starved of glutamine. Moreover, the addition of α-ketoglutarate to infected cells under glutamine-deprived conditions resulted in a significant recovery of levels of virion morphogenetic intermediates. Taken together, these data suggest that the drastic loss of

VACV protein synthesis that occurs under glutamine-deprived conditions is responsible for the observed reduction in levels of virion morphogenetic intermediates and the overall decrease in infectious virus production.

DISCUSSION

Viruses have evolved to manipulate host cellular metabolism to support the energetic and biosynthetic requirements for successful replication. Utilizing a global metabolomic screen, we have found that several metabolic pathways are perturbed by VACV infection. Interestingly, we were surprised to find that VACV infection does not appear to induce glycolysis. As our lab and others have previously described, many different viruses activate glycolysis (4, 7, 10, 23, 34, 36), indicating an important role for this metabolic pathway during virus infection. In agreement with this, inhibiting glycolysis has been shown to attenuate both HCMV and HSV-1 replication as well as induce apoptosis in cells latently infected with KSHV (34, 36, 107, 108). Recently, it was reported that the VACV protein C16 stabilizes hypoxia-induced factor 1α (HIF-1α), resulting in the transcriptional upregulation of HIF-responsive genes, including two genes involved in glucose metabolism (109). However, the metabolic consequence of C16-induced HIF-1α stabilization in the context of VACV infection has yet to be investigated. In this study, we show that depriving VACV-infected cells of exogenous glucose has no significant impact on virus production, indicating that this carbon source is not essential for VACV replication.

Our metabolic screen identified a notable perturbation in glutamine metabolism during VACV infection. Glutamine levels are increased within the first 8 h of infection, while glutamate levels remain elevated throughout the course of infection. It is possible that the continued consumption of glutamine during VACV infection leads to the decrease in glutamine levels

observed late in infection without lowering the intracellular pool of glutamate. For example, purine and pyrimidine biosynthetic pathways require the deamination of glutamine to glutamate to supply the nitrogen for these nucleotides. However, because glutamine is utilized as a nitrogen source for both pathways, nucleotide biosynthesis results in the production and accumulation of glutamate (110). The steady elevated levels of glutamate observed in VACV-infected cells may indicate that glutamine is consumed in multiple metabolic pathways during infection, including those in which glutamate serves as a product and not as an intermediate. Consistent with this notion, levels of several biochemicals involved in purine and pyrimidine metabolism are significantly increased in VACV-infected cells (Table 3-1). Further studies are in progress to assess global glutamine usage during VACV infection by metabolic carbon and nitrogen flux analysis.

In support of our metabolomic data, we show that the viral yield is drastically decreased when VACV-infected cells are deprived of exogenous glutamine, revealing that glutamine is the critical carbon source during VACV replication. Because glucose is not required to support glycolysis and the TCA cycle in VACV-infected cells, we hypothesized that glutamine is necessary for TCA cycle replenishment and ATP generation. Accordingly, we found that VACV production in glutamine-deprived cells is substantially rescued by supplementation with the TCA cycle intermediates α-ketoglutarate, oxaloacetic acid, and pyruvate. It is interesting to note that the ability of pyruvate to rescue virus production during glutamine deprivation suggests that VACV-infected cells can derive pyruvate from glutamine under normal conditions. The metabolic pathways involved in generating pyruvate from glutamine were not investigated here. However, similar results were observed when glutamine-starved HCMV-infected cells were fed pyruvate. It was speculated that this could occur when glutamine carbon enters the TCA cycle,

via α-ketoglutarate, and proceeds to citrate. Citrate can then be shuttled to the cytoplasm and converted to oxaloacetic acid and acetyl-CoA (CoA), and oxaloacetic acid can ultimately be returned to pyruvate (37). Although TCA cycle intermediate supplementation significantly restored VACV production in glutamine-deprived cells, we did not observe a complete recovery of viral yield. As mentioned above, this may be due to the requirement for glutamine to support additional metabolic pathways during VACV infection, such as providing the nitrogen for nucleotide biosynthesis. Future work to determine the importance of other pathways of glutamine metabolism during VACV replication is warranted.

Our data also show that the anaplerotic usage of glutamine for the TCA cycle is crucial for viral protein synthesis. Translation is a highly energy-exhaustive process that requires ATP for both ribosome scanning of mRNA 5' untranslated regions (UTRs) to initiate protein synthesis and the activation of amino acids during the elongation phase (111-113). Given that glutamine is a nonessential amino acid, and inhibition of glutaminolysis dramatically reduced VACV protein levels, our results suggest that glutamine may play a principal role during VACV infection by supplying the energy demand for viral protein synthesis. However, we cannot exclude the importance of glutamine utilization in the TCA cycle for providing the building blocks of protein synthesis, as several nonessential amino acids are biosynthesized from TCA cycle intermediates (reviewed in reference (114)) .

Why VACV induces such a striking alteration in carbon source utilization compared to other viruses investigated to date remains unknown. Glutamine is one of the most abundant amino acids in serum and, unlike glucose, which is solely a carbon source, additionally serves as a primary nitrogen donor for cells. Through its dual role in metabolism, glutamine may represent

a more efficient nutrient to provide the ATP, macromolecular precursors, and reducing equivalents necessary for VACV replication (reviewed in references (32, 115)).

How glutaminolysis is induced by VACV is also currently not clear. We did not observe significant changes in the protein levels of the two glutaminolytic enzymes, glutaminase and glutamate dehydrogenase, during the course of VACV infection (K.A. Fontaine and M. Lagunoff, unpublished data). However, enzyme activity could be elevated without a corresponding increase in the protein expression in VACV-infected cells. Current work is ongoing to elucidate the mechanism(s) through which VACV infection activates glutamine utilization. Given that glutamine metabolism is required for optimal VACV replication, inhibitors of glutaminolysis, such as BPTES or its newly designed analogs (116), may serve as novel therapies to target poxvirus infections. By broadening our understanding of how viruses alter host cellular metabolism, we hope to discover additional metabolic pathways that are critical to viral replication. This study is the first step in identifying the metabolic needs of poxviruses and could lead to future therapeutic avenues.

ACKNOWLEDGEMENTS

We thank Stuart Isaacs (University of Pennsylvania) for providing anti-E3L and Dennis Hruby (Oregon State University) for providing anti-P4a. We also thank Adam Geballe (Fred Hutchinson Cancer Research Center) for reagents, Jacquelyn Braggin for technical assistance, and Almira Punjabi for helpful discussions.

M.L. was supported by grants from the NIAID, the NCI, and the NIDCR of the NIH under award numbers U54AI081680, RO1CA097934, and PO1DE021954. K.A.F was supported in part by PHS NRSA T32 GM07270 from the NIGMS.

Table 3-1. VACV infection alters global host cellular metabolism.

Super Pathway	Sub Pathway	Biochemical Name	4 HPI	8 HPI	12 HPI	24 HPI
Amino acid	Glycine, serine and threonine metabolism	glycine	1.60	1.62	**1.44**	0.83
		serine	1.30	1.23	1.00	**0.70**
		N-acetylserine	2.34	**1.70**	1.19	1.14
		3-phosphoserine	1.82	2.75	1.67	0.48
		threonine	1.28	1.46	1.03	0.74
	Alanine and aspartate metabolism	aspartate	1.63	1.46	1.26	0.93
		asparagine	1.28	1.19	1.16	1.00
		beta-alanine	1.14	**1.62**	1.44	0.79
		alanine	1.12	1.18	1.05	0.77
		N-acetylalanine	1.24	1.04	1.54	1.15
	Glutamate metabolism	glutamate	1.91	2.11	1.60	1.77
		glutamine	1.66	2.02	1.23	0.96
		pyroglutamine*	**1.43**	1.92	1.10	**0.66**
		gamma-aminobutyrate (GABA)	1.00	1.00	0.46	0.67
		N-acetyl-aspartyl-glutamate (NAAG)	1.20	1.01	**0.63**	1.09
	Histidine metabolism	histidine	1.25	**1.34**	0.94	0.68
	Lysine metabolism	lysine	1.13	1.07	0.98	**0.72**
		2-aminoadipate	**1.67**	2.32	3.02	4.57
	Phenylalanine and tyrosine metabolism	phenylalanine	1.23	1.35	0.89	0.81
		tyrosine	1.24	1.30	0.97	0.79
		3-(4-hydroxyphenyl)lactate	1.96	2.88	1.52	2.11
	Tryptophan metabolism	tryptophan	1.32	1.39	0.91	**0.77**
		C-glycosyltryptophan*	1.22	1.01	0.79	**0.69**
	Valine, leucine and isoleucine metabolism	isoleucine	1.30	1.49	0.99	0.86
		leucine	**1.26**	1.28	0.97	0.77
		valine	1.20	1.26	0.93	**0.81**
		2-methylbutyroylcarnitine	1.34	0.84	0.57	0.66
	Cysteine, methionine, SAM and taurine metabolism	cysteine	1.70	1.13	0.88	0.86
		cysteine sulfinic acid	1.01	1.43	1.07	0.78
		methionine sulfoxide	1.33	1.15	0.93	0.70
		N-formylmethionine	1.46	1.43	1.20	1.68
		hypotaurine	1.21	1.65	1.00	0.43
		S-adenosylhomocysteine (SAH)	1.07	0.99	0.84	0.96
		methionine	**1.29**	**1.27**	1.00	0.85
		N-acetylmethionine	1.20	1.20	1.17	1.02
	Urea cycle; arginine and proline metabolism	dimethylarginine (SDMA + ADMA)	1.11	1.01	0.99	0.40
		arginine	1.15	1.19	0.79	0.63
		ornithine	0.95	1.12	0.90	0.66
		urea	1.22	1.22	1.15	0.83
		proline	1.33	1.35	1.31	0.84
		5-aminovalerate	0.85	2.01	1.69	1.26
	Creatine metabolism	creatine	1.43	1.46	1.14	**1.25**
	Polyamine	5-methylthioadenosine (MTA)	1.47	1.52	0.71	1.42

Heat map of fold change levels of biochemicals profiled in this study. For paired comparisons, shaded cells with white-bolded values indicate $p \leq 0.05$ (red indicates that the mean values are significantly higher in VACV-infected cells for that comparison and green indicates that the values are significantly lower). Red- and green-bolded values indicate $0.05 < p < 0.1$.

Table 3-1. VACV infection alters global host cellular metabolism. (continued)

	metabolism	spermidine	1.27	1.14	0.91	0.80
	Glutathione metabolism	glutathione, reduced (GSH)	1.61	1.73	1.62	2.73
		5-oxoproline	1.20	1.31	1.04	0.99
		glutathione, oxidized (GSSG)	1.35	1.37	1.10	2.49
		cysteine-glutathione disulfide	1.05	1.18	0.99	0.41
		S-lactoylglutathione	1.43	1.31	1.34	2.30
Peptide	Dipeptide	glycylvaline	1.10	1.22	0.97	1.31
		glycylglycine	1.13	1.23	0.89	0.51
		glycylproline	1.40	1.58	1.23	1.21
		glycylisoleucine	1.21	0.97	0.74	0.91
		glycylleucine	1.12	1.02	0.67	0.62
		glycylphenylalanine	1.24	1.17	0.91	0.89
		glycyltyrosine	0.81	1.17	1.09	0.60
		alanylvaline	1.79	0.93	0.60	1.01
		alanylleucine	1.32	1.23	0.65	1.13
		aspartylaspartate	0.92	0.57	0.74	0.73
		aspartylphenylalanine	1.21	1.49	1.18	1.34
		pro-hydroxy-pro	1.65	1.63	1.18	0.35
		valylserine	1.42	1.07	0.74	1.76
		valylleucine	1.28	1.19	1.04	1.06
		aspartylleucine	1.31	0.90	0.67	0.75
		histidylleucine	1.18	1.15	0.74	0.66
		isoleucylalanine	1.25	1.03	0.71	1.07
		isoleucylglutamine	1.15	1.05	0.79	0.97
		isoleucylglycine	1.04	0.91	0.61	0.64
		isoleucylserine	1.63	1.24	0.93	2.31
		leucylalanine	1.07	0.36	0.84	1.37
		leucylglutamate	1.38	1.04	1.11	1.37
		leucylglycine	1.22	1.11	0.73	0.86
		lysylleucine	1.37	1.29	1.05	1.24
		phenylalanylserine	1.59	1.54	0.80	0.93
		serylleucine	1.36	1.07	0.88	1.59
		serylphenyalanine	1.44	1.15	0.82	1.08
		threonylleucine	1.54	0.97	0.69	1.12
		tyrosylleucine	1.35	1.09	0.83	1.16
		valylaspartate	0.97	0.92	0.78	1.10
		alpha-glutamyltyrosine	1.00	1.02	1.54	0.80
		valylglycine	1.15	0.86	0.64	0.62
	Gamma-glutamyl	gamma-glutamylvaline	1.51	1.20	0.73	1.23
		gamma-glutamylleucine	0.99	**1.80**	0.72	0.63
		gamma-glutamylisoleucine*	0.92	1.50	1.00	1.09
		gamma-glutamylcysteine	1.14	2.02	0.93	**0.47**
		gamma-glutamylglutamate	1.34	**1.46**	1.26	1.08
		gamma-glutamylglutamine	**1.53**	**1.57**	1.19	0.59

Heat map of fold change levels of biochemicals profiled in this study. For paired comparisons, shaded cells with white-bolded values indicate $p \leq 0.05$ (red indicates that the mean values are significantly higher in VACV-infected cells for that comparison and green indicates that the values are significantly lower). Red- and green-bolded values indicate $0.05 < p < 0.1$.

Table 3-1. VACV infection alters global host cellular metabolism. (continued)

		gamma-glutamylphenylalanine	1.17	0.95	0.93	0.56
		gamma-glutamyltyrosine	1.43	0.88	0.76	0.97
Carb	Aminosugars metabolism	N-acetylglucosamine 6-phosphate	1.01	1.44	1.43	**1.57**
		erythronate*	1.62	1.43	2.23	2.88
		N-acetylneuraminate	**1.95**	2.13	1.31	1.54
	Sugar metabolism	fructose	1.63	3.47	2.80	2.98
		lactose	1.21	1.07	1.09	1.09
		mannose 6-phosphate	1.35	0.98	1.25	1.55
		sorbitol	1.75	2.25	2.06	2.63
	Glycolysis, gluconeogenesis and pyruvate metabolism	glycerate	1.53	0.87	**0.63**	1.09
		glucose 6-phosphate (G6P)	1.47	1.14	0.78	1.59
		glucose	0.92	1.43	1.25	0.74
		fructose 6-phosphate	1.22	1.34	0.84	1.80
		Isobar: fructose 1,6-diphosphate, glucose 1,6-diphosphate, myo-inositol 1,4 or 1,3-diphosphate	2.05	0.83	0.74	0.99
		3-phosphoglycerate	1.23	1.09	1.30	1.01
		dihydroxyacetone phosphate (DHAP)	1.77	1.83	1.60	2.24
		phosphoenolpyruvate (PEP)	0.95	1.29	1.52	0.76
		lactate	1.36	1.17	1.16	1.23
	Nucleotide sugars, pentose metabolism	6-phosphogluconate	2.19	**2.26**	1.46	**2.15**
		sedoheptulose 7-phosphate	1.83	0.84	0.98	0.93
		ribose	1.07	1.14	0.88	1.02
		ribose 5-phosphate	1.76	1.63	1.42	1.71
		ribulose	0.66	1.01	1.80	0.77
		Isobar: ribulose 5-phosphate, xylulose 5-phosphate	1.52	1.52	1.28	1.39
		UDP-glucuronate	**2.63**	1.99	0.64	1.22
	Nucleotide sugars	UDP-galactose	1.73	1.56	1.38	0.65
Energy	Krebs cycle	citrate	1.49	1.37	1.11	2.35
		succinate	1.47	0.89	0.68	1.39
		fumarate	1.15	1.13	0.95	1.25
		malate	1.07	1.06	1.13	1.01
	Oxidative phosphorylation	acetylphosphate	**1.22**	**1.23**	0.91	0.83
		phosphate	1.14	1.26	1.27	0.97
		pyrophosphate (PPi)	1.17	1.22	1.26	0.20
Lipid	Essential fatty acid	linoleate (18:2n6)	1.11	0.81	**0.74**	0.86
		linolenate [alpha or gamma; (18:3n3 or 6)]	1.12	0.67	0.68	0.70
		dihomo-linolenate (20:3n3 or n6)	0.98	0.83	0.96	1.79
		docosapentaenoate (n3 DPA; 22:5n3)	1.20	0.95	0.99	1.36
		docosapentaenoate (n6 DPA; 22:5n6)	1.01	0.88	0.95	1.19
		docosahexaenoate (DHA; 22:6n3)	1.25	0.92	0.90	1.16
	Medium chain fatty acid	caproate (6:0)	1.35	1.08	1.18	0.70
		caprylate (8:0)	0.78	1.05	0.96	0.92
		pelargonate (9:0)	1.09	1.15	1.00	1.11

Heat map of fold change levels of biochemicals profiled in this study. For paired comparisons, shaded cells with white-bolded values indicate $p \leq 0.05$ (red indicates that the mean values are significantly higher in VACV-infected cells for that comparison and green indicates that the values are significantly lower). Red- and green-bolded values indicate $0.05 < p < 0.1$.

Table 3-1. VACV infection alters global host cellular metabolism. (continued)

		caprate (10:0)	1.24	1.07	0.96	0.94
		undecanoate (11:0)	1.48	1.12	0.66	1.63
		laurate (12:0)	1.19	1.15	1.03	1.11
	Long chain fatty acid	myristate (14:0)	1.21	1.14	1.04	1.06
		myristoleate (14:1n5)	1.10	1.05	0.79	0.94
		pentadecanoate (15:0)	1.22	1.24	1.12	0.97
		palmitate (16:0)	1.13	1.24	1.15	1.13
		palmitoleate (16:1n7)	1.22	0.85	**0.74**	0.66
		margarate (17:0)	1.18	1.05	1.02	1.02
		10-heptadecenoate (17:1n7)	1.12	0.84	0.72	0.87
		stearate (18:0)	1.25	1.16	1.15	1.10
		oleate (18:1n9)	1.13	1.07	0.86	0.70
		cis-vaccenate (18:1n7)	1.13	1.01	0.82	0.58
		nonadecanoate (19:0)	1.30	1.19	1.13	1.05
		10-nonadecenoate (19:1n9)	1.14	0.85	0.87	0.91
		eicosenoate (20:1n9 or 11)	1.26	0.92	0.85	0.95
		dihomo-linoleate (20:2n6)	1.15	0.78	0.76	0.94
		mead acid (20:3n9)	1.16	**0.61**	**0.58**	0.48
		arachidonate (20:4n6)	1.16	0.92	0.95	1.39
		docosadienoate (22:2n6)	1.31	0.68	0.86	1.06
		docosatrienoate (22:3n3)	1.03	0.82	0.85	0.69
		adrenate (22:4n6)	1.15	0.86	0.98	1.31
	Fatty acid, ester	n-Butyl Oleate	1.19	1.34	1.50	0.63
	Fatty acid, monohydroxy	2-hydroxystearate	1.31	1.79	2.04	1.28
		2-hydroxypalmitate	1.36	**1.63**	1.68	1.21
		13-HODE + 9-HODE	1.15	0.83	0.83	0.58
	Fatty acid, dicarboxylate	2-hydroxyglutarate	**2.42**	0.47	4.41	5.19
		azelate (nonanedioate)	0.71	1.09	1.30	1.11
	Fatty acid, amide	stearamide	1.55	1.24	1.21	4.00
	Fatty acid, branched	13-methylmyristic acid	1.21	1.19	0.96	0.86
		15-methylpalmitate (isobar with 2-methylpalmitate)	1.17	1.16	1.05	1.07
	Eicosanoid	prostaglandin A2	1.06	0.84	0.68	0.55
		prostaglandin E1	0.55	0.95	0.68	0.72
		prostaglandin E2	1.09	0.81	0.72	0.65
		prostaglandin I2	1.01	0.58	0.66	0.42
		6-keto prostaglandin F1alpha	1.00	0.79	0.70	0.39
	Endocannabinoid	oleic ethanolamide	0.98	6.97	24.65	33.47
		palmitoyl ethanolamide	1.52	7.57	21.53	37.68
		stearoyl ethanolamide	0.83	4.49	24.96	51.73
	Fatty acid metabolism	propionylcarnitine	1.57	1.01	0.52	0.87
	Carnitine metabolism	deoxycarnitine	1.00	1.04	0.99	0.63
		carnitine	1.18	1.37	**1.42**	1.08

Heat map of fold change levels of biochemicals profiled in this study. For paired comparisons, shaded cells with white-bolded values indicate $p \leq 0.05$ (red indicates that the mean values are significantly higher in VACV-infected cells for that comparison and green indicates that the values are significantly lower). Red- and green-bolded values indicate $0.05 < p < 0.1$.

Table 3-1. VACV infection alters global host cellular metabolism. (continued)

		laurylcarnitine	0.87	1.64	1.49	0.56
		palmitoylcarnitine	1.26	1.41	0.89	1.01
		stearoylcarnitine	0.88	1.09	0.93	0.84
		oleoylcarnitine	0.83	1.09	0.75	0.87
	Glycerolipid metabolism	choline phosphate	1.33	1.19	1.04	1.38
		ethanolamine	1.13	0.74	0.69	0.66
		phosphoethanolamine	0.76	0.92	1.05	2.28
		choline	1.20	1.03	1.08	1.25
		glycerol 3-phosphate (G3P)	1.05	**1.39**	1.42	**1.38**
		glycerophosphorylcholine (GPC)	1.23	1.47	1.94	1.73
		cytidine 5'-diphosphocholine	2.07	2.83	1.73	1.73
	Inositol metabolism	myo-inositol	2.10	**2.06**	1.21	0.71
		inositol 1-phosphate (I1P)	1.07	0.93	0.94	0.79
	Lysolipid	1-palmitoylglycerophosphoethanolamine	1.10	1.23	1.19	1.55
		2-palmitoylglycerophosphoethanolamine*	1.08	1.07	0.83	0.85
		2-palmitoleoylglycerophosphoethanolamine*	0.91	0.96	0.75	0.69
		1-stearoylglycerophosphoethanolamine	1.08	0.92	1.01	1.12
		1-oleoylglycerophosphoethanolamine	1.08	1.33	1.25	1.40
		2-oleoylglycerophosphoethanolamine*	1.10	1.13	0.94	0.89
		2-linoleoylglycerophosphoethanolamine*	1.19	1.23	0.70	1.00
		1-arachidonoylglycerophosphoethanolamine*	1.02	1.37	1.15	1.19
		2-arachidonoylglycerophosphoethanolamine*	1.07	1.26	0.89	1.00
		2-docosapentaenoylglycerophosphoethanolamine*	1.09	1.15	0.79	0.95
		2-docosahexaenoylglycerophosphoethanolamine*	1.11	1.24	0.89	0.96
		1-myristoylglycerophosphocholine	1.02	1.10	0.75	0.99
		2-myristoylglycerophosphocholine*	1.12	1.07	0.68	0.94
		1-pentadecanoylglycerophosphocholine*	1.27	1.15	1.20	1.03
		1-palmitoylglycerophosphocholine	1.01	1.11	0.79	1.25
		2-palmitoylglycerophosphocholine*	1.06	1.05	0.78	0.88
		1-palmitoleoylglycerophosphocholine*	1.26	1.10	0.83	0.91
		2-palmitoleoylglycerophosphocholine*	1.11	1.13	0.77	0.76
		1-heptadecanoylglycerophosphocholine	0.80	1.08	0.58	0.95
		1-stearoylglycerophosphocholine	0.92	1.07	0.96	1.26
		1-oleoylglycerophosphocholine	1.00	1.07	0.76	1.14
		2-oleoylglycerophosphocholine*	1.08	1.18	0.72	1.05
		1-linoleoylglycerophosphocholine	1.45	0.99	0.74	1.22
		2-linoleoylglycerophosphocholine*	1.07	1.19	0.65	1.06
		2-arachidonoylglycerophosphocholine*	1.13	1.58	1.00	1.52
		1-docosapentaenoylglycerophosphocholine*	1.07	1.10	1.25	1.12
		2-docosapentaenoylglycerophosphocholine*	1.05	1.29	0.87	1.37
		2-docosahexaenoylglycerophosphocholine*	1.19	1.66	0.89	**1.80**
		1-palmitoylglycerophosphoinositol*	1.03	0.60	1.00	0.60
		1-stearoylglycerophosphoinositol	1.22	0.93	0.98	0.89
		1-oleoylglycerophosphoinositol*	1.09	0.73	0.85	0.55

Heat map of fold change levels of biochemicals profiled in this study. For paired comparisons, shaded cells with white-bolded values indicate $p \leq 0.05$ (red indicates that the mean values are significantly higher in VACV-infected cells for that comparison and green indicates that the values are significantly lower). Red- and green-bolded values indicate $0.05 < p < 0.1$.

Table 3-1. VACV infection alters global host cellular metabolism. (continued)

		1-arachidonoylglycerophosphoinositol*	0.93	1.10	1.60	2.42
		2-arachidonoylglycerophosphoinositol*	1.13	0.75	1.22	1.37
		1-oleoylglycerophosphoserine	1.07	1.00	1.22	0.92
		2-oleoylglycerophosphoserine*	0.63	1.24	1.69	0.74
		1-palmitoylplasmenylethanolamine*	1.49	1.44	1.61	1.72
	Monoacylglycerol	1-stearoylglycerol (1-monostearin)	1.19	1.00	1.15	0.73
	Diacylglycerol	1,2-dipalmitoylglycerol	1.23	0.71	0.91	1.65
		1,3-dipalmitoylglycerol	1.12	0.58	1.24	0.51
	Sphingolipid	sphinganine	1.31	1.25	2.06	1.78
		sphingosine	1.29	0.86	0.83	0.77
		palmitoyl sphingomyelin	0.95	0.89	0.89	0.64
		stearoyl sphingomyelin	0.75	1.07	0.99	0.89
	Sterol/steroid	lathosterol	0.95	0.81	0.95	0.59
		cholesterol	1.00	0.95	0.96	0.66
		7-dehydrocholesterol	1.03	1.00	0.79	0.42
		dihydrocholesterol	1.33	2.29	3.53	8.01
		7-alpha-hydroxycholesterol	0.98	1.23	1.17	0.80
		7-beta-hydroxycholesterol	1.35	1.50	1.66	1.46
		7-ketocholesterol	1.31	1.70	0.70	0.55
Nucleotide	Purine (hypo)xanthine/ inosine metabolism	xanthine	0.61	1.10	0.51	0.64
		hypoxanthine	1.07	**1.29**	1.21	0.98
		inosine	**1.36**	1.46	1.04	1.02
		2'-deoxyinosine	2.92	6.17	6.72	2.87
	Purine metabolism, adenine containing	adenine	1.14	0.66	1.18	1.35
		adenosine	1.66	1.24	**1.78**	0.98
		N1-methyladenosine	1.05	1.10	1.34	2.37
		adenosine 2'-monophosphate (2'-AMP)	1.00	0.92	0.72	0.62
		adenosine 3'-monophosphate (3'-AMP)	1.09	1.28	1.35	0.76
		adenosine 5'-monophosphate (AMP)	3.25	0.93	0.84	1.12
		adenosine 5'-diphosphate (ADP)	0.95	1.18	1.09	0.88
	Purine metabolism, guanine containing	guanine	1.14	**1.31**	1.22	1.08
		guanosine	1.54	1.50	1.03	1.20
	Pyrimidine, cytidine containing	cytidine	1.31	2.40	9.05	10.51
		cytidine 5'-monophosphate (5'-CMP)	1.42	**1.45**	1.57	2.40
	Pyrimidine, orotate	orotate	3.19	1.16	1.53	0.69
	Pyrimidine, thymine	thymidine	**1.88**	**1.89**	3.05	1.24
	Pyrimidine, uracil containing	uracil	1.00	0.97	1.21	0.81
		uridine	**1.40**	1.56	1.30	1.45
		uridine monophosphate (5' or 3')	1.34	1.11	1.18	1.17
Cofactors & vitamins	Folate metabolism	5-methyltetrahydrofolate (5MeTHF)	1.26	1.01	0.86	**1.54**
		folate	1.23	1.13	1.38	0.80
	Nicotinate and	nicotinamide	1.07	0.86	0.80	0.66

Heat map of fold change levels of biochemicals profiled in this study. For paired comparisons, shaded cells with white-bolded values indicate $p \leq 0.05$ (red indicates that the mean values are significantly higher in VACV-infected cells for that comparison and green indicates that the values are significantly lower). Red- and green-bolded values indicate $0.05 < p < 0.1$.

Table 3-1. VACV infection alters global host cellular metabolism. (continued)

	nicotinamide metabolism	nicotinamide ribonucleotide (NMN)	1.49	1.22	0.97	0.95
		nicotinamide adenine dinucleotide (NAD+)	1.31	1.45	1.20	**1.61**
		nicotinamide adenine dinucleotide reduced (NADH)	1.05	1.23	1.33	**2.23**
		nicotinamide adenine dinucleotide phosphate (NADP+)	1.32	1.43	0.83	0.92
		nicotinamide riboside*	0.43	1.37	1.31	0.76
		adenosine 5'diphosphoribose	1.77	1.67	0.85	2.16
		1-methylnicotinamide	1.94	1.95	1.67	1.57
	Pantothenate and CoA metabolism	pantothenate	1.54	1.75	1.65	1.69
		phosphopantetheine	0.92	0.86	1.64	1.05
		coenzyme A	1.32	1.84	2.44	5.96
		3'-dephosphocoenzyme A	1.00	1.00	1.00	**1.72**
	Pyridoxal metab	pyridoxal	1.52	1.01	0.79	1.31
	Riboflavin metabolism	flavin adenine dinucleotide (FAD)	1.15	1.16	**1.16**	1.24
		riboflavin (Vitamin B2)	0.90	1.14	1.10	**0.69**
	Thiamine metab	thiamin (Vitamin B1)	1.23	1.07	0.94	1.07
	Tocopherol metab	alpha-tocopherol	1.38	1.44	1.33	2.46
	Vitamin B6 metab	pyridoxine (Vitamin B6)	1.22	**1.26**	1.12	1.10
Xenobios	Benzoate metabolism	benzoate	1.17	1.09	1.00	1.10
		methyl-4-hydroxybenzoate	1.14	1.02	1.41	0.96
	Chemical	glycolate (hydroxyacetate)	0.68	1.90	1.05	0.76
		glycerol 2-phosphate	**1.90**	1.40	1.37	1.36
		2-ethylhexanoate (isobar with 2-propylpentanoate)	1.49	1.32	1.29	0.72
		phenol red	1.01	1.15	1.06	0.80
	Drug	penicillin G	1.21	1.19	1.13	1.09
N/A	N/A	17-(1,5-dimethylhexyl)-10,13-dimethyl-1,2,6,7,8,9,11,12,14,15,16,17-dodecahydrocyclopenta[a]phenanthren-3-one	2.14	6.50	7.62	31.65

Heat map of fold change levels of biochemicals profiled in this study. For paired comparisons, shaded cells with white-bolded values indicate $p \leq 0.05$ (red indicates that the mean values are significantly higher in VACV-infected cells for that comparison and green indicates that the values are significantly lower). Red- and green-bolded values indicate $0.05 < p < 0.1$.

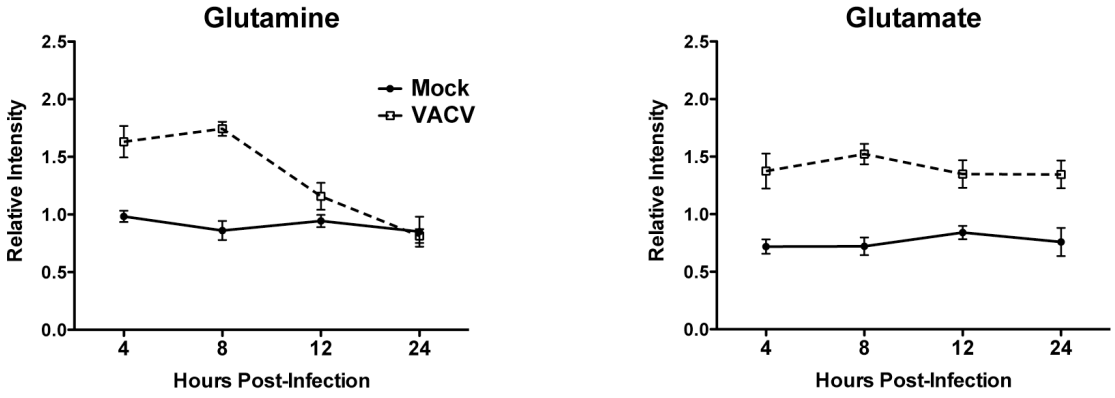

Figure 3-1. Glutamine metabolism is altered during VACV infection. Line plots of glutamine and glutamate levels in mock- and VACV-infected cells measured at 4, 8, 12, and 24 hpi. Cells were harvested at the indicated time points, and Metabolon performed global metabolic analysis of the samples.

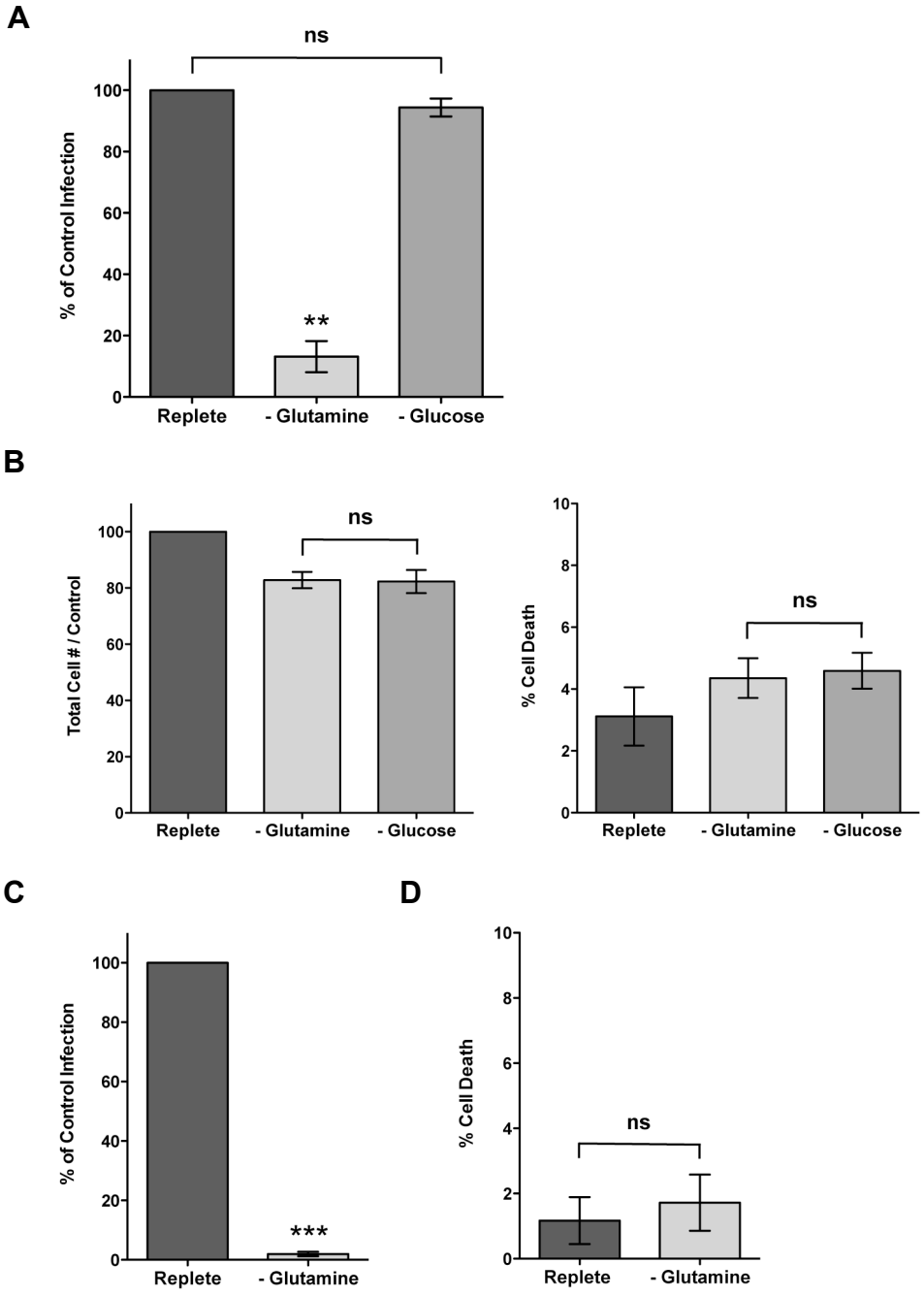

Figure 3-2. Glutamine is necessary for optimal infectious VACV production. (A and C) HFFs (A) or BSC40 cells (C) were infected with VACV at an MOI of 5 and were fed replete medium, glutamine-free medium, or glucose-free medium at 1 hpi. Cell-associated virus was harvested 24 hpi, and viral yields were determined by a plaque assay. (B and D) HFFs (B) or BSC40 cells (D) were fed replete medium, glutamine-free medium, or glucose-free medium. At 24 h posttreatment, cell counts were determined, and viability was measured by using trypan blue exclusion staining. ns, not significant.

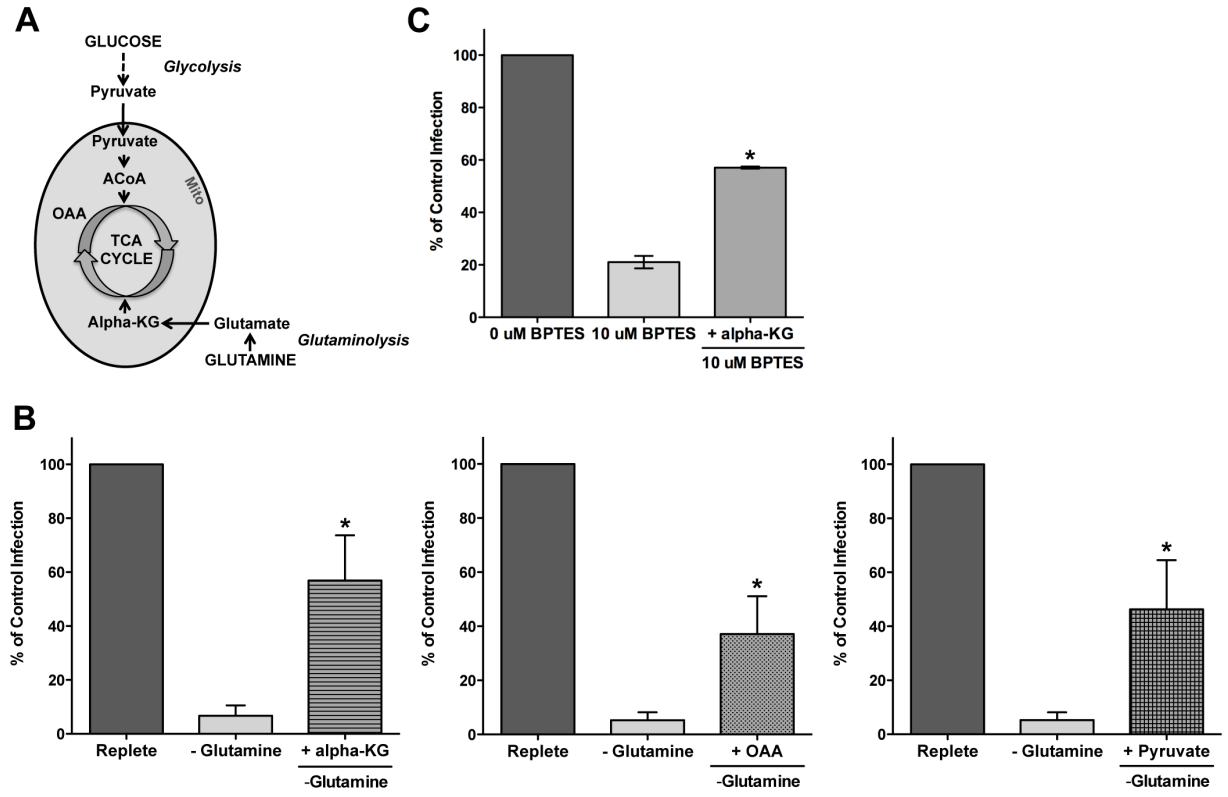

Figure 3-3. Glutamine is an essential anaplerotic substrate for the TCA cycle during VACV infection. (A) Simplified schematic of glucose and glutamine utilization. The dashed arrow represents multiple enzymatic reactions within the metabolic pathway. Abbreviations: alpha-KG, α-ketoglutarate; OAA, oxaloacetic acid; ACoA, acetyl coenzyme A. (B and C) HFFs were infected with VACV at an MOI of 5 and were fed replete medium, glutamine-free medium, or glutamine-free medium supplemented with 7 mM dimethyl-α-ketoglutarate, 4 mM oxaloacetic acid, or 4 mM pyruvate (B) or fed replete medium with 0 μM BPTES, 10 μM BPTES, or 10 μM BPTES and 7 mM dimethyl-α-ketoglutarate (C) at 1 hpi. Cell-associated virus was collected 24 hpi, and viral yields were determined by a plaque assay.

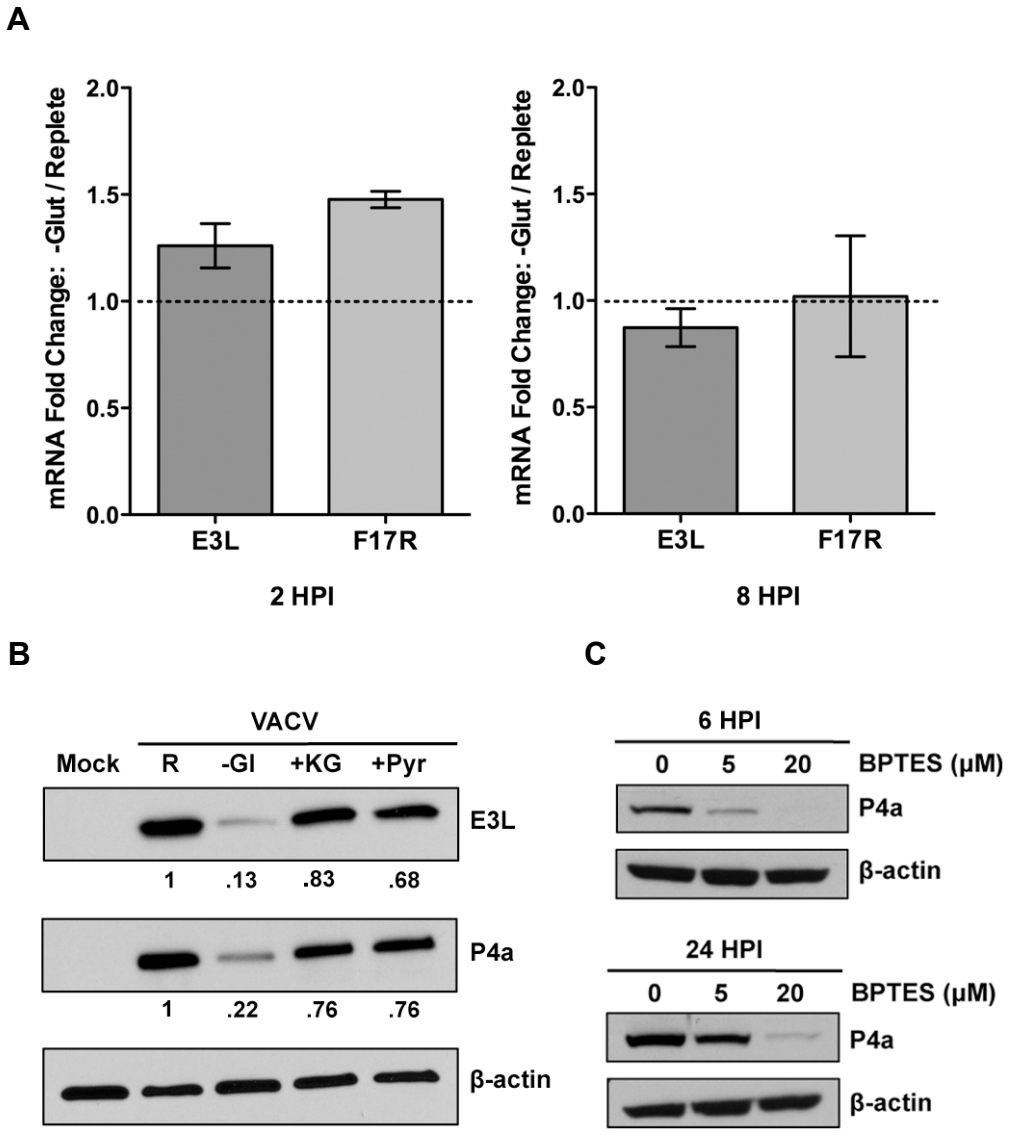

Figure 3-4. Glutamine is required to maintain the TCA cycle for VACV protein synthesis. (A) Quantitative real-time RT-PCR analysis of E3L and F17R transcript levels in VACV-infected cells supplemented with or without glutamine. HFFs were infected with VACV at an MOI of 5 and were fed replete medium or glutamine-free medium at 1 hpi. Viral mRNA expression was examined in cells harvested at 2 and 8 hpi. (B) Immunoblot analysis of E3L and P4a levels in VACV-infected cells fed replete medium (R), glutamine-free medium (-Gl), or glutamine-free medium supplemented with 7 mM dimethyl-α-ketoglutarate (KG) or 4 mM pyruvate (Pyr). Lysates from cells harvested at 24 hpi were subjected to Western blot analysis using antibodies against E3L, P4a, and the loading control β-actin. The values below the lanes indicate the relative intensity of each major band. (C) Immunoblot analysis of P4a levels in VACV-infected cells treated with increasing concentrations of BPTES. Cells were treated with 0, 5, or 20 μM BPTES at 1 hpi and harvested at 6 and 24 hpi for Western blot analysis.

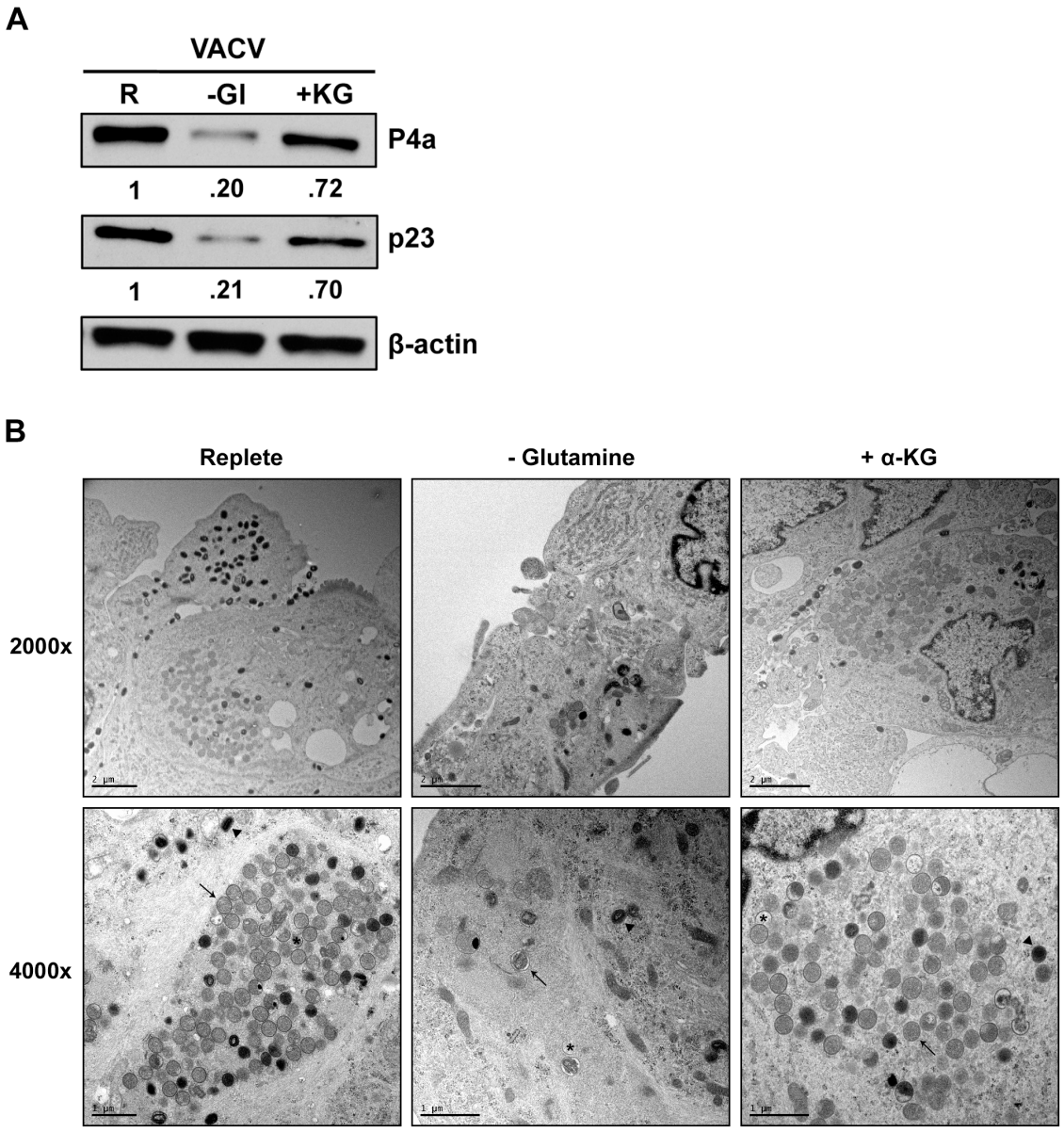

Figure 3-5. Glutamine deprivation results in reduced virion formation in VACV-infected cells. (A) Immunoblot analysis of P4a cleavage in VACV-infected cells fed replete medium, glutamine-free medium, or glutamine-free medium supplemented with 7 mM dimethyl-α-ketoglutarate. Lysates from cells harvested at 24 hpi were subjected to Western blot analysis using an antibody that recognizes both P4a and p23, a proteolytic product of P4a. The values below the lanes indicate the relative intensity of each major band. (B) Representative images of VACV morphogenesis in HFFs fed replete medium, glutamine-free medium, or glutamine-free medium supplemented with 7 mM dimethyl-α-ketoglutarate and processed for TEM at 24 hpi. Crescents (asterisks), immature virions (arrows), and mature virions (arrowheads) can be seen under all three conditions. The bottom left image was taken at a magnification of ×3000 to include the entire virus factory.

CHAPTER IV

Dengue Virus Induces and Requires Glycolysis for Optimal Replication

SUMMARY

Viruses rely on host cellular metabolism to provide the energy and biosynthetic building blocks required for their replication. Dengue virus (DENV), a member of the *Flaviviridae* family, is one of the most important arthropod-borne human pathogens worldwide. Here, we analyzed global intracellular metabolic changes associated with DENV infection of primary human cells. Our metabolic profiling data suggested that central carbon metabolism, particularly glycolysis, is strikingly altered during a time course of DENV infection. Glucose consumption is increased during DENV infection and depriving DENV-infected cells of exogenous glucose had a pronounced impact on replication. Furthermore, expression of both glucose transporter 1 (GLUT1) and hexokinase 2 (HK2), the first enzyme of glycolysis, are upregulated in DENV-infected cells. Pharmacologically inhibiting the glycolytic pathway dramatically reduced DENV RNA synthesis and infectious virion production, revealing a requirement for glycolysis during DENV infection. Thus, these experiments suggest that DENV induces the glycolytic pathway to support efficient viral replication. This study raises the possibility that metabolic inhibitors, such as those that target glycolysis, could be used to treat DENV infection in the future.

INTRODUCTION

Viruses are intracellular obligate parasites that depend on the metabolic machinery of the host cell to supply the energy and macromolecules necessary for successful replication. In recent years, research has focused on investigating how virus infection alters host metabolism with the hope that these studies will provide insight into the metabolic requirements of viral replication. Viral modulation of the host cell metabolic profile has been examined for several viruses, including human cytomegalovirus (HCMV), herpes simplex virus-1 (HSV-1), hepatitis C virus (HCV), influenza A virus (IAV), human immunodeficiency virus type 1 (HIV-1), Kaposi's sarcoma-associated herpesvirus (KSHV), vaccinia virus (VACV), and Epstein-Barr virus (4, 5, 7, 8, 10, 14, 23-25, 98, 117). These reports revealed that virus infection triggers dramatic changes in cellular metabolism, particularly in central carbon utilization pathways.

Glucose and glutamine represent the two main carbon sources used to support the energetic and biosynthetic needs of mammalian cells. In normal cells, the oxidation of glucose via glycolysis and the tricarboxylic acid (TCA) cycle is thought to be responsible for the bulk of ATP generation. However, in most cancer cells, glucose carbon is diverted away from the TCA cycle to be used biosynthetically and glutamine serves to anaplerotically replenish the TCA cycle (31-33). Extensive reprogramming of central carbon metabolism has also been observed during virus infection. For example, similar to tumor cells, HCMV-infected cells use glutamine to feed the TCA cycle so that glucose carbon can be utilized for fatty acid synthesis (5, 37). Alternatively, VACV implements a unique carbon utilization program where glutamine is essential for maximal viral replication by maintaining the TCA cycle, but glucose is completely dispensable for virus production (98, 118). These studies demonstrate that although viruses share

common metabolic requirements, they also induce distinct alterations in host cellular metabolism to complete their life cycles.

Dengue virus (DENV) is a positive-stranded RNA virus that belongs to the *Flaviviridae* family. DENV is transmitted to the human host via the *Aedes* genus mosquito vector and can cause several disease manifestations, ranging from dengue fever to the more severe dengue hemorrhagic fever and dengue shock syndrome. It is estimated that 390 million DENV infections occur annually worldwide (77), with approximately 2.5 billion people at risk of DENV transmission (76-79). There are currently no commercially available vaccines or specific antiviral therapies for DENV, making the virus a significant threat to global human health.

Previously, a multiplatform approach was developed to measure the levels of a limited number of extracellular metabolites following DENV infection of the human endothelial hybrid cell line EA.hy926 (22). However, a comprehensive examination of host cellular metabolism during DENV infection of human cells has yet to be conducted. To investigate alterations in the global metabolome following DENV infection, we performed intracellular metabolic profiling of mock- and DENV-infected primary human foreskin fibroblasts (HFFs) at multiple time points during the first 48 h of infection. Data from this analysis suggested that central carbon metabolism is significantly perturbed during DENV infection, particularly the glycolytic pathway of glucose utilization. We show that glycolysis is upregulated in DENV-infected cells and that inhibiting this metabolic pathway results in reduced DENV replication. Furthermore, the requirement for glycolysis to support production of infectious DENV is not a cell type specific phenomenon. Therefore, DENV infection activates the glycolytic pathway of glucose metabolism to promote efficient viral replication.

RESULTS

DENV infection alters glucose metabolism

To identify DENV-induced alterations in host cellular metabolism, we utilized an intracellular metabolic profiling approach. Primary cells were used for these experiments as transformed cells exhibit extensively altered metabolism and are therefore not ideal for investigating virus-induced metabolic alterations (reviewed in references (32, 102, 103)). Human foreskin fibroblasts (HFFs) were the most permissive primary cell type tested for DENV infection and thus were chosen for these studies. HFFs were serum starved approximately 16 h prior to infection to synchronize the cells in the G_0/G_1 phase. Cells were then mock or DENV infected at an MOI of 9 and harvested at 10, 24, and 48 h postinfection (hpi) for metabolic analysis. When infected at an MOI of 9 (determined as plaque-forming units (PFU)/ Vero cell), ~50% of HFFs expressed detectable levels of DENV envelope (E) glycoprotein by 24 hpi, as quantified by immunofluorescence. Each sample consisted of approximately 4×10^6 cells and samples from four independent experiments were analyzed using both gas chromatography-mass spectrometry (GC-MS) and liquid chromatography-tandem mass spectrometry (LC-MS/MS) platforms. Several major metabolic pathways were altered during DENV infection (Table 4-1), including those involved in glucose and glutamine utilization. Glycolysis was one of the most dramatically perturbed metabolic pathways following DENV infection. As shown in Figure 4-1A, the levels of all detected glycolytic metabolites were significantly altered in DENV-infected cells as compared to mock-infected cells during the first 48 h of infection. Levels of several intermediates of glycolysis were significantly increased early during DENV infection, whereas glycolytic metabolites were only measured at significantly decreased levels at the latest time point examined postinfection. Interestingly, we observed two main trends in metabolite levels

throughout the course of DENV infection. Early glycolytic intermediates, such as glucose 6-phosphate and fructose 6-phosphate, increased over time, whereas late glycolytic intermediates, including 3-phosphoglycerate and phosphoenolpyruvate, were initially higher at 10 hpi, but decreased over time (Figure 4-1B). It is important to note that elevated levels of a given intracellular metabolite may reflect either an increase in its production or a decrease in its consumption. Although an upregulation in glycolytic flux cannot be inferred from our global metabolomic screen, these data indicate that DENV infection modulates glucose utilization in HFFs.

In addition, we observed a considerable perturbation in glutamine metabolism during the course of DENV infection. Glutamine is catabolized via glutaminolysis, a pathway consisting of two deamination steps. Glutamine is first deaminated to glutamate and subsequently deaminated to the TCA cycle intermediate α-ketoglutarate. Figure 4-2 shows that both glutamine and glutamate levels were elevated in DENV-infected cells as compared to their mock-infected counterparts. Glutamine levels were significantly increased at 10 hpi, whereas glutamate levels were significantly elevated at all three time points examined. Taken together, these data reveal that DENV implements a distinct carbon utilization program during infection.

Exogenous glucose is required during DENV infection

Since our metabolomic screen identified DENV-induced perturbations in central carbon metabolism, we investigated the impact of both glucose and glutamine deprivation on DENV production. HFFs were infected with DENV at an MOI of 3 and subsequently fed replete medium containing both glucose and glutamine or medium lacking either glucose or glutamine. At 24 hpi, the release of infectious extracellular virus was quantified by focus-forming unit

reduction assays. As shown in Figure 4-3, depriving DENV-infected cells of exogenous glucose reduced the production of infectious virus by greater than 2 logs. We have previously shown that 24 h of glucose or glutamine starvation only has a modest impact on HFF proliferation and no significant impact on cell viability (98). Furthermore, depriving HFFs of exogenous glucose does not inhibit vaccinia virus (VACV) replication, thus indicating that the block in DENV production was not due to the effects of glucose deprivation on cellular integrity. Interestingly, depriving DENV-infected cells of exogenous glutamine, the other primary carbon source for mammalian cells, only reduced infectious virus production by approximately 60% (Figure 4-3). These results indicate that DENV demonstrates a selective dependence on exogenous glucose during infection.

Glycolysis is activated during DENV infection

The metabolomic data shows that the glycolytic pathway of glucose metabolism is perturbed in DENV-infected cells and we found that DENV requires exogenous glucose for optimal replication. To determine if DENV activates glycolysis, we first examined glucose consumption following DENV infection. HFFs were mock or DENV infected at an MOI of 9 and uptake of the radiolabeled glucose analog [^{3}H]2-deoxy-D-glucose was measured at 24 hpi. As seen in Figure 4-4A, DENV-infected cells exhibited a subtle, but statistically significant, increase in glucose uptake as compared to their mock-infected counterparts. Importantly, an approximate 50% infection rate was achieved in these experiments. Therefore, the population of uninfected cells in the culture masked the full impact DENV infection has on glucose consumption.

Exogenous glucose uptake into mammalian cells is mediated by a family of at least 14 isoforms of facilitative transporter membrane proteins known as the glucose transporters

(GLUTs). GLUT1 is ubiquitously expressed in many different cell types of various tissues and is responsible for basal glucose transport (reviewed in reference (119)). To determine if the increase in glucose consumption observed in DENV-infected cells is due to upregulation of GLUT expression, we measured GLUT1 protein levels via Western blot analysis. Because GLUT1 expression is enhanced by hypoxia, we treated mock- and DENV-infected cells with deferoxamine mesylate (DFO), a hypoxia-mimetic agent, to better visualize the relative levels of GLUT1. HFFs were mock or DENV infected at an MOI of 9 and cytoplasmic extracts were harvested from normoxic and DFO-treated cells at 24 hpi. As shown in Figure 4-4B, GLUT1 protein levels were elevated in DENV-infected cells, with the greatest increase in GLUT1 expression detected under conditions of DFO treatment. These results suggest that GLUT1 induction is likely responsible, at least in part, for enhanced glucose consumption during DENV infection.

To further examine if DENV activates glycolysis, we also measured hexokinase expression in mock- and DENV-infected cells. Hexokinase is the first rate-limiting enzyme of the glycolytic pathway and the hexokinase 2 (HK2) isoform, in particular, has been shown to be a key mediator of aerobic glycolysis (96, 120). We utilized quantitative real-time RT-PCR to measure HK2 mRNA levels during DENV infection. HFFs were mock and DENV infected at an MOI of 5 and total RNA was isolated from cells harvested at 24 hpi. Figure 4-4C shows that HK2 expression was significantly elevated in DENV-infected cells compared to mock-infected cells. Levels of the three isoforms of phosphofructokinase-1 (PFK), the second rate-limiting enzyme of glycolysis, were not significantly increased during DENV infection (data not shown). We next confirmed HK2 upregulation via Western blot analysis. As HK2 levels are low in normal cells, we again utilized DFO to enhance HK2 protein expression for comparison between

mock- and DENV-infected cells at 24 hpi. Figure 4-4D shows that HK2 protein levels were increased in DENV-infected cells, which similar to GLUT1 levels, were enhanced following DFO treatment. Again, the detected increases in GLUT1 and HK2 protein expression are diminished by the lower infection rates obtained with DENV infection of HFFs. Combined with the metabolic profiling data, these results reveal that glycolysis is induced during DENV infection.

Glycolysis is required for optimal infectious DENV production

Because glycolysis is activated during DENV infection and exogenous glucose is essential for virion production, we hypothesized that glycolysis is necessary for efficient DENV replication. Thus, we next examined infectious DENV production following treatment with oxamate, a glycolytic inhibitor. Oxamate is a pyruvate analog that specifically inhibits lactate dehydrogenase (LDH), the enzyme that catalyzes the conversion of pyruvate to lactate (121-123). Figure 4-5A shows that DENV-infected HFFs treated with increasing concentrations of oxamate exhibited a dose-dependent decrease in release of extracellular infectious virus. Moreover, viral RNA levels were similarly reduced following oxamate treatment (Figure 4-5B), indicating that the glycolytic pathway is required at an early stage in the DENV life cycle. To determine if glycolysis is necessary for DENV replication in cell types other than HFFs, we measured the impact of glycolytic inhibition on infectious DENV production in tert-immortalized microvascular endothelial (TIME) cells. While immortal, this cell line has been shown to exhibit metabolism similar to primary endothelial cells (8, 34). DENV-infected endothelial cells have been found in dengue patients and murine models of DENV disease and may contribute to DENV pathogenesis (124-131). Infected TIME cells treated with 100 mM oxamate also showed

a block in infectious DENV production (Figure 4-5C), revealing that the requirement for glycolysis is not HFF specific. Together, these data indicate that glycolysis is a critical metabolic pathway for optimal DENV replication.

DISCUSSION

Viruses require host cellular metabolism to provide the energy and molecular building blocks needed for successful viral replication. In this study, we utilized a metabolomic approach to identify intracellular metabolic alterations that occur during a time course of DENV infection. Among other changes, this screen detected striking DENV-induced perturbations in glucose and glutamine utilization. Dynamic changes in the levels of numerous glycolytic intermediates are observed throughout the first 48 h of DENV infection. As elevated metabolite concentrations may reflect either an increase in the production of intermediates or a decrease in their consumption, we sought to determine if glucose metabolism is required during DENV infection. In support of our metabolomic data, we show that infectious DENV production is drastically decreased when DENV-infected cells are deprived of exogenous glucose. Furthermore, depriving DENV-infected cells of exogenous glutamine only has a modest impact on viral yield, though this effect is statistically significant. We previously found that glutamine metabolism is considerably altered during vaccinia virus (VACV) infection of HFFs and is necessary to anaplerotically replenish the TCA cycle (98). Interestingly, the changes in glutamine and glutamate levels throughout the course of infection are similar between VACV-infected cells and DENV-infected cells, raising the possibility that glutamine also serves as an anaplerotic substrate for the TCA cycle during DENV infection. However, glutamine is consumed in multiple metabolic pathways, such as providing the nitrogen for nucleotide biosynthesis. The observed

block in DENV production under conditions of glutamine-deprivation could also be due to the requirement for increased intracellular nucleotide pools during DENV replication. Consistent with this notion, levels of several biochemicals involved in purine and pyrimidine metabolism are significantly elevated in DENV-infected cells (see Table 4-1). Therefore, it may be that DENV requires glutamine as both a carbon source and nitrogen source to support its replicative needs. Metabolic carbon and nitrogen flux analysis is warranted to gain further insight into global glucose and glutamine usage during DENV infection. However, the results presented here reveal that glucose is the more critical carbon source for DENV replication.

Data from our metabolic screen suggest that the glycolytic pathway of glucose utilization is specifically altered during DENV infection. As our laboratory and others have previously described, many human viruses activate glycolysis (4, 7, 10, 23, 34, 36). Moreover, inhibition of the glycolytic pathway has been shown to restrict HCMV and HSV-1 replication and induce apoptosis in cells latently infected with KSHV (34, 36, 107, 108). Here, we report the activation of glycolysis by DENV infection. We show that GLUT1 and HK2 expression are upregulated in DENV-infected cells, with a concurrent increase in glucose uptake. Several viruses have been found to upregulate the expression and/or activity of GLUT1 and HK2 (13, 34, 117, 132, 133), thus revealing common strategies viruses use to reprogram carbon metabolism.

Our data further implicates a broad role for the glycolytic pathway during virus infection. Accordingly, we found that inhibiting the glycolytic pathway via oxamate treatment resulted in a significant reduction in DENV RNA levels and infectious virion production. While the requirement for increased glycolysis during DENV infection is clear, how glycolysis is utilized for viral replication remains to be determined. HCMV induces enhanced flux through the glycolytic pathway to direct glucose carbon toward the TCA cycle and away from the

mitochondrion in the form of citrate to fuel fatty acid synthesis (FAS) (5, 7). DENV may also activate glycolysis to support lipid biogenesis. DENV infection upregulates FAS (18), and inhibiting fatty acid synthase (FASN), a major enzyme in the metabolic pathway, significantly impairs DENV replication in both human (18, 134) and mosquito cells (21). Furthermore, FASN is relocalized to sites of viral replication by the DENV nonstructural protein 3 (NS3) (18). Thus, it has been proposed that DENV modulates fatty acid metabolism to generate the lipid material needed for DENV replication complex (RC) formation (18), as these structures are assembled on invaginated cytoplasmic membranes (17, 135). Therefore, DENV might induce glycolysis to ultimately promote the establishment of DENV RCs. However, fatty acids also play a role in other processes during DENV infection, including ATP synthesis (136). Autophagy-dependent processing of lipid droplets in DENV-infected cells releases free fatty acids, which undergo β-oxidation to produce ATP. Importantly, these processes are necessary for optimal DENV replication (136). Hence, lipid metabolism may be required at multiple stages during the DENV life cycle. Although enhanced glycolytic flux has been connected to increased fatty acid synthesis during virus infection, we cannot exclude the possibility that DENV requires the activation of glycolysis to directly support other replicative needs, such as generating ATP and NADH. Metabolic carbon flux analysis will provide further insight into global glucose usage during DENV infection.

This study and others have identified glycolysis as an essential metabolic pathway for the life cycle of several important human viruses. Pharmacological inhibitors of the glycolytic pathway show promising anticancer activity since a wide variety of human cancers exhibit increased aerobic glycolysis (reviewed in references (105, 137-139)). As several of these glycolytic inhibitors are currently in preclinical and clinical development, it is intriguing to

consider the possibility that these compounds may also be used as novel broad-spectrum antiviral therapies.

ACKNOWLEGEMENTS

The authors would like to thank Dr. Sharon Isern and Dr. Scott Michael (Florida Gulf Coast University) for reagents and helpful discussions and Dr. Michael Gale, Jr. (University of Washington) for reagents.

M.L was supported by grants from the NIAID, the NCI, and NIDCR of the NIH under award numbers U54AI081680, RO1CA097934, and PO1DE021954. K.A.F was supported in part by PHS NRSA T32 GM07270 from NIGMS. The content is solely the responsibility of the authors and does not necessarily represent the official views of the National Institutes of Health.

Table 4-1. DENV infection alters global host cellular metabolism.

Super Pathway	Sub Pathway	Biochemical Name	10 HPI	24 HPI	48 HPI
Amino acid	Glycine, serine and threonine metabolism	glycine	**1.53**	1.26	0.99
		serine	**1.39**	1.11	**0.54**
		N-acetylserine	1.32	1.11	1.08
		3-phosphoserine	0.75	**0.16**	**0.06**
		threonine	1.19	1.17	0.91
	Alanine and aspartate metabolism	aspartate	**1.76**	1.41	1.02
		asparagine	**1.43**	1.25	**0.63**
		beta-alanine	**2.03**	1.28	1.23
		alanine	**1.29**	1.14	**0.61**
	Glutamate metabolism	glutamate	**1.5**	**1.48**	**1.61**
		glutamine	**1.98**	1.2	1.7
		pyroglutamine*	1.22	1.25	**1.32**
		gamma-aminobutyrate (GABA)	1.25	0.55	1.08
		N-acetylglutamate	1.05	1.07	1.13
	Histidine metabolism	histidine	**1.46**	**1.41**	**0.81**
	Lysine metabolism	lysine	**1.37**	1.19	**0.62**
		2-aminoadipate	1.07	0.58	**0.35**
	Phenylalanine and tyrosine metabolism	phenylalanine	**1.32**	1.13	**0.74**
		tyrosine	**1.23**	1.1	**0.72**
		phenylacetylglycine	1.34	1.2	1.03
	Tryptophan metabolism	kynurenine	2.01	**100.96**	**48.74**
		tryptophan	1.28	**0.06**	**0.16**
		C-glycosyltryptophan*	**1.41**	1.19	**0.68**
	Valine, leucine and isoleucine metabolism	isoleucine	**1.33**	1.13	**0.87**
		leucine	**1.35**	1.14	**0.71**
		valine	**1.26**	**1.14**	**0.72**
	Cysteine, methionine, SAM and taurine metabolism	cysteine	0.93	0.93	0.76
		cystathionine	**1.95**	1.19	1.7
		hypotaurine	1.12	0.76	0.67
		S-adenosylhomocysteine (SAH)	**1.46**	**1.72**	**1.5**
		methionine	**1.31**	1.14	**0.67**
		N-acetylmethionine	1.2	1.09	**0.54**
		homocysteine	1.96	1.79	1.18
	Urea cycle; arginine and proline metabolism	dimethylarginine (SDMA + ADMA)	0.92	0.91	**0.18**
		arginine	1.24	1.22	**0.63**
		ornithine	1.12	0.96	0.97
		urea	1.06	1.27	**1.34**
		proline	**1.26**	1.16	**0.72**
	Creatine metabolism	creatine	1.55	0.93	0.73
	Polyamine metabolism	spermidine	1.45	1.4	**2.34**
	Glutathione metabolism	glutathione, reduced (GSH)	1.71	0.87	1.05

Heat map of fold change levels of biochemicals profiled in this study. For paired comparisons, shaded cells with white-bolded values indicate $p \leq 0.05$ (red indicates that the mean values are significantly higher in DENV-infected cells for that comparison and green indicates that the values are significantly lower). Red- and green-bolded values indicate $0.05 < p < 0.1$ (red indicates that the mean values trend higher in DENV-infected cells and green indicates that the values trend lower).

Table 4-1. DENV infection alters global host cellular metabolism. (continued)

		5-oxoproline	1.15	1.05	0.96
		glutathione, oxidized (GSSG)	1.29	0.82	1.28
		cysteine-glutathione disulfide	1.12	1.4	1.25
Peptide	Dipeptide	glycylglycine	1.27	1.06	0.43
		glycylproline	0.88	1.11	0.57
		glycylleucine	1.35	0.77	0.47
		pro-hydroxy-pro	1.49	1.17	0.5
		aspartylleucine	1.41	1.07	0.86
		isoleucylglycine	1.56	1.08	0.71
		leucylglutamate	0.81	1.17	1.34
		leucylglycine	1.05	1.17	2.2
	Gamma-glutamyl	gamma-glutamylglutamate	2.89	2.6	2.52
		gamma-glutamylglutamine	2.6	2.52	1.8
Carb	Aminosugars metabolism	N-acetylglucosamine 6-phosphate	1.58	0.92	0.37
		erythronate*	1.62	1.83	2.02
	Sugar metabolism	fructose	1.67	1.47	0.94
		mannose 6-phosphate	0.86	3.04	5.23
		sorbitol	1.89	2.18	1.89
		maltotriose	0.66	0.96	1.77
	Oligosaccharide	maltotetraose	0.56	0.73	1.45
	Glycolysis, gluconeogenesis and pyruvate metabolism	glycerate	1.74	1.22	0.36
		glucose 6-phosphate (G6P)	0.49	3.94	8.23
		glucose	0.49	0.6	0.58
		fructose 6-phosphate	0.74	4.12	5.97
		fructose 1-phosphate	3.31	3.61	1.5
		Isobar: fructose 1,6-diphosphate, glucose 1,6-diphosphate, myo-inositol 1,4 or 1,3-diphosphate	8.81	4.13	0.99
		2-phosphoglycerate	1.86	1.2	0.41
		3-phosphoglycerate	1.9	0.98	0.31
		dihydroxyacetone phosphate (DHAP)	3.97	2.25	2.96
		phosphoenolpyruvate (PEP)	1.75	1.11	0.28
		lactate	1.78	1.11	0.9
	Nucleotide sugars, pentose metabolism	6-phosphogluconate	1.88	1.97	1.77
		sedoheptulose 7-phosphate	2.33	1.17	1.67
		ribose	1.65	1.61	1.11
		ribose 5-phosphate	3.33	1.25	1.18
		ribulose	2.11	1.83	0.9
		Isobar: ribulose 5-phosphate, xylulose 5-phosphate	2.45	1.49	1.67
Energy	Krebs cycle	citrate	1.15	1.23	1.9
		fumarate	1.22	1.51	0.87
		malate	1.14	1.27	0.93
	Oxidative phosphorylation	phosphate	1.12	1.3	1.43
		pyrophosphate (PPi)	1.75	1.19	0.93

Heat map of fold change levels of biochemicals profiled in this study. For paired comparisons, red and green shaded cells with white-bolded values indicate $p \leq 0.05$ (red indicates that the mean values are significantly higher in DENV-infected cells for that comparison and green indicates that the values are significantly lower). Red- and green-bolded values indicate $0.05 < p < 0.1$ (red indicates that the mean values trend higher in DENV-infected cells and green indicates that the values trend lower).

Table 4-1. DENV infection alters global host cellular metabolism. (continued)

Lipid	Essential fatty acid	linoleate (18:2n6)	1.14	1.16	0.99
		linolenate [alpha or gamma; (18:3n3 or 6)]	0.96	1.02	1.01
		dihomo-linolenate (20:3n3 or n6)	1.44	1.58	1.19
		eicosapentaenoate (EPA; 20:5n3)	**1.34**	**1.26**	**1.27**
		docosapentaenoate (n3 DPA; 22:5n3)	**1.39**	1.33	1.14
		docosapentaenoate (n6 DPA; 22:5n6)	1.14	1.41	0.95
		docosahexaenoate (DHA; 22:6n3)	1.28	**1.4**	1.19
	Medium chain fatty acid	pelargonate (9:0)	0.99	1.16	1.17
		caprate (10:0)	1.18	**1.31**	1.19
		laurate (12:0)	1.05	1.2	**1.32**
	Long chain fatty acid	myristate (14:0)	1.09	1.07	**1.2**
		myristoleate (14:1n5)	0.81	0.89	1.05
		pentadecanoate (15:0)	1.05	1.29	**1.33**
		palmitoleate (16:1n7)	0.98	0.99	0.87
		margarate (17:0)	**1.23**	**1.41**	**1.62**
		10-heptadecenoate (17:1n7)	1.19	1.23	1.16
		oleate (18:1n9)	1.24	**1.26**	1.14
		cis-vaccenate (18:1n7)	1.15	1.27	1.1
		nonadecanoate (19:0)	1.16	**1.43**	**1.36**
		10-nonadecenoate (19:1n9)	**1.33**	1.27	1.33
		eicosenoate (20:1n9 or 11)	1.05	1.25	1
		dihomo-linoleate (20:2n6)	1.11	1.1	1.2
		mead acid (20:3n9)	0.74	0.8	**0.56**
		arachidonate (20:4n6)	1.35	1.44	0.86
		docosadienoate (22:2n6)	1.03	1.12	1.19
		docosatrienoate (22:3n3)	0.9	0.79	0.76
		adrenate (22:4n6)	1.3	1.39	**2.06**
	Fatty acid, monohydroxy	2-hydroxystearate	**1.59**	0.74	**0.33**
		2-hydroxypalmitate	**1.43**	0.67	**0.26**
		13-HODE + 9-HODE	1.2	1.14	1.34
	Fatty acid, branched	17-methylstearate	1.27	**1.75**	**0.49**
	Eicosanoid	prostaglandin A2	1.81	1.57	**2.58**
		prostaglandin B2	0.96	**2.41**	**3.29**
		prostaglandin E1	1.16	1.6	**4.22**
		prostaglandin E2	1.5	**2.05**	**3.63**
		6-keto prostaglandin F1alpha	**1.87**	1.56	**0.38**
	Carnitine metabolism	acetylcarnitine	1.22	0.99	**0.44**
	Glycerolipid metabolism	choline phosphate	1.5	1.32	1.12
		ethanolamine	1.4	1.5	**1.65**
		phosphoethanolamine	1.61	**2.27**	**2.15**
		choline	**1.57**	**1.61**	**1.94**
		glycerol 3-phosphate (G3P)	**3.22**	0.95	0.61

Heat map of fold change levels of biochemicals profiled in this study. For paired comparisons, red and green shaded cells with white-bolded values indicate $p \leq 0.05$ (red indicates that the mean values are significantly higher in DENV-infected cells for that comparison and green indicates that the values are significantly lower). Red- and green-bolded values indicate $0.05 < p < 0.1$ (red indicates that the mean values trend higher in DENV-infected cells and green indicates that the values trend lower).

Table 4-1. DENV infection alters global host cellular metabolism. (continued)

		glycerophosphorylcholine (GPC)	0.78	1.23	**2.02**
	Inositol metabolism	myo-inositol	2	1.38	0.39
		inositol 1-phosphate (I1P)	1.04	1.22	**1.38**
		scyllo-inositol	2.65	1.64	0.54
	Lysolipid	1-palmitoylglycerophosphoethanolamine	1.27	1.08	1.03
		2-palmitoylglycerophosphoethanolamine*	1.11	0.74	**0.16**
		1-stearoylglycerophosphoethanolamine	1.11	1.33	1.44
		1-oleoylglycerophosphoethanolamine	1.1	1.21	1.32
		2-oleoylglycerophosphoethanolamine*	1.34	1.11	0.93
		1-arachidonoylglycerophosphoethanolamine*	**1.58**	1.33	1.16
		2-arachidonoylglycerophosphoethanolamine*	**1.74**	1.41	1.09
		2-docosapentaenoylglycerophosphoethanolamine*	1.2	0.68	**0.08**
		2-docosahexaenoylglycerophosphoethanolamine*	1.43	0.81	**0.11**
		1-palmitoylglycerophosphocholine	1.18	0.63	**0.18**
		2-palmitoylglycerophosphocholine*	1.15	0.73	**0.09**
		1-palmitoleoylglycerophosphocholine*	0.96	0.66	**0.27**
		2-palmitoleoylglycerophosphocholine*	1.01	0.69	**0.33**
		1-stearoylglycerophosphocholine	1.33	0.67	**0.18**
		1-oleoylglycerophosphocholine	1.01	0.68	**0.19**
		2-oleoylglycerophosphocholine*	1.15	0.46	**0.12**
		2-arachidonoylglycerophosphocholine*	1.2	0.79	**0.3**
		1-palmitoylglycerophosphoinositol*	0.65	1.32	0.8
		1-stearoylglycerophosphoinositol	0.76	1.51	1.09
		1-oleoylglycerophosphoinositol*	0.71	1.49	0.74
		1-arachidonoylglycerophosphoinositol*	**1.57**	1.31	**0.61**
		2-oleoylglycerophosphoinositol*	0.83	1.06	0.61
		1-oleoylglycerophosphoserine	1.15	1.2	0.88
		1-palmitoylplasmenylethanolamine*	1.38	1.54	**1.9**
	Monoacylglycerol	1-stearoylglycerol (1-monostearin)	0.98	1.26	1.21
	Sphingolipid	sphinganine	1.06	1.16	0.47
		sphingosine	0.93	0.7	**0.19**
		palmitoyl sphingomyelin	1.04	**1.35**	1.24
		stearoyl sphingomyelin	0.96	0.82	1.35
	Sterol/steroid	lathosterol	**0.51**	1.25	1.47
		cholesterol	1.15	**1.29**	**1.41**
		7-dehydrocholesterol	1.14	0.85	0.98
		7-alpha-hydroxycholesterol	1.65	0.56	1.03
		7-beta-hydroxycholesterol	1.14	0.95	1.04
Nucleotide	Purine (hypox)anthine/inosine metabolism	xanthine	1.33	**1.38**	**1.8**
		hypoxanthine	**1.3**	**1.32**	1.1
		inosine	**1.72**	1.31	0.75
	Purine metabolism,	adenine	**3.21**	1.67	**2.48**

Heat map of fold change levels of biochemicals profiled in this study. For paired comparisons, red and green shaded cells with white-bolded values indicate $p \leq 0.05$ (red indicates that the mean values are significantly higher in DENV-infected cells for that comparison and green indicates that the values are significantly lower). Red- and green-bolded values indicate $0.05 < p < 0.1$ (red indicates that the mean values trend higher in DENV-infected cells and green indicates that the values trend lower).

Table 4-1. DENV infection alters global host cellular metabolism. (continued)

	adenine	adenosine	0.81	1.56	**4.8**
		adenosine 2'-monophosphate (2'-AMP)	**1.33**	**1.33**	0.93
		adenosine 5'-monophosphate (AMP)	**1.58**	1.25	0.56
		adenosine 5'-diphosphate (ADP)	**1.31**	**1.29**	0.85
	Purine metabolism, guanine containing	guanine	**1.31**	**1.27**	1.02
		guanosine	**1.96**	1.46	0.88
	Pyrimidine, cytidine	cytidine 5'-monophosphate (5'-CMP)	**1.51**	**1.78**	**1.35**
	Pyrimidine, thymine	thymine	0.66	0.83	**3.5**
	Pyrimidine metabolism, uracil containing	uracil	1.25	1.02	0.77
		uridine	**1.76**	1.29	1.01
	Purine/pyrimidine	methylphosphate	1.01	**1.34**	1.15
Cofactors & vitamins	Nicotinate and nicotinamide metabolism	nicotinamide	1.01	**1.7**	**1.53**
		nicotinamide adenine dinucleotide (NAD+)	**2.65**	**0.14**	**0.03**
		nicotinamide riboside*	**2**	0.6	**0.21**
		1-methylnicotinamide	**2.2**	1.56	1.66
	Pantothenate and CoA	pantothenate	**1.87**	**1.49**	**2.19**
	Riboflavin metabolism	riboflavin (Vitamin B2)	1.13	0.79	0.95
	Tocopherol metabolism	alpha-tocopherol	1.97	0.93	1.13
	Vitamin B6 metabolism	pyridoxine (Vitamin B6)	1.09	1.07	1.06
Xenobios	Chemical	glycerol 2-phosphate	**2.5**	1.52	1.24
		phenol red	0.83	1.02	0.96
	Drug	penicillin G	0.85	0.92	0.84
		streptomycin	0.75	1.15	**1.54**
	Sugar/sugar substitute	erythritol	1.59	1.45	1.4

Heat map of fold change levels of biochemicals profiled in this study. For paired comparisons, red and green shaded cells with white-bolded values indicate $p \leq 0.05$ (red indicates that the mean values are significantly higher in DENV-infected cells for that comparison and green indicates that the values are significantly lower). Red- and green-bolded values indicate $0.05 < p < 0.1$ (red indicates that the mean values trend higher in DENV-infected cells and green indicates that the values trend lower).

A

Glycolytic Intermediate	10 HPI	24 HPI	48 HPI
Glucose 6-phosphate	0.49	3.94	8.23
Fructose 6-phosphate	0.74	4.12	5.97
Dihydroxyacetone phosphate	3.97	*2.25*	2.96
3-Phosphoglycerate	1.9	0.98	0.31
2-Phosphoglycerate	1.86	1.2	0.41
Phosphoenolpyruvate	*1.75*	1.11	0.28
Lactate	1.78	1.11	0.9

B

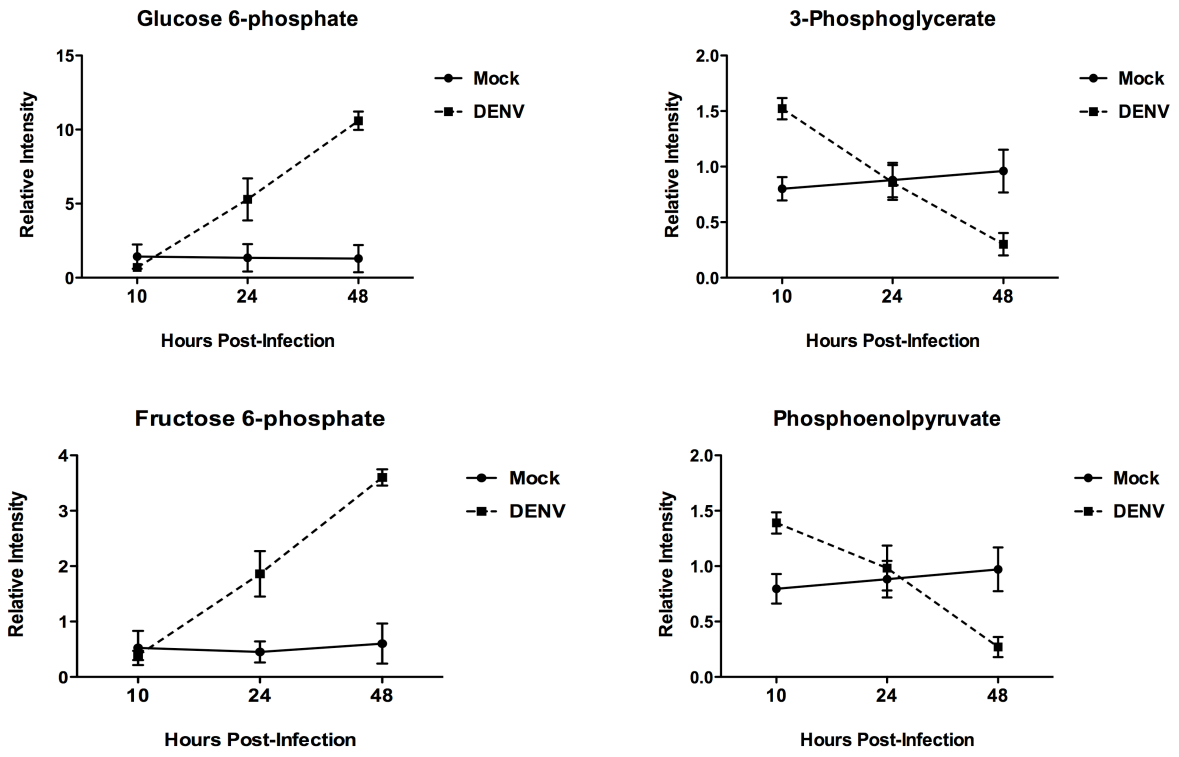

Figure 4-1. The glycolytic pathway of glucose metabolism is altered during DENV infection HFFs were mock or DENV infected (MOI of 9) and harvested at 10, 24, and 48 hpi for intracellular metabolic analysis by Metabolon. (A) Heat map of fold change levels of glycolytic intermediates profiled during a time course of DENV infection. For paired comparisons, shaded cells indicate $p \leq 0.05$ (dark gray indicates that the mean values are significantly higher in DENV-infected cells for that comparison and light gray indicates that the values are significantly lower). Italicized values indicate $0.1 < p < 0.05$. (B) Line plots of selected glycolytic intermediates in mock- and DENV-infected cells measured at the indicated time points.

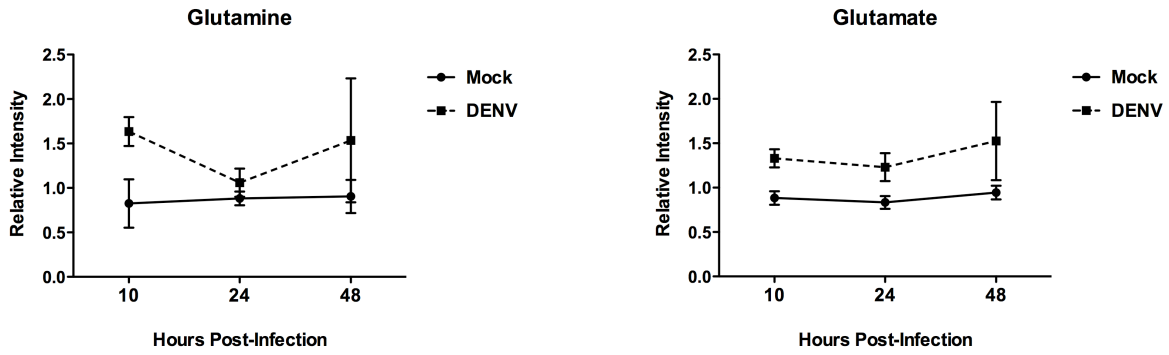

Figure 4-2. Glutamine metabolism is perturbed in DENV-infected cells. Line plots of glutamine and glutamate levels in mock- and DENV-infected cells measured at 10, 24, and 48 hpi. Cells were harvested at the indicated time points, and Metabolon performed global metabolic analysis of the samples.

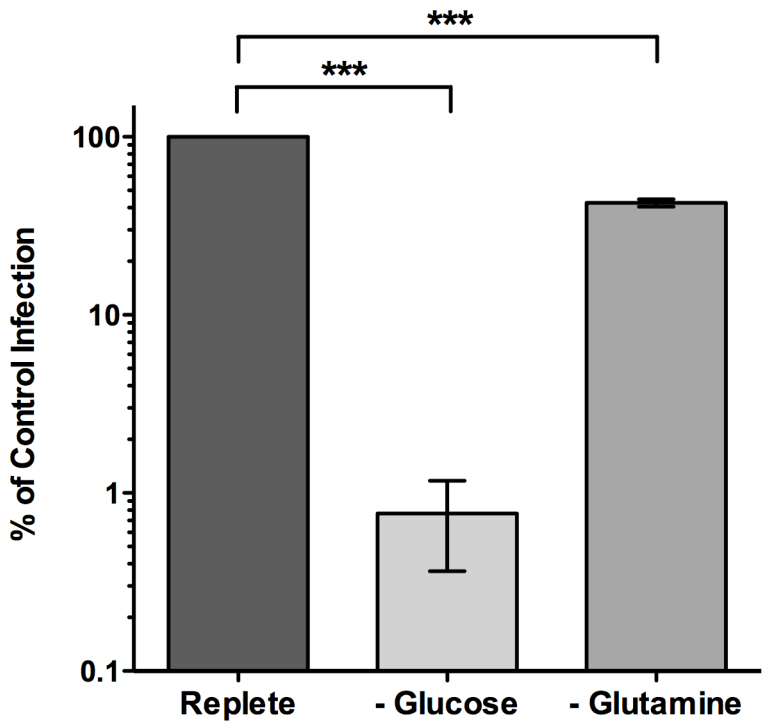

Figure 4-3. Exogenous glucose is necessary for optimal infectious DENV production. HFFs were infected with DENV at an MOI of 3 and were fed replete medium, glucose-free medium, or glutamine-free medium at 2 hpi. Released infectious virus was harvested at 24 hpi and quantified by focus-forming unit reduction assays in Vero cells.

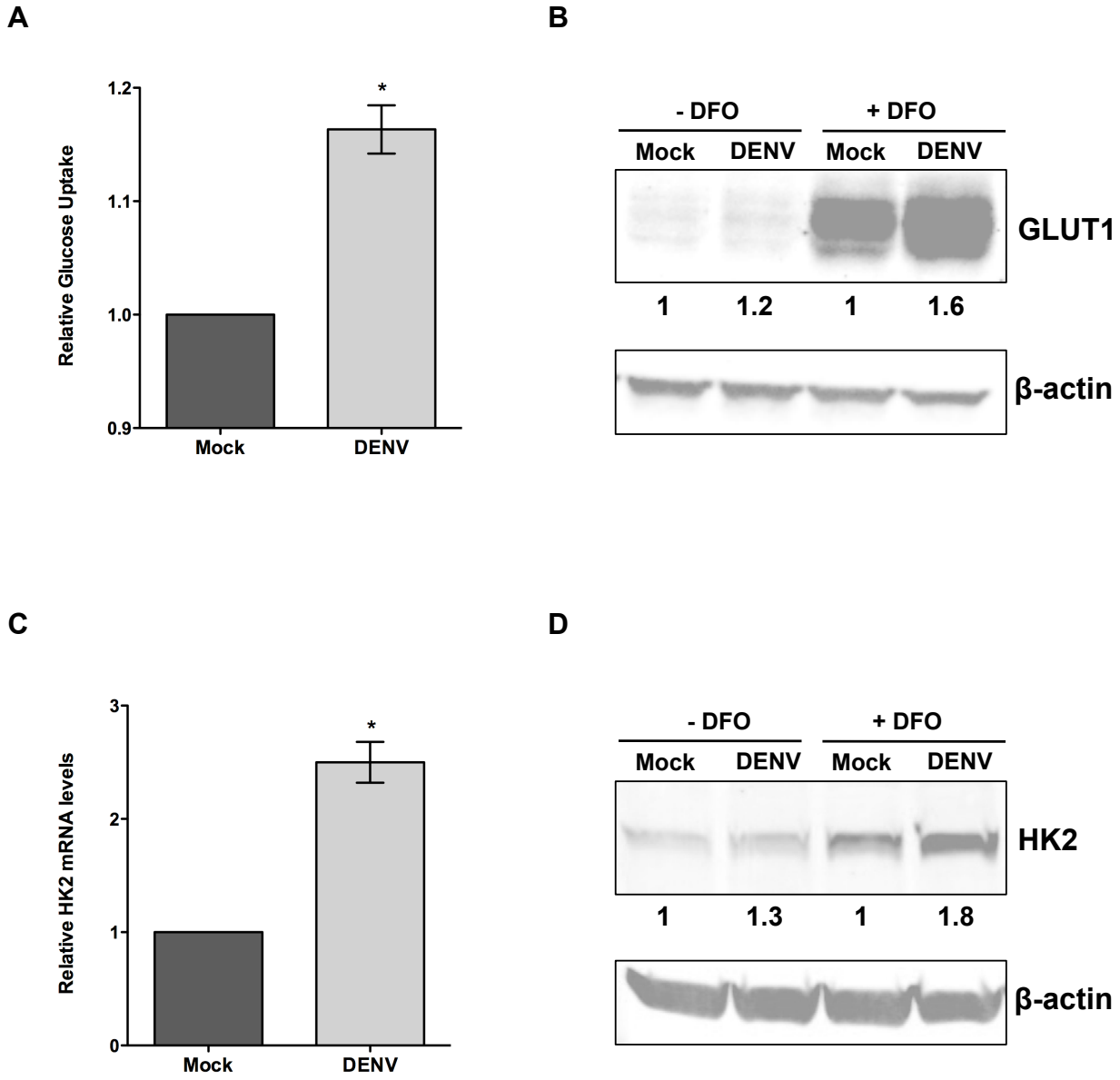

Figure 4-4. Glycolysis is induced during DENV infection. (A) Glucose uptake is increased during DENV infection. Twenty-four hours postinfection, mock- and DENV-infected (MOI of 9) HFFs were exposed to a radiolabeled glucose analog for 5 min followed by intracellular quantification of radioactivity. (B, C, and D) Expression levels of GLUT1 and HK2 are elevated in DENV-infected cells. HFFs were mock or DENV infected (MOI of 9) and were treated with 0 μM DFO or 150 μM DFO at 2 hpi. Cell lysates harvested at 24 hpi were subjected to immunoblot analysis using the indicated antibodies. The values below the lanes indicate the relative intensity of each major band, with β-actin serving as a loading control. (C) Quantitative real-time RT-PCR analysis of HK2 transcript levels in mock- and DENV-infected cells (MOI of 5) harvested at 24 hpi. Relative abundance of HK2 mRNA was normalized by the delta threshold cycle method to the abundance of GAPDH mRNA.

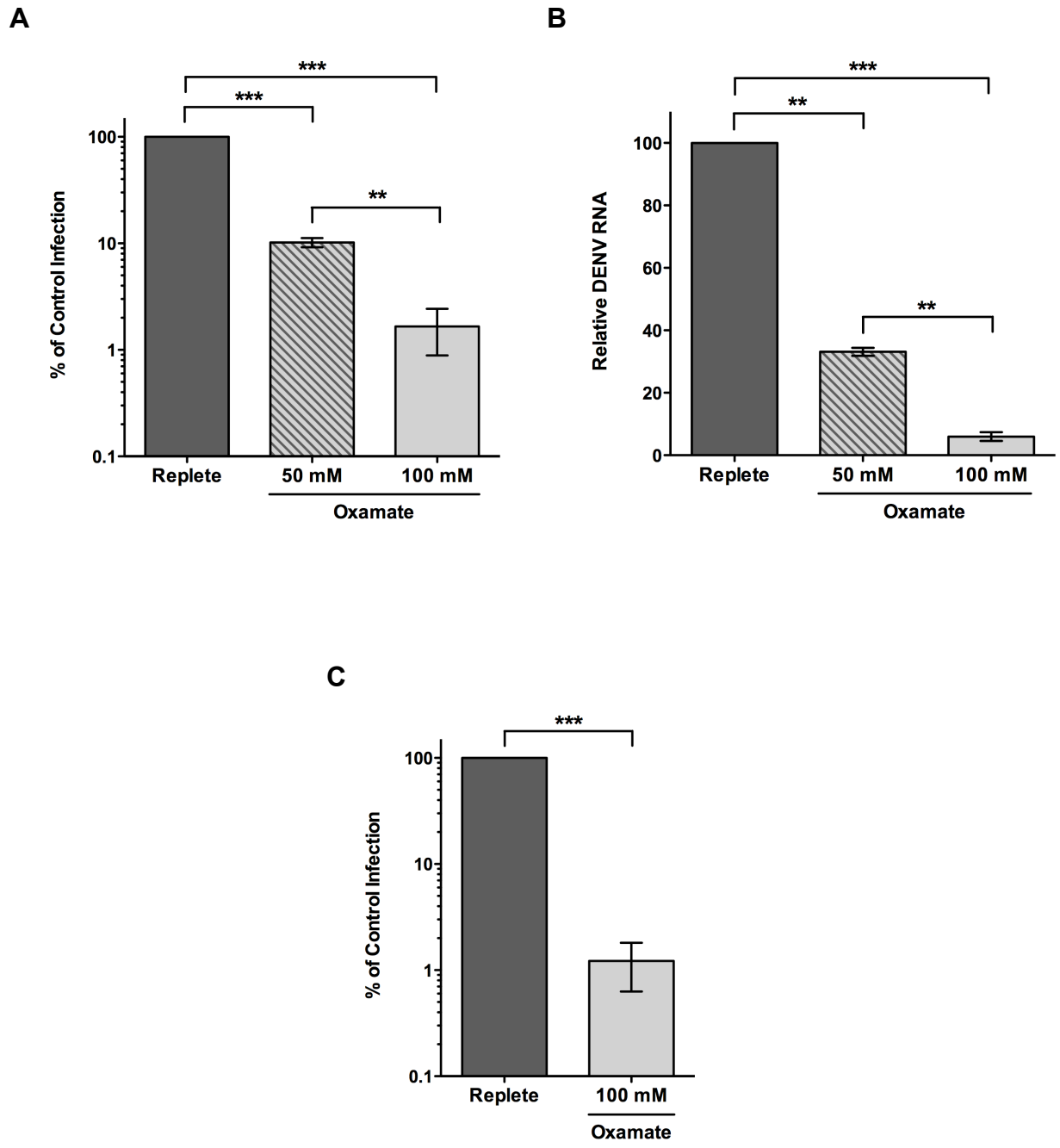

Figure 4-5. Glycolysis is required for maximal DENV replication. HFFs were infected with DENV at an MOI of 3 and were fed replete medium (0 mM oxamate) or replete medium supplemented with 50 mM oxamate or 100 mM oxamate at 2 hpi. Twenty-four hours postinfection, released infectious virus (A) and viral RNA (B) were quantified by focus-forming unit reduction assays or quantitative real-time RT-PCR, respectively. (C) TIME cells were infected with DENV at an MOI of 1 and were fed replete medium supplemented with 0 mM oxamate or 100 mM oxamate at 2 hpi. Infectious extracellular virus was collected at 24 hpi and quantified as above.

CHAPTER V

Conclusions and Future Directions

SUMMARY

Cellular metabolism is a tightly regulated system of biochemical pathways that provides the energy and biosynthetic needs of the cell. All viruses are dependent on the host cell metabolic machinery and therefore reprogram the global metabolome to support viral replication. Understanding how viruses alter host cellular metabolism may illuminate novel therapeutic avenues to combat human pathogens, including those that have the potential to be used as bioterrorism agents. We have found that vaccinia virus (VACV) and dengue virus (DENV), two viruses that are important for biodefense, dramatically reprogram the host cell metabolic network. In particular, these viruses exhibit unique central carbon utilization requirements upon infection of primary human foreskin fibroblasts (HFFs). VACV perturbs the glutaminolytic pathway of glutamine utilization to promote efficient infectious virion production. Specifically, we define a role for glutamine carbon to maintain the TCA cycle during infection and identify the stage of the VACV life cycle that is affected when glutamine utilization is inhibited (98). Conversely, our experiments suggest that DENV activates the glycolytic pathway of glucose metabolism for optimal replication. Interestingly, glucose is dispensable for VACV replication and glycolysis does not appear to be activated during VACV infection (98). This body of work demonstrates that although viruses share many common metabolic requirements, they also induce distinct alterations in host cellular metabolism to support their replication. We believe that identifying such differences could lead to the design of specific metabolic inhibitors to target virus infections that represent public health threats.

CONCLUSIONS

VACV induces glutaminolysis during infection

The impact virus infection has on the host metabolic network is currently an active area of investigation in the field of virology. Before this thesis work had been conducted, global metabolomic analyses had not yet been performed on members of the *Poxviridae* family. The complex nature of the poxvirus life cycle provided an excellent opportunity to examine how a DNA virus that replicates exclusively in the cytoplasm alters host cellular metabolism. In Chapter III, we described the utilization of intracellular metabolic profiling to investigate the effect VACV infection has on the global metabolome (98). We found that VACV perturbs numerous metabolic pathways during infection of primary HFFs, including pathways involved in carbon utilization. We showed that the glutaminolytic pathway of glutamine metabolism is markedly altered in VACV-infected cells and is necessary to replenish the TCA cycle during infection. Furthermore, we demonstrated that glutaminolysis is required for maximal VACV replication by facilitating the robust viral protein synthesis needed for infectious virion production. Interestingly, we found that exogenous glucose is a dispensable carbon source during VACV infection (98). This was an unexpected finding as studies that have examined the impact of glucose and glutamine deprivation on virus production have found that both carbon sources are required for optimal viral replication in other systems (37, 100, 101). A subsequent report showed that exogenous glucose is also expendable during VACV infection of the African green monkey BSC40 cell line. Moreover, the authors of that study found that glutamine is an essential anaplerotic substrate for the TCA cycle in VACV-infected BSC40 cells (118). These results provide further evidence that VACV implements a strikingly unique carbon utilization program to promote successful replication.

DENV induces glycolysis during infection

My thesis work was also dedicated to examining the metabolic effect of DENV infection on primary HFFs. In Chapter IV, we performed a parallel metabolomic analysis to identify DENV-induced perturbations of host cellular metabolic pathways. As DENV is a small RNA virus, we were able to compare how highly divergent viruses alter the intracellular metabolome of the same cell type during infection. From these analyses, we identified several metabolic alterations that are conserved between VACV- and DENV-infected HFFs, such as broad changes in lipid and amino acid metabolism. However, we were again intrigued by how a specific virus manipulates carbon utilization during infection. Interestingly, we found that DENV infection activates the glycolytic pathway of glucose metabolism, at least in part, by upregulating glucose transporter 1 (GLUT1) and hexokinase 2 (HK2) expression. In support of increased glucose utilization during DENV infection, we showed that glucose uptake is enhanced in DENV-infected cells and exogenous glucose is essential for efficient replication. Exogenous glutamine is also necessary for maximal DENV production, albeit to a much lesser extent than glucose. This observation is in line with previous reports that have shown that both nutrients are needed to support replication in other viral systems (37, 100, 101). Lastly, we demonstrated that glycolysis is required for optimal production of infectious DENV. These results reveal that DENV represents another human virus that could potentially be targeted by glycolytic inhibitors. Importantly, these two studies suggest that the specific carbon utilization programs executed during VACV and DENV infection are critical, as supplementation with a secondary carbon source does not restore viral replication. Thus, broad-spectrum antivirals based on metabolic inhibitors that target aberrant central carbon metabolism may offer therapeutic promise.

FUTURE DIRECTIONS: Elucidating the mechanistic details of viral-induced activation of carbon utilization pathways

Determining the cellular mechanism of VACV-induced activation of glutaminolysis

In Chapter III, we demonstrated the induction of glutaminolysis during VACV infection of HFFs (98). We found that exogenous glutamine, via its conversion to α-ketoglutarate by the glutaminolytic pathway, is necessary to maintain the TCA cycle in VACV-infected cells. Moreover, this anaplerotic usage of glutamine is critical in supporting viral protein synthesis (98). Although we have identified why VACV requires glutaminolysis, we have yet to determine how this pathway is being modulated during VACV infection. Two enzymes are responsible for the conversion of glutamine to α-ketoglutarate in the glutaminolytic pathway. Glutamine is first deaminated to glutamate by glutaminase (GLS), and glutamate dehydrogenase (GDH) subsequently deaminates glutamate to α-ketoglutarate. Chambers *et al.* found that HCMV infection temporally regulates both the protein levels and enzymatic activity of GLS and GDH (37). We therefore first examined glutaminolytic enzyme expression via Western blot analysis and observed no significant changes in the protein levels of GLS and GDH following VACV infection (Figure 5-1, unpublished data). Although glutaminolytic enzyme levels are not altered in VACV-infected cells, enzymatic activity could be elevated without a corresponding increase in protein expression. GLS and GDH activity can be measured in the future by utilizing biochemical methods or commercially available kits to determine if increased glutaminolytic enzyme activity is responsible for enhanced glutaminolysis during VACV infection.

Alternatively, enhanced glutaminolytic flux could be due to the upregulation of glutamine transporter expression during VACV infection. Exogenous glutamine uptake is mediated by a

number of transporters, including ASC amino acid transporter 2 (ASCT2) and L-type amino acid transporter 1 (LAT1), both of which are elevated in a variety of human cancers (reviewed in references (140, 141)). To begin to address this possibility, our lab has obtained anti-ASCT2 antibody and radiolabeled glutamine to measure ASCT2 protein levels and glutamine consumption in VACV-infected cells. These reagents, along with other glutamine transporter specific antibodies, can be utilized in future experiments to provide mechanistic insight into glutaminolytic activation by VACV.

Lastly, we speculate that the Myc oncoprotein may be involved in the regulation of glutaminolysis during VACV infection. Myc is a transcription factor that has a central role in both normal cell physiology and tumorigenesis (reviewed in reference (141)). Myc stimulates mitochondrial glutaminolysis through a coordinated transcriptional program that results in cancer cells developing a dependence on exogenous glutamine for their survival, a phenomenon known as glutamine addiction (33). A number of genes involved in the glutaminolytic pathway are induced by Myc, including multiple glutamine transporters and GLS (reviewed in reference (141)). Furthermore, several viruses have been shown to activate Myc (142-144). For example, adenovirus-induced activation of Myc reprograms host cell glucose metabolism and enables optimal virion production (144). Thus, it is possible that VACV also modulates Myc to promote an intracellular metabolic state supportive of viral replication. Our lab has acquired a number of anti-Myc antibodies for immunoblot analysis that can be used to determine if Myc expression is upregulated following VACV infection. In addition, these antibodies can be utilized for immunofluorescence to examine if nuclear localization of Myc, and therefore potentially its transcriptional activity, is increased in VACV-infected cells. Our lab is also currently working on the design of a Myc shRNA lentiviral construct. Once this construct has been successfully

created, intracellular glutamine and glutamate levels or glutaminolytic flux can be measured in mock- and VACV-infected cells following the knockdown of Myc. If Myc knockdown inhibits VACV-induced glutaminolysis, it would demonstrate a role for Myc in regulating glutamine metabolism during VACV infection.

Determining the cellular and viral mechanisms of DENV-induced activation of glycolysis

In Chapter IV, we demonstrated the induction of glycolysis during DENV infection of HFFs. We found that GLUT1 and HK2 expression are upregulated in DENV-infected cells and observed a concomitant enhancement in glucose consumption as compared to their mock-infected counterparts. However, the cellular mechanism responsible for DENV-induced glycolytic activation is not currently known. As the hypoxia-induced factors (HIFs) are master regulators of cellular glycolysis, we directed our focus toward examining the potential role of HIFs during DENV infection.

HIFs are trancription factors that modulate energy metabolism to facilitate cell survival during conditions of low oxygen, or hypoxia (145). Transcriptionally active HIF is a heterodimer consisting of an oxygen-labile α subunit and a constitutively expressed β subunit. The α subunit is generally the ubiquitously expressed HIF-1α (145) or the cell type limited HIF-2α (146). A much less characterized third isoform of HIF (HIF-3α) has also been identified (147). During normoxia, HIF-1α and HIF-2α are rapidly degraded as a result of hydroxylation by oxygen-dependent prolyl hydroxylases (PHDs), which targets the proteins for ubiquitination. However, PHDs cannot function under hypoxic conditions, resulting in the cytoplasmic stabilization of HIF α subunits. The stabilized proteins can then translocate to the nucleus, heterodimerize, and transcriptionally activate genes containing hypoxia response elements (HREs). Several genes

involved in glucose transport and glycolysis harbor HREs, including GLUT1 and HK2 (reviewed in reference (148)) .

HIF α proteins can also be induced under normoxic conditions by a variety of growth factors, cytokines, and vasomodulatory hormones (reviewed in reference (149)). As aerobic glycolysis is a hallmark of cancer, HIF-1α overexpression is observed in many human cancers and is associated with poor treatment response and increased mortality (reviewed in reference (150)). Interestingly, an impressive number of human oncogenic viruses activate HIF-1α, including Kaposi's sarcoma-associated herpesvirus (KSHV), Epstein-Barr virus (EBV), human papillomavirus (HPV), hepatitis B virus (HBV), hepatitis C virus (HCV), and human T-lymphotropic virus (HTLV-1) (11, 151-157). Nononcogenic viruses have also been shown to stabilize HIF-1α (109, 158). For example, VACV protein C16 enhances HIF-1α stabilization by binding to the PHD2 isoform and inhibiting its activity (109). These reports highlight HIF-1α as a major regulator manipulated by viruses to facilitate the metabolic reprogramming needed to complete their life cycles.

Viruses upregulate HIF-1α levels by altering the transcription, translation, or stabilization of the protein (reviewed in reference (159)). To determine if HIF-1α is induced during DENV infection, we first measured HIF-1α transcripts by quantitative real-time RT-PCR. HIF-1α mRNA levels were elevated in DENV-infected cells, suggesting that DENV may transcriptionally modulate HIF-1α (Figure 5-2, unpublished data). Further work will include confirming HIF-1α induction at the protein level via immunoblot analysis and examining if HIF-1α activates the glycolytic pathway during DENV infection. Work is ongoing to construct a lentiviral shRNA vector that targets HIF-1α. Glucose uptake, as well as GLUT1 and HK2 expression, will then be examined following stable knockdown of HIF-1α in DENV-infected

cells to determine if this transcription factor is responsible for upregulating glycolysis during infection.

Although less extensively studied compared to HIF-1α, we will also investigate a potential role for HIF-2α in manipulating glucose metabolism in DENV-infected cells. We have previously shown that KSHV activates HIF-2α (151), revealing that this HIF α protein is also modulated during virus infection. The above-described experiments can also be conducted to determine if HIF-2α is upregulated to increase glycolysis during DENV infection. If, however, the HIFs do not appear to be responsible for DENV-induced glycolytic activation, we will subsequently examine the potential involvement of Myc. In addition to regulating glutamine metabolism, Myc has been shown to transcriptionally activate glycolytic genes, such as phosphofructokinase M (PFKM), enolase I (ENO1), GLUT1, and HK2 (reviewed in reference (160)). Using the Myc reagents previously mentioned, future studies could include performing experiments similar to those outlined for the HIFs to determine if Myc induction upregulates glycolysis during DENV infection.

We would also like to identify the viral mechanism responsible for DENV-induced activation of glycolysis. As previously described, the DENV genome encodes only three structural proteins and seven nonstructural (NS) proteins (reviewed in reference (68)). Recent reports have demonstrated physical interactions between flavivirus NS proteins and key cellular metabolic enzymes. Heaton *et al.* found that DENV NS3 interacts with fatty acid synthase (FASN) in the absence of other viral proteins and purified NS3 stimulates FASN activity *in vitro* (18). Furthermore, NS3 relocalizes FASN to sites of DENV replication and *de novo* lipogenesis was detected in subcellular fractions that contain DENV replication complexes. Thus, NS3 upregulates fatty acid synthesis during DENV infection, a metabolic alteration that is required

for efficient replication (18). Similarly, HCV NS5A directly interacts with the glycolytic enzyme hexokinase 2 (HK2) and enhances its activity *in vitro* (13). Accordingly, NS5a expression results in the increase of both glucose consumption and lactate secretion in Huh-7.5 cells. Hence, the activation of glycolysis during HCV infection is mediated, at least in part, by NS5A (13). Together, these studies suggest that a single DENV protein can upregulate the glycolytic pathway to promote successful viral replication.

We speculate that one of the seven NS proteins of DENV is responsible for the induction of glycolysis observed during DENV infection of HFFs. Our lab recently obtained expression constructs that contain each of the individual DENV NS proteins (a generous gift from Glenn Randall, University of Chicago). These expression plasmids were previously used to transfect Huh-7.5 cells to determine the mechanism of FASN relocalization during DENV infection (18). We will also use Huh-7.5 cells (provided by Michael Gale, Jr., University of Washington) to determine if any of the NS proteins are sufficient to activate glycolysis. Although we have achieved optimal infection rates with Huh-7.5 cells, glycolytic induction following DENV infection of this cell type remains to be determined. Importantly, Huh-7.5 cells are transformed and may fundamentally exhibit altered glycolysis. In the case that Huh-7.5 cells are not suitable for these studies, HFFs will be utilized in future transfection experiments. To identify the viral mechanism responsible for activating glycolysis during DENV infection, individual DENV NS genes will be transfected into Huh-7.5 cells or HFFs, and glucose consumption, along with GLUT1 and HK2 expression, will be examined.

In conclusion, we have shown that VACV and DENV implement remarkably different metabolic programs following infection of primary HFFs. Furthermore, both viruses exhibit distinct preferences in central carbon metabolism that are essential for efficient replication.

Future studies are needed to provide a more complete understanding of why VACV and DENV require these specific carbon utilization pathways and to address how these pathways are activated during virus infection. Importantly, this thesis work demonstrates that identifying unique viral-induced alterations in host cellular metabolism may reveal an Achilles' heel of a particular virus. Such studies can lead to the development of novel therapeutic approaches to control viral outbreaks in the future.

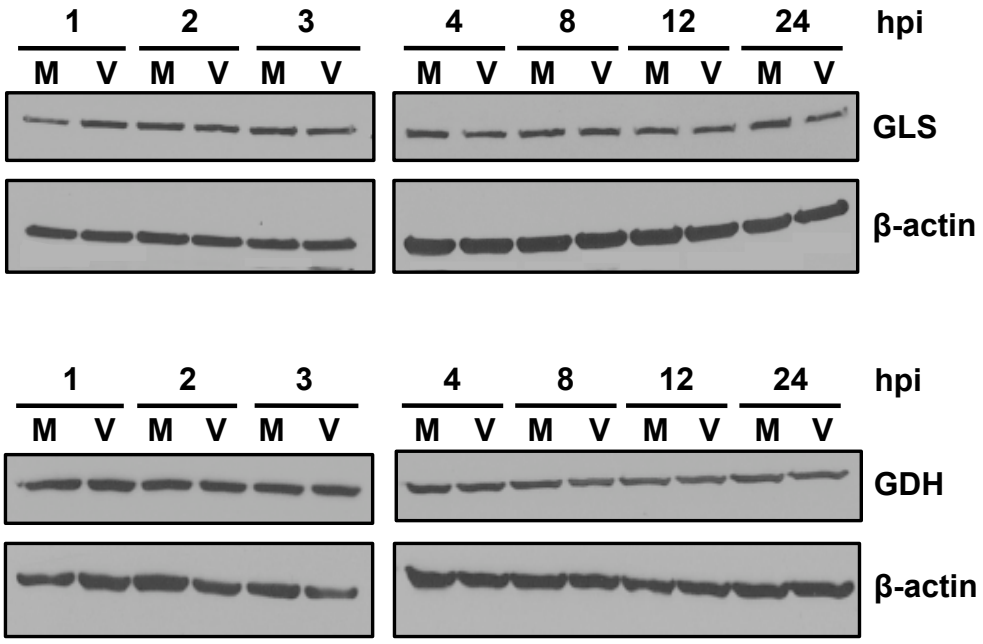

Figure 5-1. Glutaminolytic enzyme levels are not elevated during VACV infection. Western blot analysis of glutaminase (GLS) and glutamate dehydrogenase (GDH) levels in VACV-infected cells. HFFs were mock (M) or VACV (V) infected (MOI of 5) and lysates from cells harvested at the indicated times postinfection were subjected to immunoblot analysis using antibodies against GLS, GDH, and the loading control β-actin.

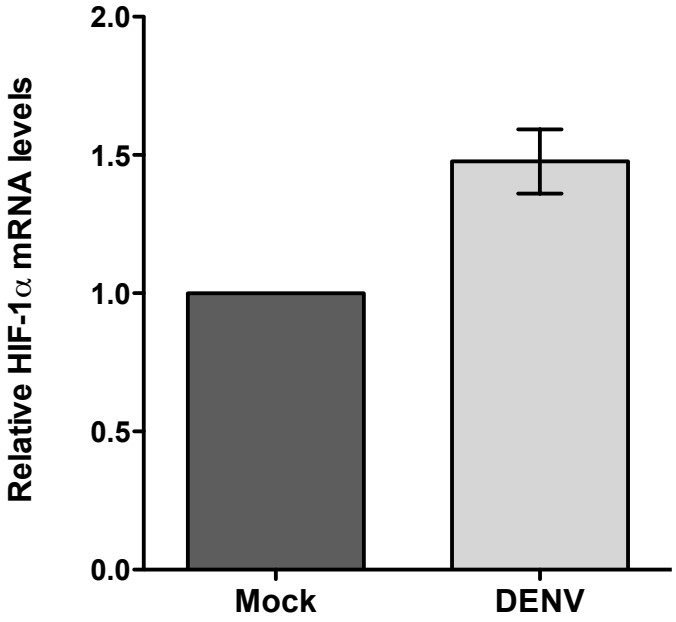

Figure 5-2. HIF-1α mRNA levels are increased during DENV infection. Quantitative real-time RT-PCR analysis of HIF-1α transcript levels in mock- and DENV-infected cells (MOI of 5) harvested at 24 hpi. Relative abundance of HIF-1α mRNA was normalized by the delta threshold cycle method to the abundance of GAPDH mRNA.

REFERENCES

1. **Fiehn O.** 2002. Metabolomics--the link between genotypes and phenotypes. Plant Mol Biol **48:**155-171.

2. **Nicholson JK, Connelly J, Lindon JC, Holmes E.** 2002. Metabonomics: a platform for studying drug toxicity and gene function. Nat Rev Drug Discov **1:**153-161.

3. **Sauer U.** 2006. Metabolic networks in motion: 13C-based flux analysis. Mol Syst Biol **2:**62.

4. **Munger J, Bajad SU, Coller HA, Shenk T, Rabinowitz JD.** 2006. Dynamics of the cellular metabolome during human cytomegalovirus infection. PLoS Pathog **2:**e132.

5. **Munger J, Bennett BD, Parikh A, Feng XJ, McArdle J, Rabitz HA, Shenk T, Rabinowitz JD.** 2008. Systems-level metabolic flux profiling identifies fatty acid synthesis as a target for antiviral therapy. Nat Biotechnol **26:**1179-1186.

6. **Koyuncu E, Purdy JG, Rabinowitz JD, Shenk T.** 2013. Saturated very long chain fatty acids are required for the production of infectious human cytomegalovirus progeny. PLoS Pathog **9:**e1003333.

7. **Vastag L, Koyuncu E, Grady SL, Shenk TE, Rabinowitz JD.** 2011. Divergent effects of human cytomegalovirus and herpes simplex virus-1 on cellular metabolism. PLoS Pathog **7:**e1002124.

8. **Delgado T, Sanchez EL, Camarda R, Lagunoff M.** 2012. Global metabolic profiling of infection by an oncogenic virus: KSHV induces and requires lipogenesis for survival of latent infection. PLoS Pathog **8:**e1002866.

9. **Antman K, Chang Y.** 2000. Kaposi's sarcoma. N Engl J Med **342:**1027-1038.

10. **Diamond DL, Syder AJ, Jacobs JM, Sorensen CM, Walters KA, Proll SC, McDermott JE, Gritsenko MA, Zhang Q, Zhao R, Metz TO, Camp DG, 2nd, Waters KM, Smith RD, Rice CM, Katze MG.** 2010. Temporal proteome and lipidome profiles reveal hepatitis C virus-associated reprogramming of hepatocellular metabolism and bioenergetics. PLoS Pathog **6:**e1000719.

11. **Ripoli M, D'Aprile A, Quarato G, Sarasin-Filipowicz M, Gouttenoire J, Scrima R, Cela O, Boffoli D, Heim MH, Moradpour D, Capitanio N, Piccoli C.** 2010. Hepatitis C virus-linked mitochondrial dysfunction promotes hypoxia-inducible factor 1 alpha-mediated glycolytic adaptation. J Virol **84:**647-660.

12. **Vassilaki N, Kalliampakou KI, Kotta-Loizou I, Befani C, Liakos P, Simos G, Mentis AF, Kalliaropoulos A, Doumba PP, Smirlis D, Foka P, Bauhofer O, Poenisch M, Windisch MP, Lee ME, Koskinas J, Bartenschlager R, Mavromara P.** 2013. Low oxygen tension enhances hepatitis C virus replication. J Virol **87:**2935-2948.

13. **Ramiere C, Rodriguez J, Enache LS, Lotteau V, Andre P, Diaz O.** 2014. Activity of hexokinase is increased by its interaction with hepatitis C virus protein NS5A. J Virol **88:**3246-3254.

14. **Roe B, Kensicki E, Mohney R, Hall WW.** 2011. Metabolomic profile of hepatitis C virus-infected hepatocytes. PLoS One **6:**e23641.

15. **Syed GH, Amako Y, Siddiqui A.** 2010. Hepatitis C virus hijacks host lipid metabolism. Trends Endocrinol Metab **21:**33-40.

16. **Herker E, Ott M.** 2011. Unique ties between hepatitis C virus replication and intracellular lipids. Trends Endocrinol Metab **22:**241-248.

17. **Welsch S, Miller S, Romero-Brey I, Merz A, Bleck CK, Walther P, Fuller SD, Antony C, Krijnse-Locker J, Bartenschlager R.** 2009. Composition and three-dimensional architecture of the dengue virus replication and assembly sites. Cell Host Microbe **5:**365-375.

18. **Heaton NS, Perera R, Berger KL, Khadka S, Lacount DJ, Kuhn RJ, Randall G.** 2010. Dengue virus nonstructural protein 3 redistributes fatty acid synthase to sites of viral replication and increases cellular fatty acid synthesis. Proc Natl Acad Sci U S A **107:**17345-17350.

19. **Hase T, Summers PL, Eckels KH, Baze WB.** 1987. An electron and immunoelectron microscopic study of dengue-2 virus infection of cultured mosquito cells: maturation events. Arch Virol **92:**273-291.

20. **Ko KK, Igarashi A, Fukai K.** 1979. Electron microscopic observations on Aedes albopictus cells infected with dengue viruses. Arch Virol **62:**41-52.

21. **Perera R, Riley C, Isaac G, Hopf-Jannasch AS, Moore RJ, Weitz KW, Pasa-Tolic L, Metz TO, Adamec J, Kuhn RJ.** 2012. Dengue virus infection perturbs lipid homeostasis in infected mosquito cells. PLoS Pathog **8:**e1002584.

22. **Birungi G, Chen SM, Loy BP, Ng ML, Li SF.** 2010. Metabolomics approach for investigation of effects of dengue virus infection using the EA.hy926 cell line. J Proteome Res **9:**6523-6534.

23. **Hollenbaugh JA, Munger J, Kim B.** 2011. Metabolite profiles of human immunodeficiency virus infected CD4+ T cells and macrophages using LC-MS/MS analysis. Virology **415:**153-159.

24. **Rabinowitz JD, Purdy JG, Vastag L, Shenk T, Koyuncu E.** 2011. Metabolomics in drug target discovery. Cold Spring Harb Symp Quant Biol **76:**235-246.

25. **Ritter JB, Wahl AS, Freund S, Genzel Y, Reichl U.** 2010. Metabolic effects of influenza virus infection in cultured animal cells: Intra- and extracellular metabolite profiling. BMC Syst Biol **4:**61.

26. **Yu Y, Clippinger AJ, Alwine JC.** 2011. Viral effects on metabolism: changes in glucose and glutamine utilization during human cytomegalovirus infection. Trends Microbiol **19:**360-367.

27. **Kuhajda FP.** 2006. Fatty acid synthase and cancer: new application of an old pathway. Cancer Res **66:**5977-5980.

28. **Menendez JA, Lupu R.** 2007. Fatty acid synthase and the lipogenic phenotype in cancer pathogenesis. Nat Rev Cancer **7:**763-777.

29. **Swinnen JV, Brusselmans K, Verhoeven G.** 2006. Increased lipogenesis in cancer cells: new players, novel targets. Curr Opin Clin Nutr Metab Care **9:**358-365.

30. **Warburg O.** 1924. Uber den Stoffwechsel der Carcinomzelle. Biochem. Z. **152:**319-344.

31. **DeBerardinis RJ, Mancuso A, Daikhin E, Nissim I, Yudkoff M, Wehrli S, Thompson CB.** 2007. Beyond aerobic glycolysis: transformed cells can engage in glutamine metabolism that exceeds the requirement for protein and nucleotide synthesis. Proc Natl Acad Sci U S A **104:**19345-19350.

32. **Deberardinis RJ, Sayed N, Ditsworth D, Thompson CB.** 2008. Brick by brick: metabolism and tumor cell growth. Curr Opin Genet Dev **18:**54-61.

33. **Wise DR, DeBerardinis RJ, Mancuso A, Sayed N, Zhang XY, Pfeiffer HK, Nissim I, Daikhin E, Yudkoff M, McMahon SB, Thompson CB.** 2008. Myc regulates a transcriptional program that stimulates mitochondrial glutaminolysis and leads to glutamine addiction. Proc Natl Acad Sci U S A **105:**18782-18787.

34. **Delgado T, Carroll PA, Punjabi AS, Margineantu D, Hockenbery DM, Lagunoff M.** 2010. Induction of the Warburg effect by Kaposi's sarcoma herpesvirus is required for the maintenance of latently infected endothelial cells. Proc Natl Acad Sci U S A **107:**10696-10701.

35. **Nakashima K, Takeuchi K, Chihara K, Hotta H, Sada K.** 2011. Inhibition of hepatitis C virus replication through adenosine monophosphate-activated protein kinase-dependent and -independent pathways. Microbiol Immunol **55:**774-782.

36. **McArdle J, Schafer XL, Munger J.** 2011. Inhibition of calmodulin-dependent kinase kinase blocks human cytomegalovirus-induced glycolytic activation and severely attenuates production of viral progeny. J Virol **85:**705-714.

37. **Chambers JW, Maguire TG, Alwine JC.** 2010. Glutamine metabolism is essential for human cytomegalovirus infection. J Virol **84:**1867-1873.

38. **Moss B.** 2001. Poxviridae: The Viruses and Their Replication, p. 2849-2883, Fields Virology, 4th ed. Lippincott Williams & Wilkins, Philadelphia.

39. **Smith GL, Vanderplasschen A, Law M.** 2002. The formation and function of extracellular enveloped vaccinia virus. J Gen Virol **83:**2915-2931.

40. **Roberts KL, Smith GL.** 2008. Vaccinia virus morphogenesis and dissemination. Trends Microbiol **16:**472-479.

41. **Payne LG.** 1980. Significance of extracellular enveloped virus in the in vitro and in vivo dissemination of vaccinia. J Gen Virol **50:**89-100.

42. **Blasco R, Moss B.** 1991. Extracellular vaccinia virus formation and cell-to-cell virus transmission are prevented by deletion of the gene encoding the 37,000-Dalton outer envelope protein. J Virol **65:**5910-5920.

43. **Dales S, Siminovitch L.** 1961. The development of vaccinia virus in Earle's L strain cells as examined by electron microscopy. J Biophys Biochem Cytol **10:**475-503.

44. **Tooze J, Hollinshead M, Reis B, Radsak K, Kern H.** 1993. Progeny vaccinia and human cytomegalovirus particles utilize early endosomal cisternae for their envelopes. Eur J Cell Biol **60:**163-178.

45. **Hiller G, Weber K.** 1985. Golgi-derived membranes that contain an acylated viral polypeptide are used for vaccinia virus envelopment. J Virol **55:**651-659.

46. **Schmelz M, Sodeik B, Ericsson M, Wolffe EJ, Shida H, Hiller G, Griffiths G.** 1994. Assembly of vaccinia virus: the second wrapping cisterna is derived from the trans Golgi network. J Virol **68:**130-147.

47. **Payne LG, Kristensson K.** 1982. The effect of cytochalasin D and monensin on enveloped vaccinia virus release. Arch Virol **74:**11-20.

48. **Blasco R, Moss B.** 1992. Role of cell-associated enveloped vaccinia virus in cell-to-cell spread. J Virol **66:**4170-4179.

49. **Frischknecht F, Moreau V, Rottger S, Gonfloni S, Reckmann I, Superti-Furga G, Way M.** 1999. Actin-based motility of vaccinia virus mimics receptor tyrosine kinase signalling. Nature **401:**926-929.

50. **Parkinson JE, Smith GL.** 1994. Vaccinia virus gene A36R encodes a M(r) 43-50 K protein on the surface of extracellular enveloped virus. Virology **204:**376-390.

51. **Sanderson CM, Frischknecht F, Way M, Hollinshead M, Smith GL.** 1998. Roles of vaccinia virus EEV-specific proteins in intracellular actin tail formation and low pH-induced cell-cell fusion. J Gen Virol **79 (Pt 6):**1415-1425.

52. **Hanna W, Baxby D.** 2002. Studies in smallpox and vaccination. 1913. Rev Med Virol **12:**201-209.

53. **Moss B.** 2011. Smallpox vaccines: targets of protective immunity. Immunol Rev **239:**8-26.

54. **McFadden G.** 2005. Poxvirus tropism. Nat Rev Microbiol **3:**201-213.

55. **Damon IK, Damaso CR, McFadden G.** 2014. Are we there yet? The smallpox research agenda using variola virus. PLoS Pathog **10:**e1004108.

56. **Lewis-Jones S.** 2004. Zoonotic poxvirus infections in humans. Curr Opin Infect Dis **17:**81-89.

57. **Frey SE, Belshe RB.** 2004. Poxvirus zoonoses--putting pocks into context. N Engl J Med **350:**324-327.

58. **Esposito JJ.** 2001. Poxviruses, p. 2885-2921, Fields Virology, 4th ed. Lippincott Williams & Wilkins, Philadelphia.

59. **Chen X, Anstey AV, Bugert JJ.** 2013. Molluscum contagiosum virus infection. Lancet Infect Dis **13:**877-888.

60. **Breman JG.** 2000. Monkeypox: an Emerging Infection for Humans?, p. 45-67. *In* Schield WM, Craig, W.A., Hughes, J.M. (ed.), Emerging Infections 4. ASM Press, Washington DC.

61. **Damon IK.** 2011. Status of human monkeypox: clinical disease, epidemiology and research. Vaccine **29 Suppl 4:**D54-59.

62. **Hutin YJ, Williams RJ, Malfait P, Pebody R, Loparev VN, Ropp SL, Rodriguez M, Knight JC, Tshioko FK, Khan AS, Szczeniowski MV, Esposito JJ.** 2001. Outbreak of human monkeypox, Democratic Republic of Congo, 1996 to 1997. Emerg Infect Dis **7:**434-438.

63. **Meyer H, Perrichot M, Stemmler M, Emmerich P, Schmitz H, Varaine F, Shungu R, Tshioko F, Formenty P.** 2002. Outbreaks of disease suspected of being due to human monkeypox virus infection in the Democratic Republic of Congo in 2001. J Clin Microbiol **40:**2919-2921.

64. **Breman JG, Kalisa R, Steniowski MV, Zanotto E, Gromyko AI, Arita I.** 1980. Human monkeypox, 1970-79. Bull World Health Organ **58:**165-182.

65. **Rimoin AW, Mulembakani PM, Johnston SC, Lloyd Smith JO, Kisalu NK, Kinkela TL, Blumberg S, Thomassen HA, Pike BL, Fair JN, Wolfe ND, Shongo RL, Graham BS, Formenty P, Okitolonda E, Hensley LE, Meyer H, Wright LL, Muyembe JJ.** 2010. Major increase in human monkeypox incidence 30 years after smallpox vaccination

campaigns cease in the Democratic Republic of Congo. Proc Natl Acad Sci U S A **107:**16262-16267.

66. **Heymann DL, Szczeniowski M, Esteves K.** 1998. Re-emergence of monkeypox in Africa: a review of the past six years. Br Med Bull **54:**693-702.

67. **Ligon BL.** 2004. Monkeypox: a review of the history and emergence in the Western hemisphere. Semin Pediatr Infect Dis **15:**280-287.

68. **Chambers TJ, Hahn CS, Galler R, Rice CM.** 1990. Flavivirus genome organization, expression, and replication. Annu Rev Microbiol **44:**649-688.

69. **Miller S, Krijnse-Locker J.** 2008. Modification of intracellular membrane structures for virus replication. Nat Rev Microbiol **6:**363-374.

70. **Fernandez-Garcia MD, Mazzon M, Jacobs M, Amara A.** 2009. Pathogenesis of flavivirus infections: using and abusing the host cell. Cell Host Microbe **5:**318-328.

71. **Gubler DJ.** 1998. Dengue and dengue hemorrhagic fever. Clin Microbiol Rev **11:**480-496.

72. **Effler PV, Pang L, Kitsutani P, Vorndam V, Nakata M, Ayers T, Elm J, Tom T, Reiter P, Rigau-Perez JG, Hayes JM, Mills K, Napier M, Clark GG, Gubler DJ.** 2005. Dengue fever, Hawaii, 2001-2002. Emerg Infect Dis **11:**742-749.

73. **Whitehead SS, Blaney JE, Durbin AP, Murphy BR.** 2007. Prospects for a dengue virus vaccine. Nat Rev Microbiol **5:**518-528.

74. **Kyle JL, Harris E.** 2008. Global spread and persistence of dengue. Annu Rev Microbiol **62:**71-92.

75. **Guzman MG, Alvarez M, Halstead SB.** 2013. Secondary infection as a risk factor for dengue hemorrhagic fever/dengue shock syndrome: an historical perspective and role of antibody-dependent enhancement of infection. Arch Virol **158:**1445-1459.

76. **Beatty ME, Stone A, Fitzsimons DW, Hanna JN, Lam SK, Vong S, Guzman MG, Mendez-Galvan JF, Halstead SB, Letson GW, Kuritsky J, Mahoney R, Margolis HS.**

2010. Best practices in dengue surveillance: a report from the Asia-Pacific and Americas Dengue Prevention Boards. PLoS Negl Trop Dis **4:**e890.

77. **Bhatt S, Gething PW, Brady OJ, Messina JP, Farlow AW, Moyes CL, Drake JM, Brownstein JS, Hoen AG, Sankoh O, Myers MF, George DB, Jaenisch T, Wint GR, Simmons CP, Scott TW, Farrar JJ, Hay SI.** 2013. The global distribution and burden of dengue. Nature **496:**504-507.

78. **Guzman MG, Halstead SB, Artsob H, Buchy P, Farrar J, Gubler DJ, Hunsperger E, Kroeger A, Margolis HS, Martinez E, Nathan MB, Pelegrino JL, Simmons C, Yoksan S, Peeling RW.** 2010. Dengue: a continuing global threat. Nat Rev Microbiol **8:**S7-16.

79. **Halstead SB.** 2007. Dengue. Lancet **370:**1644-1652.

80. **Endy TP, Chunsuttiwat S, Nisalak A, Libraty DH, Green S, Rothman AL, Vaughn DW, Ennis FA.** 2002. Epidemiology of inapparent and symptomatic acute dengue virus infection: a prospective study of primary school children in Kamphaeng Phet, Thailand. Am J Epidemiol **156:**40-51.

81. **Burke DS, Nisalak A, Johnson DE, Scott RM.** 1988. A prospective study of dengue infections in Bangkok. Am J Trop Med Hyg **38:**172-180.

82. **Carlos CC, Oishi K, Cinco MT, Mapua CA, Inoue S, Cruz DJ, Pancho MA, Tanig CZ, Matias RR, Morita K, Natividad FF, Igarashi A, Nagatake T.** 2005. Comparison of clinical features and hematologic abnormalities between dengue fever and dengue hemorrhagic fever among children in the Philippines. Am J Trop Med Hyg **73:**435-440.

83. **Nimmannitya S.** 1987. Clinical spectrum and management of dengue haemorrhagic fever. Southeast Asian J Trop Med Public Health **18:**392-397.

84. **Halstead SB, Simasthien P.** 1970. Observations related to the pathogenesis of dengue hemorrhagic fever. II. Antigenic and biologic properties of dengue viruses and their association with disease response in the host. Yale J Biol Med **42:**276-292.

85. **Kliks SC, Nimmanitya S, Nisalak A, Burke DS.** 1988. Evidence that maternal dengue antibodies are important in the development of dengue hemorrhagic fever in infants. Am J Trop Med Hyg **38:**411-419.

86. **Halstead SB.** 2003. Neutralization and antibody-dependent enhancement of dengue viruses. Adv Virus Res **60:**421-467.

87. **Halstead SB.** 1988. Pathogenesis of dengue: challenges to molecular biology. Science **239:**476-481.

88. **Heinz FX.** 1986. Epitope mapping of flavivirus glycoproteins. Adv Virus Res **31:**103-168.

89. **Roehrig JT, Bolin RA, Kelly RG.** 1998. Monoclonal antibody mapping of the envelope glycoprotein of the dengue 2 virus, Jamaica. Virology **246:**317-328.

90. **Littaua R, Kurane I, Ennis FA.** 1990. Human IgG Fc receptor II mediates antibody-dependent enhancement of dengue virus infection. J Immunol **144:**3183-3186.

91. **Morens DM, Venkateshan CN, Halstead SB.** 1987. Dengue 4 virus monoclonal antibodies identify epitopes that mediate immune infection enhancement of dengue 2 viruses. J Gen Virol **68 (Pt 1):**91-98.

92. **Lin YW, Wang KJ, Lei HY, Lin YS, Yeh TM, Liu HS, Liu CC, Chen SH.** 2002. Virus replication and cytokine production in dengue virus-infected human B lymphocytes. J Virol **76:**12242-12249.

93. **Halstead SB.** 1979. In vivo enhancement of dengue virus infection in rhesus monkeys by passively transferred antibody. J Infect Dis **140:**527-533.

94. **Goncalvez AP, Engle RE, St Claire M, Purcell RH, Lai CJ.** 2007. Monoclonal antibody-mediated enhancement of dengue virus infection in vitro and in vivo and strategies for prevention. Proc Natl Acad Sci U S A **104:**9422-9427.

95. **DiMaio TA, Gutierrez KD, Lagunoff M.** 2011. Latent KSHV infection of endothelial cells induces integrin beta3 to activate angiogenic phenotypes. PLoS Pathog **7:**e1002424.

96. **Wolf A, Agnihotri S, Micallef J, Mukherjee J, Sabha N, Cairns R, Hawkins C, Guha A.** 2011. Hexokinase 2 is a key mediator of aerobic glycolysis and promotes tumor growth in human glioblastoma multiforme. J Exp Med **208:**313-326.

97. **Carroll PA, Brazeau E, Lagunoff M.** 2004. Kaposi's sarcoma-associated herpesvirus infection of blood endothelial cells induces lymphatic differentiation. Virology **328:**7-18.

98. **Fontaine KA, Camarda R, Lagunoff M.** 2014. Vaccinia virus requires glutamine but not glucose for efficient replication. J Virol **88:**4366-4374.

99. **Schneider CA, Rasband WS, Eliceiri KW.** 2012. NIH Image to ImageJ: 25 years of image analysis. Nat Methods **9:**671-675.

100. **Lewis VJ, Jr., Scott LV.** 1962. Nutritional requirements for the production of herpes simplex virus. I. Influence of glucose and glutamine of herpes simplex virus production by HeLa cells. J Bacteriol **83:**475-482.

101. **Eagle H, Habel K.** 1956. The nutritional requirements for the propagation of poliomyelitis virus by the HeLa cell. J Exp Med **104:**271-287.

102. **Vander Heiden MG, Cantley LC, Thompson CB.** 2009. Understanding the Warburg effect: the metabolic requirements of cell proliferation. Science **324:**1029-1033.

103. **Munoz-Pinedo C, El Mjiyad N, Ricci JE.** 2012. Cancer metabolism: current perspectives and future directions. Cell Death Dis **3:**e248.

104. **Kim JW, Dang CV.** 2006. Cancer's molecular sweet tooth and the Warburg effect. Cancer Res **66:**8927-8930.

105. **Pelicano H, Martin DS, Xu RH, Huang P.** 2006. Glycolysis inhibition for anticancer treatment. Oncogene **25:**4633-4646.

106. **Vanslyke JK, Whitehead SS, Wilson EM, Hruby DE.** 1991. The multistep proteolytic maturation pathway utilized by vaccinia virus P4a protein: a degenerate conserved cleavage motif within core proteins. Virology **183:**467-478.

107. **Radsak KD, Weder D.** 1981. Effect of 2-deoxy-D-glucose on cytomegalovirus-induced DNA synthesis in human fibroblasts. J Gen Virol **57:**33-42.

108. **Courtney RJ, Steiner SM, Benyesh-Melnick M.** 1973. Effects of 2-deoxy-D-glucose on herpes simplex virus replication. Virology **52:**447-455.

109. **Mazzon M, Peters NE, Loenarz C, Krysztofinska EM, Ember SW, Ferguson BJ, Smith GL.** 2013. A mechanism for induction of a hypoxic response by vaccinia virus. Proc Natl Acad Sci U S A **110:**12444-12449.

110. **Cory J.** 2006. Purine and Pyrimidine Nucleotide Metabolism p. 789-822. *In* Devlin T (ed.), Textbook of Biochemistry with Clinical Correlations, 6th ed. Wiley-Liss, Hoboken.

111. **Pestova TV, Kolupaeva VG.** 2002. The roles of individual eukaryotic translation initiation factors in ribosomal scanning and initiation codon selection. Genes Dev **16:**2906-2922.

112. **Jackson RJ.** 1991. The ATP requirement for initiation of eukaryotic translation varies according to the mRNA species. Eur J Biochem **200:**285-294.

113. **Alberts B. JA, Lewis J., Raff M., Roberts K., and Walter P.** 2002. Molecular Biology of the Cell, 4th ed. Garland Science, New York.

114. **Berg J.M. TJL, and Stryer L.** 2002. Biochemistry, 5 ed. W.H. Freeman, New York

115. **Lu W, Pelicano H, Huang P.** 2010. Cancer metabolism: is glutamine sweeter than glucose? Cancer Cell **18:**199-200.

116. **Shukla K, Ferraris DV, Thomas AG, Stathis M, Duvall B, Delahanty G, Alt J, Rais R, Rojas C, Gao P, Xiang Y, Dang CV, Slusher BS, Tsukamoto T.** 2012. Design, synthesis, and pharmacological evaluation of bis-2-(5-phenylacetamido-1,2,4-thiadiazol-2-yl)ethyl sulfide 3 (BPTES) analogs as glutaminase inhibitors. J Med Chem **55:**10551-10563.

117. **Xiao L, Hu ZY, Dong X, Tan Z, Li W, Tang M, Chen L, Yang L, Tao Y, Jiang Y, Li J, Yi B, Li B, Fan S, You S, Deng X, Hu F, Feng L, Bode AM, Dong Z, Sun LQ, Cao Y.** 2014. Targeting Epstein-Barr virus oncoprotein LMP1-mediated glycolysis sensitizes nasopharyngeal carcinoma to radiation therapy. Oncogene.

118. **Greseth MD, Traktman P.** 2014. De novo fatty acid biosynthesis contributes significantly to establishment of a bioenergetically favorable environment for vaccinia virus infection. PLoS Pathog **10:**e1004021.

119. **Augustin R.** 2010. The protein family of glucose transport facilitators: It's not only about glucose after all. IUBMB Life **62:**315-333.

120. **Gershon TR, Crowther AJ, Tikunov A, Garcia I, Annis R, Yuan H, Miller CR, Macdonald J, Olson J, Deshmukh M.** 2013. Hexokinase-2-mediated aerobic glycolysis is integral to cerebellar neurogenesis and pathogenesis of medulloblastoma. Cancer Metab **1:**2.

121. **Papaconstantinou J, Colowick SP.** 1961. The role of glycolysis in the growth of tumor cells. I. Effects of oxamic acid on the metabolism of Ehrlich ascites tumor cells in vitro. J Biol Chem **236:**278-284.

122. **Papaconstantinou J, Colowick SP.** 1961. The role of glycolysis in the growth of tumor cells. II. The effect of oxamic acid on the growth of HeLa cells in tissue culture. J Biol Chem **236:**285-288.

123. **Elwood JC.** 1968. Effect of oxamate on glycolysis and respiration in sarcoma 37 ascites cells. Cancer Res **28:**2056-2060.

124. **Jessie K, Fong MY, Devi S, Lam SK, Wong KT.** 2004. Localization of dengue virus in naturally infected human tissues, by immunohistochemistry and in situ hybridization. J Infect Dis **189:**1411-1418.

125. **Bhoopat L, Bhamarapravati N, Attasiri C, Yoksarn S, Chaiwun B, Khunamornpong S, Sirisanthana V.** 1996. Immunohistochemical characterization of a new monoclonal antibody reactive with dengue virus-infected cells in frozen tissue using immunoperoxidase technique. Asian Pac J Allergy Immunol **14:**107-113.

126. **Hall WC, Crowell TP, Watts DM, Barros VL, Kruger H, Pinheiro F, Peters CJ.** 1991. Demonstration of yellow fever and dengue antigens in formalin-fixed paraffin-embedded human liver by immunohistochemical analysis. Am J Trop Med Hyg **45:**408-417.

127. **Balsitis SJ, Coloma J, Castro G, Alava A, Flores D, McKerrow JH, Beatty PR, Harris E.** 2009. Tropism of dengue virus in mice and humans defined by viral nonstructural protein 3-specific immunostaining. Am J Trop Med Hyg **80:**416-424.

128. **Avirutnan P, Malasit P, Seliger B, Bhakdi S, Husmann M.** 1998. Dengue virus infection of human endothelial cells leads to chemokine production, complement activation, and apoptosis. J Immunol **161:**6338-6346.

129. **Huang YH, Lei HY, Liu HS, Lin YS, Chen SH, Liu CC, Yeh TM.** 2003. Tissue plasminogen activator induced by dengue virus infection of human endothelial cells. J Med Virol **70:**610-616.

130. **Huang YH, Lei HY, Liu HS, Lin YS, Liu CC, Yeh TM.** 2000. Dengue virus infects human endothelial cells and induces IL-6 and IL-8 production. Am J Trop Med Hyg **63:**71-75.

131. **Warke RV, Xhaja K, Martin KJ, Fournier MF, Shaw SK, Brizuela N, de Bosch N, Lapointe D, Ennis FA, Rothman AL, Bosch I.** 2003. Dengue virus induces novel changes in gene expression of human umbilical vein endothelial cells. J Virol **77:**11822-11832.

132. **Loisel-Meyer S, Swainson L, Craveiro M, Oburoglu L, Mongellaz C, Costa C, Martinez M, Cosset FL, Battini JL, Herzenberg LA, Atkuri KR, Sitbon M, Kinet S, Verhoeyen E, Taylor N.** 2012. Glut1-mediated glucose transport regulates HIV infection. Proc Natl Acad Sci U S A **109:**2549-2554.

133. **Gonnella R, Santarelli R, Farina A, Granato M, D'Orazi G, Faggioni A, Cirone M.** 2013. Kaposi sarcoma associated herpesvirus (KSHV) induces AKT hyperphosphorylation, bortezomib-resistance and GLUT-1 plasma membrane exposure in THP-1 monocytic cell line. J Exp Clin Cancer Res **32:**79.

134. **Samsa MM, Mondotte JA, Iglesias NG, Assuncao-Miranda I, Barbosa-Lima G, Da Poian AT, Bozza PT, Gamarnik AV.** 2009. Dengue virus capsid protein usurps lipid droplets for viral particle formation. PLoS Pathog **5:**e1000632.

135. **den Boon JA, Diaz A, Ahlquist P.** 2010. Cytoplasmic viral replication complexes. Cell Host Microbe **8:**77-85.

136. **Heaton NS, Randall G.** 2010. Dengue virus-induced autophagy regulates lipid metabolism. Cell Host Microbe **8:**422-432.

137. **Scatena R, Bottoni P, Pontoglio A, Mastrototaro L, Giardina B.** 2008. Glycolytic enzyme inhibitors in cancer treatment. Expert Opin Investig Drugs **17:**1533-1545.

138. **Ganapathy-Kanniappan S, Geschwind JF.** 2013. Tumor glycolysis as a target for cancer therapy: progress and prospects. Mol Cancer **12:**152.

139. **Tennant DA, Duran RV, Gottlieb E.** 2010. Targeting metabolic transformation for cancer therapy. Nat Rev Cancer **10:**267-277.

140. **Fuchs BC, Bode BP.** 2005. Amino acid transporters ASCT2 and LAT1 in cancer: partners in crime? Semin Cancer Biol **15:**254-266.

141. **Wise DR, Thompson CB.** 2010. Glutamine addiction: a new therapeutic target in cancer. Trends Biochem Sci **35:**427-433.

142. **Rodrigues L, Popov N, Kaye KM, Simas JP.** 2013. Stabilization of Myc through heterotypic poly-ubiquitination by mLANA is critical for gamma-herpesvirus lymphoproliferation. PLoS Pathog **9:**e1003554.

143. **Higgs MR, Lerat H, Pawlotsky JM.** 2013. Hepatitis C virus-induced activation of beta-catenin promotes c-Myc expression and a cascade of pro-carcinogenetic events. Oncogene **32:**4683-4693.

144. **Thai M, Graham NA, Braas D, Nehil M, Komisopoulou E, Kurdistani SK, McCormick F, Graeber TG, Christofk HR.** 2014. Adenovirus E4ORF1-induced MYC activation promotes host cell anabolic glucose metabolism and virus replication. Cell metabolism **19:**694-701.

145. **Wang GL, Jiang BH, Rue EA, Semenza GL.** 1995. Hypoxia-inducible factor 1 is a basic-helix-loop-helix-PAS heterodimer regulated by cellular O2 tension. Proc Natl Acad Sci U S A **92:**5510-5514.

146. **Tian H, McKnight SL, Russell DW.** 1997. Endothelial PAS domain protein 1 (EPAS1), a transcription factor selectively expressed in endothelial cells. Genes Dev **11:**72-82.

147. **Makino Y, Cao R, Svensson K, Bertilsson G, Asman M, Tanaka H, Cao Y, Berkenstam A, Poellinger L.** 2001. Inhibitory PAS domain protein is a negative regulator of hypoxia-inducible gene expression. Nature **414:**550-554.

148. **Schofield CJ, Ratcliffe PJ.** 2004. Oxygen sensing by HIF hydroxylases. Nat Rev Mol Cell Biol **5:**343-354.

149. **Dery MA, Michaud MD, Richard DE.** 2005. Hypoxia-inducible factor 1: regulation by hypoxic and non-hypoxic activators. Int J Biochem Cell Biol **37:**535-540.

150. **Semenza GL.** 2003. Targeting HIF-1 for cancer therapy. Nat Rev Cancer **3:**721-732.

151. **Carroll PA, Kenerson HL, Yeung RS, Lagunoff M.** 2006. Latent Kaposi's sarcoma-associated herpesvirus infection of endothelial cells activates hypoxia-induced factors. J Virol **80:**10802-10812.

152. **Wakisaka N, Kondo S, Yoshizaki T, Murono S, Furukawa M, Pagano JS.** 2004. Epstein-Barr virus latent membrane protein 1 induces synthesis of hypoxia-inducible factor 1 alpha. Mol Cell Biol **24:**5223-5234.

153. **Li G, He L, Zhang E, Shi J, Zhang Q, Le AD, Zhou K, Tang X.** 2011. Overexpression of human papillomavirus (HPV) type 16 oncoproteins promotes angiogenesis via enhancing HIF-1alpha and VEGF expression in non-small cell lung cancer cells. Cancer Lett **311:**160-170.

154. **Yoo YG, Oh SH, Park ES, Cho H, Lee N, Park H, Kim DK, Yu DY, Seong JK, Lee MO.** 2003. Hepatitis B virus X protein enhances transcriptional activity of hypoxia-inducible factor-1alpha through activation of mitogen-activated protein kinase pathway. J Biol Chem **278:**39076-39084.

155. **Yoo YG, Cho S, Park S, Lee MO.** 2004. The carboxy-terminus of the hepatitis B virus X protein is necessary and sufficient for the activation of hypoxia-inducible factor-1alpha. FEBS Lett **577:**121-126.

156. **Nasimuzzaman M, Waris G, Mikolon D, Stupack DG, Siddiqui A.** 2007. Hepatitis C virus stabilizes hypoxia-inducible factor 1alpha and stimulates the synthesis of vascular endothelial growth factor. J Virol **81:**10249-10257.

157. **Tomita M, Semenza GL, Michiels C, Matsuda T, Uchihara JN, Okudaira T, Tanaka Y, Taira N, Ohshiro K, Mori N.** 2007. Activation of hypoxia-inducible factor 1 in human T-cell leukaemia virus type 1-infected cell lines and primary adult T-cell leukaemia cells. Biochem J **406:**317-323.

158. **Moin SM, Chandra V, Arya R, Jameel S.** 2009. The hepatitis E virus ORF3 protein stabilizes HIF-1alpha and enhances HIF-1-mediated transcriptional activity through p300/CBP. Cell Microbiol **11:**1409-1421.

159. **Cuninghame S, Jackson R, Zehbe I.** 2014. Hypoxia-inducible factor 1 and its role in viral carcinogenesis. Virology **456-457C:**370-383.

160. **Dang CV, Le A, Gao P.** 2009. MYC-induced cancer cell energy metabolism and therapeutic opportunities. Clin Cancer Res **15:**6479-6483.

CURRICULUM VITAE

Krystal Ann Fontaine

EDUCATION

Ph.D. in Microbiology, 2014
University of Washington
Seattle, Washington, USA
Thesis Advisor: Michael Lagunoff

B.S. in Biotechnology, Summa Cum Laude, 2006
Florida Gulf Coast University
Fort Myers, Florida, USA

PUBLICATIONS

Fontaine KA, Camarda R, and Lagunoff M. 2014. Vaccinia virus requires glutamine but not glucose for efficient replication. *Journal of Virology*. 88(8): 4366-74.

Lok S, Costin JM, Hrobowski YM, Hoffman AR, Rowe DK, Kukkaro P, Holdaway H, Chipman P, **Fontaine KA**, Holbrook MR, Garry RF, Kostyuchenko V, Wimley WC, Isern S, Rossmann MG, and Michael SF. 2012. Expulsion of dengue virus genome induced by a peptide inhibitor. *PLoS ONE*. 7(11);e50995.

Costin JM, Jenwitheesuk E, Lok S, Hunsperger E, Conrads K, **Fontaine KA**, Rees CR, Rossmann MG, Isern S, Samudrala R, and Michael SF. 2010. Structural Optimization and *de novo* design of dengue virus entry inhibitory peptides. *PLoS Negl Trop Dis*. 4(6):e721.

Schieffelin JS, Costin JM, Nicholson CO, Orgeron NM, **Fontaine KA**, Isern S, Michael SF, and Robinson JE. 2010. Neutralizing and non-neutralizing monoclonal antibodies against dengue virus E glycoprotein from a naturally infected patient. *Virology Journal*. 7:28.

Rees CR, Costin JM, Fink RC, McMichael M, **Fontaine KA,** Isern S, and Michael SF. 2008. *In vitro* inhibition of dengue virus entry by p-sulfoxy-cinnamic acid and structurally related combinatorial chemistries. *Antiviral Research*. 80(2):135-142.

NATIONAL AND INTERNATIONAL POSTER PRESENTATIONS

Fontaine KA, Camarda R, and Lagunoff M. 2013. Analysis of global cellular metabolic alterations during poxvirus infection: glutamine metabolism is required for vaccinia virus replication. *Gordon Research Conference on Viruses and Cells, Lucca, Italy.*

Fontaine KA, Camarda R, and Lagunoff M. 2012. Analysis of global cellular metabolic alterations during poxvirus infection: glutamine metabolism is required for vaccinia virus replication. *American Society for Virology 31st Annual Meeting, University of Wisconsin, Madison, WI.*

Costin JM, McMichael M, **Fontaine K**, Rees CR, Hamelin S, Williams KB, Sansing AV, Roschek Jr. W, Michael SF and Isern S. 2007. Inhibition of influenza and dengue virus by zosteric acid and related combinatorial chemistries. *American Society for Virology 26th Annual Meeting, OSU, Corvallis, OR.*

Costin JM, Rees CR, Jenwitheesuk E, **Fontaine K**, Samudrala R, Garry RF, Isern S, and Michael SF. 2007. Dengue virus entry inhibitors. *American Society for Virology 26th Annual Meeting, OSU*, *Corvallis, OR.*